T-2312

A FEASIBILITY STUDY USING BOREHOLE DATA AS APPLIED TO THE SEISMIC DETECTION OF CARBONATE POROSITY IN THE MADISON AND RED RIVER FORMATIONS, NORTHEASTERN POWDER RIVER BASIN

by

Robert C. Anderson

ProQuest LLC.
789 East Eisenhower Parkway
P.O. Box 1346
Ann Arbor, MI 48106 – 1346

T-2312

A thesis submitted to the Faculty and the Board of Trustees of the Colorado School of Mines in partial fulfillment of the requirements for the degree of Master of Science in Geophysics.

Signed: Robert C. Anderson
Robert C. Anderson

Golden, Colorado

April 16, 1982

Approved: George V. Keller
George R. Pickett
Thesis Advisor

Approved: George V. Keller
George V. Keller
Head of Department

Golden, Colorado

May 3, 1982

ABSTRACT

The Madison Limestone Formation, Red River Formation, and associated rocks in the northeastern part of the Powder River Basin have been investigated by the U.S. Geological Survey (USGS) and state agencies in Wyoming, Montana, and South Dakota as possible sources of large quantities of fresh water for coal development and transportation. Presently the Madison Formation is supplying water for domestic and industrial uses in some areas, although large-scale withdrawals have not been attempted. Because of the large areal extent of the Madison and Red River Formations, their complex hydrologic nature, and their great depth (2,000 to 16,000 feet below the surface), the cost of random drilling to the aquifer would be prohibitive. This thesis is concerned with using seismic reflection exploration methods to locate the best areas for drilling development water wells.

The objectives of this thesis are to investigate the seismic responses of the Madison and Red River Formations, and to select criteria for differentiating between water producing and non-water producing strata. To do this, two areas along the northeastern Wyoming-Montana border with different water productivity rates were selected, in which

water wells, log data, and surface multichannel seismic reflection profiles were available for analysis and publication. Using the velocity and density log data from the wells, synthetic seismic responses were generated and correlated to lithology and zones of high water productivity in the Madison and Red River Formations.

This study demonstrates that the best aquifers occur in dolomitic carbonate zones of the Madison and Red River Formations with high secondary porosity and permeability due to diagenetic effects and fracturing. The correlation of these prolific water-producing zones with synthetic seismic traces showed that water producing zones can be detected by careful interpretation of seismic data. The high porosity zones within the Madison and Red River Formations are thin, and mostly below the resolution of usual seismic exploration methods. Consequently their seismic reflection response is subtle, requiring specialized interpretation techniques for their detection.

TABLE OF CONTENTS

LIST OF ILLUSTRATIONS

ACKNOWLEDGEMENTS

My graduate studies at the Colorado School of Mines, culminating in this thesis, was made possible by my employer, the Branch of Oil and Gas Resources, U.S. Geological Survey. I am grateful to this organization for providing the flexibility in my schedule to pursue this work, and for the resources and data that make up this thesis.

I wish to thank Dr. Alfred H. Balch of the USGS for his support of this work, and to my advisor, Dr. George Pickett, for his suggestions and technical input.

I am also grateful to my wife, Lynda, and daughter, Amy, for their patience and understanding throughout my graduate tenure.

A FEASIBILITY STUDY USING BOREHOLE DATA AS APPLIED TO THE SEISMIC DETECTION OF CARBONATE POROSITY IN THE MADISON AND RED RIVER FORMATIONS, NORTHEASTERN POWDER RIVER BASIN

Introduction

Large quantities of fresh water are necessary for the development of a major part of the United States' coal reserves in the Fort Union coal region of the Northern Great Plains. Development of the coal would include on-site steam power generation, gasification, liquefaction, and slurry pipeline transportation. The quantities of water required are estimated to exceed 200,000 acre-feet/year (USGS, 1975). In 1976, the Water Resources Division of the U.S. Geological Survey (USGS) instituted a five year project to study Paleozoic sedimentary rocks in the northeastern Powder River Basin regarding their aquifer properties.

Deep water-bearing sedimentary rocks are required as the source since most shallow and surface water has been fully appropriated to other users. One of the problems associated with using deep aquifers is locating the best water producing zones in the subsurface. The best aquifers are expected to yield more than 500 gallons per minute (MacCary and others, 1981). To date, the study of deep aquifers has been confined to studies of borehole

information from oil and gas wells, and from a limited amount of water test wells drilled by the USGS.

Recently the USGS conducted experiments with seismic reflection data as an exploration tool for locating Paleozoic aquifers as deep as 16,000 ft. Several conventional multichannel common-depth-point (CDP) reflection seismic lines were obtained, and were purposely recorded near two deep USGS water test wells to allow calibration of the seismic waveforms to lithologic zones that have the best water production.

The geologic target under consideration in this study is the Madison Limestone Formation and associated rocks, which underlie most of the basin. Permeability in this unit was created by fracturing as a result of structural folding and faulting, and secondary solution (Lageson, 1977). Thickness of the Madison Formation is not uniform because of varying depositional rates and erosion. Other potential sources of ground water would include a part of the Sundance Formation, the Minnekahta Limestone, and the upper sandy part of the Minnelusa Formation.

Water wells that produce from the Madison Formation have varying production rates, ranging from 20 gal/min to 9,000 gal/min (Blakennagel and others, 1977). The varying water production rates are a function of the variability of the porosity and fracture permeability within the Madison

Formation over the area. The USGS therefore selected two areas with separate Madison geologic properties, and drilled one well at each location to test the hydrologic properties of the carbonate reservoir formations. Log data from these wells were used to generate synthetic seismic traces in order to study seismic response characteristics of Madison rocks with a large range in productivity. Results of the synthetic modeling are discussed later in this report.

Many aspects of the Madison aquifer have already been investigated by the USGS, including the amount of water expected, the chemical and physical properties of the water, the recharge and discharge mechanisms, patterns of ground-water flow, and the hydrologic effects resulting from large-scale water withdrawals at various locations. Work performed in these investigations is described in USGS Open File Report No. 75-631. Many wells have been drilled to the Madison aquifer as oil exploration tests on geologic structures. Data from these wells provide some information to define the geologic framework and aquifer properties of the Madison Formation. Unfortunately, well data is not plentiful in the area, and consequently does not adequately map the high porosity and permeability zones within the aquifer. The main purpose of performing the seismic study, then, is to detect the high porosity and permeability zones in the Madison Formation to provide favorable choices for

drilling locations.

The criteria used by the USGS in selecting areas to study for potential large water-yield aquifers were (1) the presence of more than 100 net feet of rock with porosity of 10 percent or more; (2) the presence of more than 100 net feet of dolomite with average grain size of .0625 mm, and (3) the presence of structure that would cause higher secondary permeability, and corresponding higher water yields (MacCary and others, 1981).

Other minor factors considered include the depths to the aquifers, concentration of dissolved solids, water temperature, and the relation of piezometric head to the land surface. The problem of dissolved solids was evaluated on the basis of apparent resistivity of formation water. According to MacCary et al (1981), an apparent water resistivity of 1 ohm-meter corresponds to a sodium chloride solution of approximately 5,500 milligram per liter concentration at 75^{o} F. Recognizing that other ions are also present, the USGS decided on 1 ohm-meter as the maximum acceptable concentration of dissolved solids.

Geophysical work accomplished to date in this study by the USGS has been the recording of vertical seismic profiles (VSP) in several deep oil and water wells. Vertical seismic profiles are down-hole seismic surveys in a well in which the full seismic wave train is recorded at many different

depth locations within the borehole. Both the downgoing signal from the source at the surface, and upcoming reflections from below, can be observed for each recording location in the well, allowing precise identification of the position of reflecting horizons and their associated seismic reflection characteristics.

In addition to the VSP data, several surface multichannel seismic reflection profiles have been collected near the wells and VSP data, allowing correlation of the seismic response on the surface lines with the porosity and permeability changes of the formation. This seismic data will not be discussed further, as this report deals primarily with the log interpretation and seismic modeling. However, the seismic data can be obtained from the USGS as Oil and Gas Investigation Charts OC-110 and OC-114.

This investigation will concentrate on defining an interpretation criteria to associate seismic waveform changes to lithlogic and porosity conditions in the subsurface. Lithologic characteristics will be obtained directly from an analysis of the well logs in the area and compared to synthetic seismic reflection traces generated from the acoustic and density data. Having established seismic response patterns of the aquifer and surrounding rock layers using log data for calibration, it should be possible to determine whether seismic data can be used to

explore for these subsurface water-bearing formations.

REGIONAL GEOLOGIC FRAMEWORK OF THE MADISON AQUIFER

The study area and major structural features of the northern Rocky Mountain province are shown in Figure 1. The area of seismic reflection data acquisition and deep Madison test wells, outlined by the box in the figure, includes the northeastern part of Wyoming (Powder River County and Converse County), and the southeastern part of Montana (Custer County). The U.S. Geological Survey has evaluated a much larger area for Madison aquifers, but these studies will not be discussed in this thesis.

The Madison Limestone Formation was originally named for lower Mississippian limestones in a region adjacent to Three Forks, Montana. Petroleum exploration of the Madison reservoir has yielded little oil or gas. A few areas of petroleum accumulations occur in the Williston Basin, the Bighorn Basin, and in the north-central part of Montana, but no important deposits have been found in the Powder River Basin. However, the Madison Formation has produced large quantities of water from test wells for many years.

The area of study contains several oil fields, but most have been drilled to shallower horizons. One of the most important oil fields in the area is the Bell Creek field in southeastern Montana. The Bell Creek field produces oil

from a Lower Cretaceous sandstone unit, but operators of the field have used water from deeper wells penetrating the Madison Formation for secondary recovery purposes.

As a consequence of the disappointing petroleum potential of the Madison Formation, the rocks within the study area have not been tested with many wells, and little is known concerning the Madison reservoir and the spatial distribution of permeability and porosity.

Tectonic Features

The Madison Limestone Formation in Wyoming (which is equivalent to the Pahasapa Limestone Formation in western South Dakota) is predominately a shelf carbonate rock of Early to Late Mississippian age (Sando, 1976). Minor amounts of anhydrite become more abundant to the north into Montana. Dolomite content increases generally to the south and southeast.

During Mississippian time, the northern Rocky Mountain region was part of a craton, which included the Precambrian basement rocks of the Canadian Shield, and the Transcontinental Arch, a linear positive element extending southward from the Canadian Shield. The Transcontinental Arch apparently divided the craton into two areas of marine deposition during the Mississippian. The Cordilleran

platform was west of the arch and consisted of a broad flat region. During Early Mississippian time, the platform was a shelf that received carbonate and evaporite sediments, and was later separated into three basins, which received shallow water carbonate sediments.

Structural features present today, shown in Figure 1, significantly affect water movement within the Madison aquifer. The folding and faulting of the Madison rocks have probably fractured the carbonate rock units, providing increased permeability and water flow.

Stratigraphic Framework

The sequence of rocks within the Madison Formation and equivalent units in the eastern Powder River Basin represents a major upward shoaling or shallowing of carbonate units, deposited by a sea which spread out of the shallow Williston basin. Cycles of argillaceous limestone were mixed with oolitic limestone, and as the sea retreated during later Mississippian time, the deposition became more evaporitic. The Madison Formation is subdivided in the northern part of the basin into the Lodgepole Limestone at the base, the Mission Canyon Limestone, and Charles Formation. Figure 2 shows the correlation of formation names for Paleozoic rocks occuring in the Williston Basin

and Powder River Basin. Madison correlatives in other parts of the basin include many different formation names, and will not be discussed further in this thesis.

Thinning of the Madison Group occurs gradually from the depocenter of the Williston Basin, where the interval is over 600 feet thick, to about 200 feet near the east-central part of Wyoming. Through much of Mississippian time, thinning was controlled by the Transcontinental Arch along the eastern side of the basin. Within this thinning edge the Madison Formation is predominantly a fine-grained limestone, called micrite.

Underlying the Madison Formation are rocks of Silurian and Ordovician age, which include the Red River Formation (Ordovician) inside the study area. Along the top of the Madison Formation, differential truncation in part is responsible for the southward thinning of the unit. Karst development is associated with this regional unconformity, and is characterized by breccia zones, calcites, and other features that are now largely filled with sediments.

Paleokarst geology in the Madison Limestone Formation would seem to provide the rock with good permeability for ground water circulation. However, studies by Hunton (1976) show that these features are virtually ineffective in terms of ground water circulation because they are plugged with impermeable shales and silts, destroying the lateral

continuity of the reservoir. Also the absence of large springs producing from the Madison Formation supports the discontinuous nature of the Madison top.

The limestone unit is composed of either crinoidal remains or oolite banks in separate and distinct beds. However, each facies type commonly has little dolomitization and porosity development. The better porosity and permeability developments occur in rock facies composed of relatively coarsely grained crystalline sucrosic dolomite rock, but in general an individual lithologic bed will not be more than 10 to 25 feet thick (Peterson, 1978).

The other important carbonate rock unit that is a potential water producing zone is the Ordovician Red River Formation. The Red River Formation, like the Madison Formation above it, is primarily a shallow marine, tidal-flat dolomite unit, in which the amount of dolomite increases from approximately 25 percent in the southeastern part of the Powder River Basin, to nearly 90 percent along the Wyoming-Montana border. Oil production does occur from the Red River Formation, but has been confined closer to the center of the Williston Basin. Thinning of the unit from southeastern Montana southward occurs as a result of pre-Madison truncation of the top of the Red River Formation.

Studies performed on the Madison and Red River Formations have shown that the best areas for developing

large water yields will be those in which the carbonate rocks are predominately coarsely grained dolomite, and therefore have better porosity development (Blankennagel and others, 1977). As a result of these studies, the USGS selected two locations and drilled two test wells.

The objectives of drilling these wells were to: (1) evaluate the importance of dolomitization in the development of interstitial porosity; (2) evaluate the fracturing of the limestone rocks in the area; and (3) obtain better subsurface hydrologic information on the Madison reservoir. Although fracturing of the Madison and Red River Formations through tectonic folding and faulting has increased the rocks ability to produce water, the degree to which fracturing occurs is difficult to access. In order to make a complete and adequate interpretation of poorosity and permeability of the aquifer, the USGS acquired conventional well log data, borehole televiewer logs, radioactive tracer log, and ran pump tests. A description of the interpretation methods and results of the radioactive tracer logs is given by Blankennagel and others (1977).

Data from two of the water test wells that were drilled were used to study the seismic characteristics of the Madison and Red River aquifers. The USGS Madison No. 1 well, located in Cook County of northeastern Wyoming, was drilled in an apparent structurally active area, indicating

a good potential for secondary fracture porosity. The well was also expected to encounter a high percentage of dolomite facies, also associated with higher porosity. The USGS Madison No. 2 test was drilled in Custer County, Montana. The area is also apparently structurally active, but based on lithofacies maps, the Madison Formation and associated rocks are predominantly low porosity limestones.

Lithologic Description of Aquifers

A majority of the aquifers in the Madison and River Formations contains vuggy, fine to medium crystalline dolomite, and solution-brecciated dolomite and limestone. In some areas, grainstone beds may produce water, but are generally cemented with calcite. Also acting as aquifers are karst-filled deposits, which also may be impervious to clay plugging or cementation.

Fracturing of Madison and Red River aquifers through tectonic faulting and folding has enhanced the water productivity in many areas, but the contribution of fractures to water productivity is very difficult to document with available information. Generally, to make an adequate interpretation of fracture-controlled porosity and permeability requires a complex suite of data, which include cores, pump-tests, borehole televiewer logs and radioactive logs (Blankennagel, 1967).

Measurements from cores of porosity and permeability made by Blankennagel and others (1977), and Brown and others (1978), show values of probable dolomite aquifers average about 17 percent (20 samples) and 11 md (16 samples) respectively in the Madison, and 18 percent (30 samples) and 357.5 md (27) samples in the Red River Formation. A 3 to 6 ft vuggy dolomite section in the Red River with

with permeabilities of 2,490 and 4,890 md (Blankennagel and others, 1977 p. 54), biases the average permeability for the formation. Without these two high values the average permeability in the Red River is then 91 md.

The type of dolomite in the Madison and Red River is thought to be similar to Paleozoic carbonates in and around the Williston basin. Origin of the dolomite results from early replacement of calcite and aragonite mud, which was deposited in shallow subtidal, intertidal, and supratidal environments. Evaporation changes the pore water of the calcareous mud into a brine. After precipitation of gypsum, the brine is rich in magnesium, and the dolomitization process begins.

Porosity and permeability are developed when dolomite crystals grow larger at the expense of leached remnants of calcium carbonate (Murray, 1960). Also, ground water and sea water mixing dolomitzation (Hanshaw and others, 1971) may also have significantly enhanced the porosity and permeability of these dolomite aquifers.

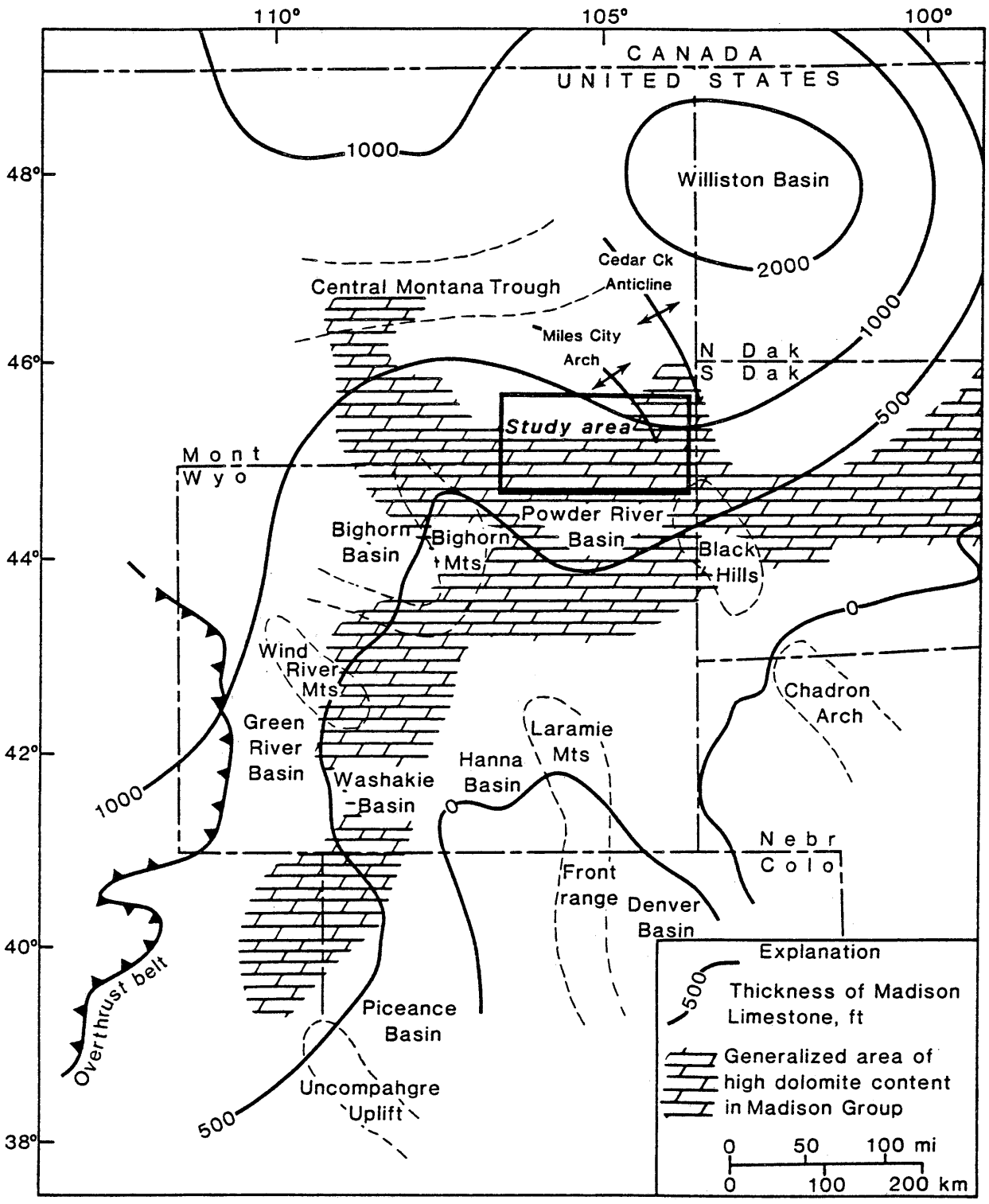

Figure 1. Generalized tectonic features of the study area and surrounding sedimentary basins, and a generalized outline of the areas of high dolomite rock content of the Madison Group. Contour lines show the thickness of the Madison Group.

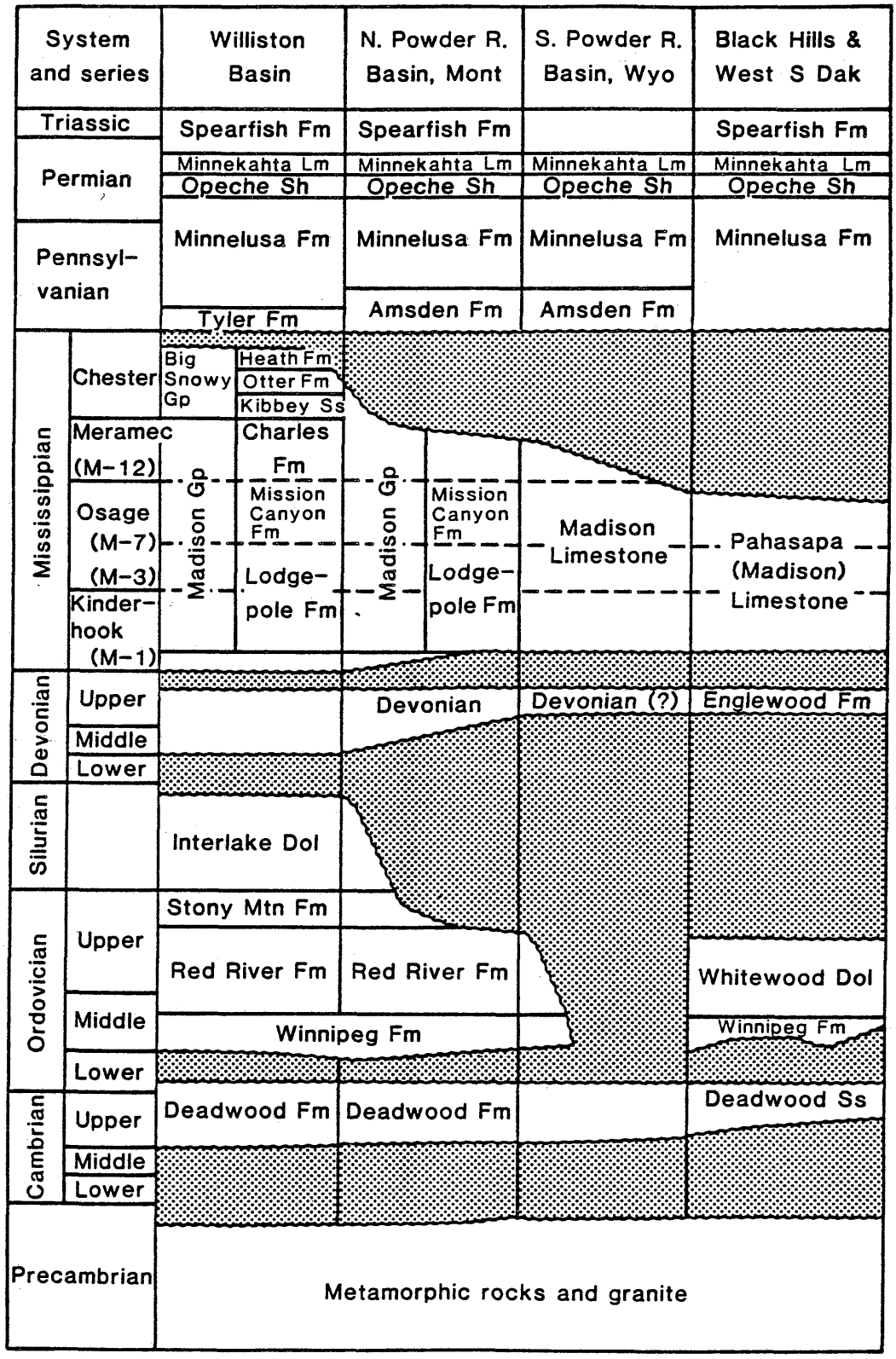

Figure 2. Correlation chart of Paleozoic rocks in the southern and northern Powder River Basin, and the Williston Basin (after Peterson).

EVALUATION OF WELL LOG DATA

An important step in any stratigraphic study is to carefully evaluate and interpret available well log data. Well log data provides the in-situ measurements of velocity and density for modeling the seismic response of a stratigraphic horizon. The model should then indicate the best interpretation criteria to apply regarding the detection of porosity and permeability changes in the Madison and Red River intervals.

The two water test wells evaluated in this thesis encountered different Madison and Red River carbonate environments, with corresponding differences in water producing capabilities. This was fortuitous, because it provided an ideal data set for a seismic exploration feasibility study, since the stratigraphy encountered in the two wells most likely represents the two extreme conditions of porous, water-producing strata versus tight, non-producing strata. Therefore the modeled seismic responses from these two wells should show contrasting waveform characteristics, perhaps providing an exploration method for discrimination of water-producing strata from non-producing strata based on seismic data alone. Although in this study there is a sampling at only two locations of the Madison Formation, the variations detected can be

generalized to include the expected distribution of porosity, density, and interval velocity for the area of exploration.

The only alternative for studying the stratigraphic effects on seismic response is to simulate the effects of permeability and porosity by mathematical methods, or by simulating in-situ stress conditions on rock samples in the laboratory. Mathematical modeling has been applied with some success in the case of sandstone reservoirs in which the effects of porosity, fluid type within the pores, and bulk properties of the rock matrix are accounted for in terms of velocity and density. A reliable mathematical procedure has not been derived for modeling carbonate rocks, probably because of the heterogeneous material comprising the matrix and pore structure. Mathematical modeling of the Madison carbonate reservoir was not attempted in this thesis.

Description of Well Data

The two test wells were drilled and tested in a manner designed to yield the maximum amount of stratigraphic, structural, geophysical, and hydrologic information about the Madison Formation. Information collected from these wells included cores of selected intervals, well logs, and productivity tests. Conventional well logs were recorded digitally at the well site and subsequently analyzed by programs for this thesis.

The particular locations of these wells was chosen by the USGS because:

(1) The depth to the Madison Formation was not excessive, in which the top of the Madison was 2,200 feet in the USGS Madison No. 1 well, and 4,000 feet in the USGS Madison No. 2 well.

(2) Pressures in the aquifer were adequate to allow flowage of water at the surface without pumping.

(3) Locations were on state or federally owned land, and easily accessible.

The USGS Madison No. 1 well was drilled in the northeast quarter of the southeast quarter of section 15, T57N, R65W in Crook County, Wyoming, about thirty miles north of Hulett, Wyoming, and fifty miles northwest of Belle Fourche, South Dakota. The well was drilled to Precambrian

crystalline rocks at a total depth of 4,355 feet below the land surface.

The Madison Formation in this well is approximately 750 feet thick, and is bounded by Devonian rocks of unknown formation name at the base, and the lower portion of the Minnelusa Formation at the top. The Red River Formation in this well is about 460 feet thick, and rests on the Winnipeg Formation. It is overlain unconformably by the Stony Mountain Formation. Dolomite comprises about sixty percent of the Madison Formation, while approximately ninety percent of the Red River Formation is dolomite, with the rest being limestone and anhydrite.

The USGS Madison No. 1 well was productive and flowed water freely at the surface at a rate of approximately 650 to 700 gal/min. Stratigraphic units in the open-hole part of the well that flowed water included the Madison Formation, Red River, Winnipeg and Flathead Formations. It is therefore expected that analysis of the well logs in this well will show several zones that are porous and permeable.

The USGS Madison No. 2 well is located in the southeastern quarter of section 18, T1N, R54W, in Custer County, Montana. The well penetrated Precambrian crystalline rocks at a total depth of 9,394 feet. The Madison Formation in this well is approximately 1,185 feet thick and consists predominantly of limestone, with lesser

amounts of dolomite and anhydrite. The Amsden Formation (Pennsylvanian-Mississippian) is above the Madison and the Madison Formation is bounded below by the Jefferson Group (Devonian). Below the Madison Formation, the Red River Formation is about 450 feet thick, and rests conformably on the Winnipeg Formation and is overlain unconformably by the Stony Mountain Formation. The Red River Formation is approximately 70 percent limestone and 30 percent dolomite. The water yield in this well was about 50 gal/min from the Madison and Red River interval, which is significantly smaller than the production rate of the USGS Madison No. 1 well. Interpretation of tracer logs suggested that the majority of water flow was from Red River dolomite zones (Blankennagel and others, 1977).

Well Log Analysis

The objective of the well log analysis was to determine relationships of rock type, pore structure, permeability, and fluid content to velocity and density. Velocity and density are the primary parameters of acoustic impedance (the product of velocity with density), which is used in the reflection coefficient formula for generating normally incident plane-wave synthetic seismograms. Having established the zones of important water flow using well log

evaluation techniques, the acoustic impedance parameters can be easily determined. These can then be used to predict the seismic reponse characteristics of these zones. The seismic response from the well is a guide for interpreting seismic data -- the interpreter has calibrated a seismic waveform to denote a special lithologic condition.

If the stratigraphic interval under consideration is thick enough the response may be measured directly on seismic data. However, if the zone is too thin, the seismic response may not be directly apparent, but may manifest itself in some other way. For example, a series of thin beds that have high acoustic impedence contrast may not be individually resolved on a seismic trace, but taken together as a group of reflections over an interval may be diagnostic of geologic conditions in the interval.

Automatic Blocking of Log Data

While methods of interpreting well log data are widely known, techniques for obtaining the data from the logs vary. Many log analysts still use the quick and economical method of picking values directly from the paper records of a log curve and plotting these points on paper for evaluation. Another method widely used is to digitize log data at evenly spaced intervals, and allow a computer

program to generate crossplots, statistical computations, and other variables at the selected intervals of interest.

Both of these techniques have their merits and shortcomings. The hand-picking method allows curve data to be edited as it is picked, but is a very slow and time-consuming procedure when large intervals or many wells are to be evaluated. On the other hand, the more automatic computer interpretation methods of digital log data often result in too many points being introduced into the crossplots, with a relatively large point scatter. On such crossplots it is difficult to accurately select trends and simultaneously retain a record of depths of data values. It is also difficult to tell whether a particular data value represents the true reading of a formation, or is only a transition value between bed layers due to averaging effects of the logging tool.

Therefore, to overcome these problems, a computer program (not publicly available) was written to automatically block well log curve data, and reduce the number of data points making up a crossplot. Blocking is a technique of automatically selecting an average value of log data over an interval where the log curve is not varying more than a predefined deviation. Blocked log values therefore represent lithologic layers and excludes the transition between curves, and very thin beds. The

technique allows for a user to make a decision as to which blocked data is to be used in a given crossplot. Figure 3 shows the digitized curve data from the USGS Madison No. 2 well with the blocking overlain. The resulting blocked curves are then overlayed and handpicked to produce the data points for graphical analysis.

Results of picking the Madison and Red River Formations are shown in Table I (Appendix A) for the productive USGS Madison No. 1 well, and Table II (Appendix A) for the non-productive USGS Madison No. 2 well. Along with the values picked from the well logs, several computed parameters are listed also, including the reflection coefficients and two-way travel times from the surface to the top of each horizon.

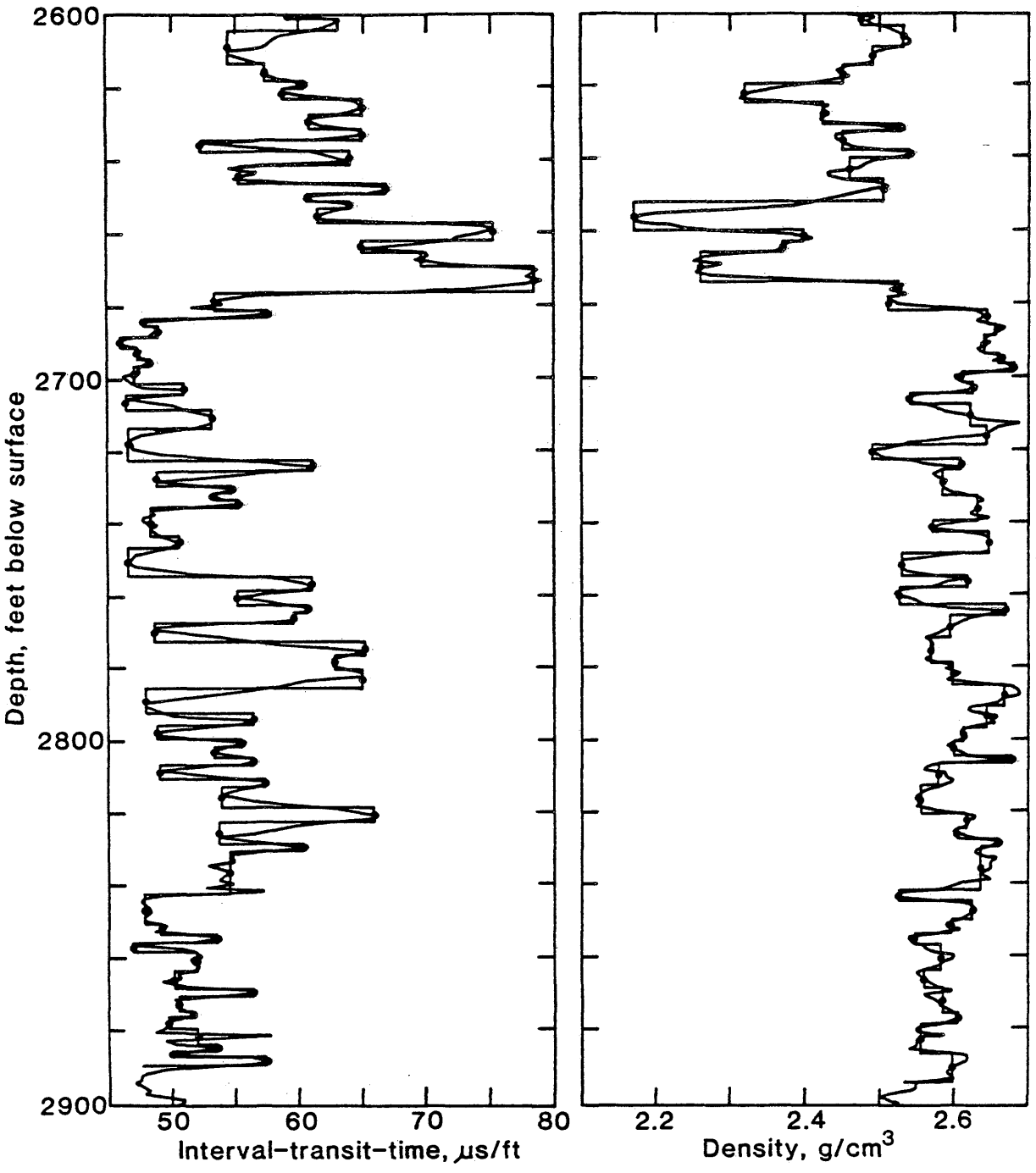

Figure 3. Automatic blocking of the interval-transit-time curve and density curve. Blocked values were then selected and used in the crossplot analysis.

Frequency Distribution

Displays of relative frequencies of porosity, density, and velocity from the Madison Formation and Red River Formation for the two wells are shown by the histogram plots starting on page 31. To contrast the lithologies from the two wells, the format of the plot is to show data values from the productive USGS Madison No. 1 well along the left side of the plot, and values from the non-productive USGS Madison No. 2 well along the right side of the plot. Data from the Madison interval is shown in the upper half of each figure, and data for the Red River interval is shown in the lower half.

The relative frequency distribution for porosity, obtained from the neutron porosity log, is shown in Figure 4. This plot shows higher porosity zones in the USGS Madison No. 1 well, particularly in the Red River interval, where the majority of points cluster around the 20 percent porosity value. Porosity in the Madison interval from the productive USGS Madison No. 1 well are more uniformly distributed.

The histogram of porosity for the non-productive USGS Madison No. 2 well demonstrates the occurence of low porosity zones. Porosity values have a skewed distribution for the upper Madison and Red River interval, while in the

lower Madison interval the values are somewhat higher, peaking around an average porosity of 10 percent.

Figure 5 is the histogram plot of density values, plotted with a format similar to Figure 4. Since density has an inverse relationship with porosity, the distribution of density values was expected to reflect the distribution of the porosity histogram.

The porous zone of the Red River interval from the productive USGS Madison No. 1 well shows a clustering of low density values, agreeing with the porosity histogram. However, the Madison interval shows a peak of density values around 2.50 gm/cm^3, while the porosity histogram is relatively flat. This is an indication that there is probably a mixture of rock types in this interval, in which a wide range of porosity occurs over a relatively narrow range of density. This would be expected in a tidal flat environment in which mixtures of subtidal, intertidal, and supratidal carbonate rocks are deposited as the tidal flats propagate seaward. This is unfortunate because the relative amplitude of a reflecting layer is directly proportional to density, and the discrimination power for detecting porosity will be reduced somewhat.

The distribution of density values for the non-productive Madison and Red River intervals in the USGS Madison No. 2 well are in good agreement with the porosity

distribution. Generally the low porosity zones have high density values.

The final histogram plot, Figure 6, is for interval velocity, which also has a direct effect on seismic reflection strength. In both wells, though, the distribution of velocity values is relatively uniform, with the possible exception of the Red River interval in the non-productive USGS Madison No. 2 well. In this case, the histogram peak is definitely shifted to higher velocities, corresponding to the histogram peak of low porosity values. Generally these plots indicate that a wide range of velocities exist for the narrow range of porosity values. Again this detracts from using seismic data as an exploration tool, because the velocity contrasts of two layers with different porosities will be low, resulting in a small reflection amplitude. The upper Madison Formation in the No. 2 well also shows a shift to higher velocities, which correlates to the histogram peak of low porosities. The lower Madison shows a more uniform distribution of velocities, while the histogram plot of porosities peaks around 8 to 10 percent.

Secondary Porosity

Since the Madison and Red River intervals are relatively free of shale or gas, the overlay of porosity derived from the acoustic log with the neutron porosity log provides a means of locating secondary porosity zones (Schlumberger, 1972, p. 71). When secondary porosity occurs in a carbonate rock, such as vugs or fractures, the acoustic log yields a low value for porosity when "normal" response relations are used. When plotted on the same scale with the neutron porosity log, assuming that the proper scaling for mineral type has been used, the separation of the two curves may indicate the effects of secondary porosity.

Figure 7 shows this overlay plot for the blocked data from the water producing USGS Madison No. 1 well. The upper part of the Madison Formation, from 2,600 to 2,850 feet shows little separation, but beginning at 2,900 feet the two curves separate, and are significantly separated past 3,050 feet, which comprises the Red River interval.

The same plot for the non-productive USGS Madison No. 2 well is shown in Figure 8. Both the Madison and Red River intervals appear to have little secondary porosity effects, as the curves track each other through the interval.

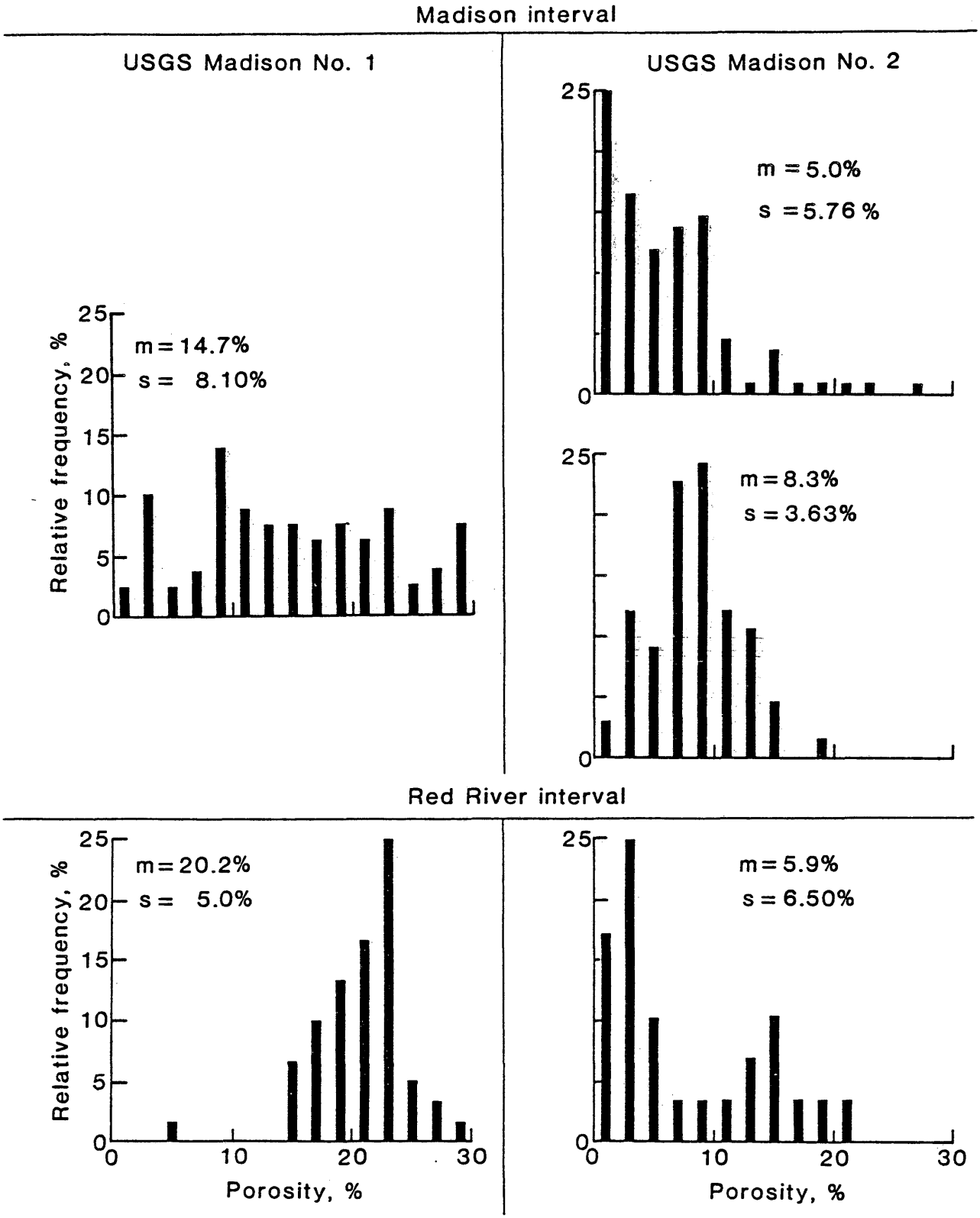

Figure 4. Comparison of porosity distribution between the water productive USGS Madison No. 1 well (left side) with the non-productive USGS Madison No. 2 well (right side) for the Madison Formation (top) and Red River Formation (bottom).

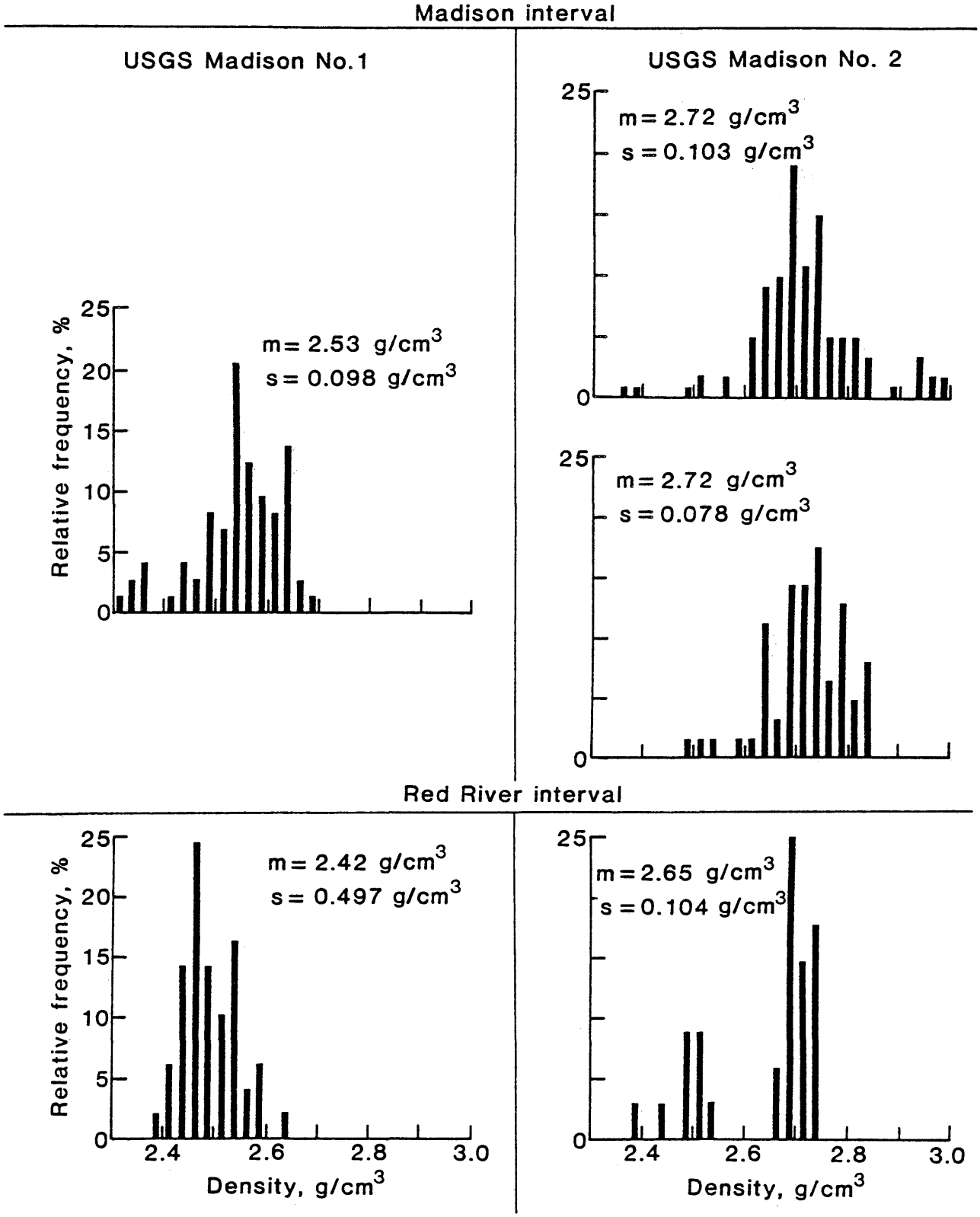

Figure 5. Comparison of the density distribution between the water producing USGS Madison No. 1 well (left side) and the non-productive USG Madison No. 2 well (right side) for the Madison Formation (top) and the Red River Formation (bottom).

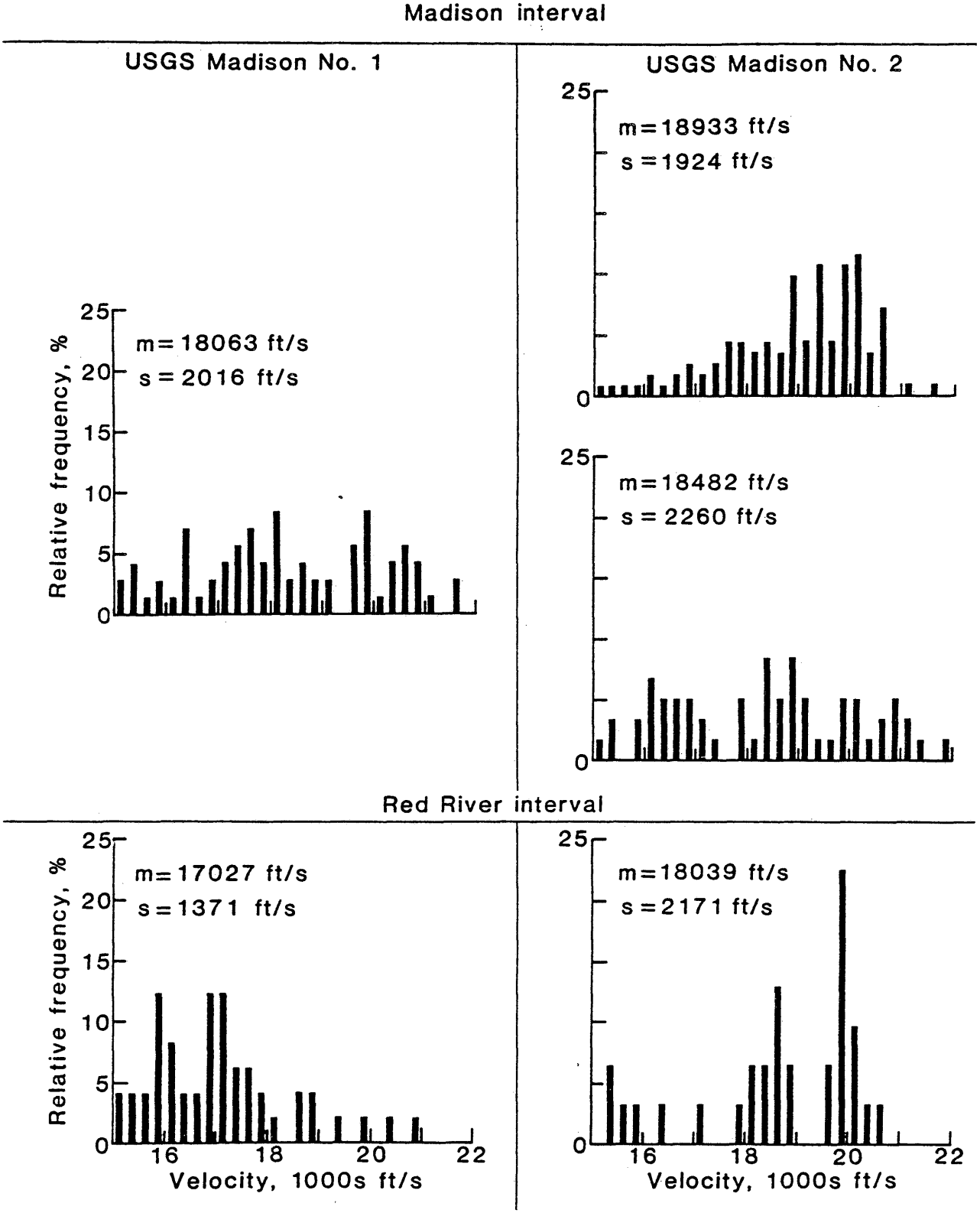

Figure 6. Comparison of velocity distribution between the water producing USGS Madison No. 1 well (left side) with the non-productive USGS Madison No. 2 well (right side) for the Madison Formation (top) and Red River Formation (bottom).

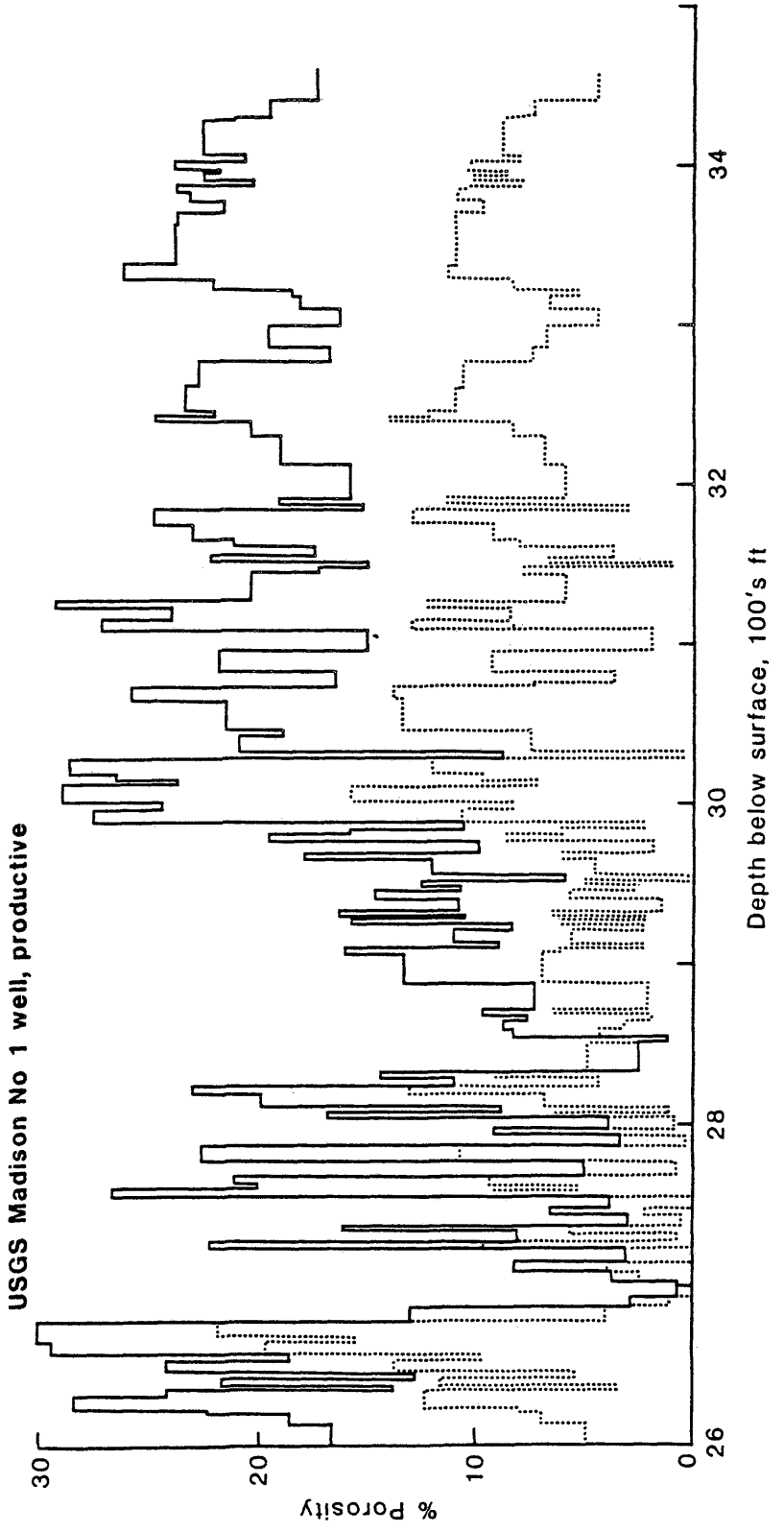

Figure 7. Porosity versus depth from the productive USGS Madison No. 1 well, using two blocked porosity curves to locate zones of secondary porosity. The solid curve is the neutron porosity log, and the dashed curve is porosity computed from the sonic travel time curve using limestone as the rock matrix.

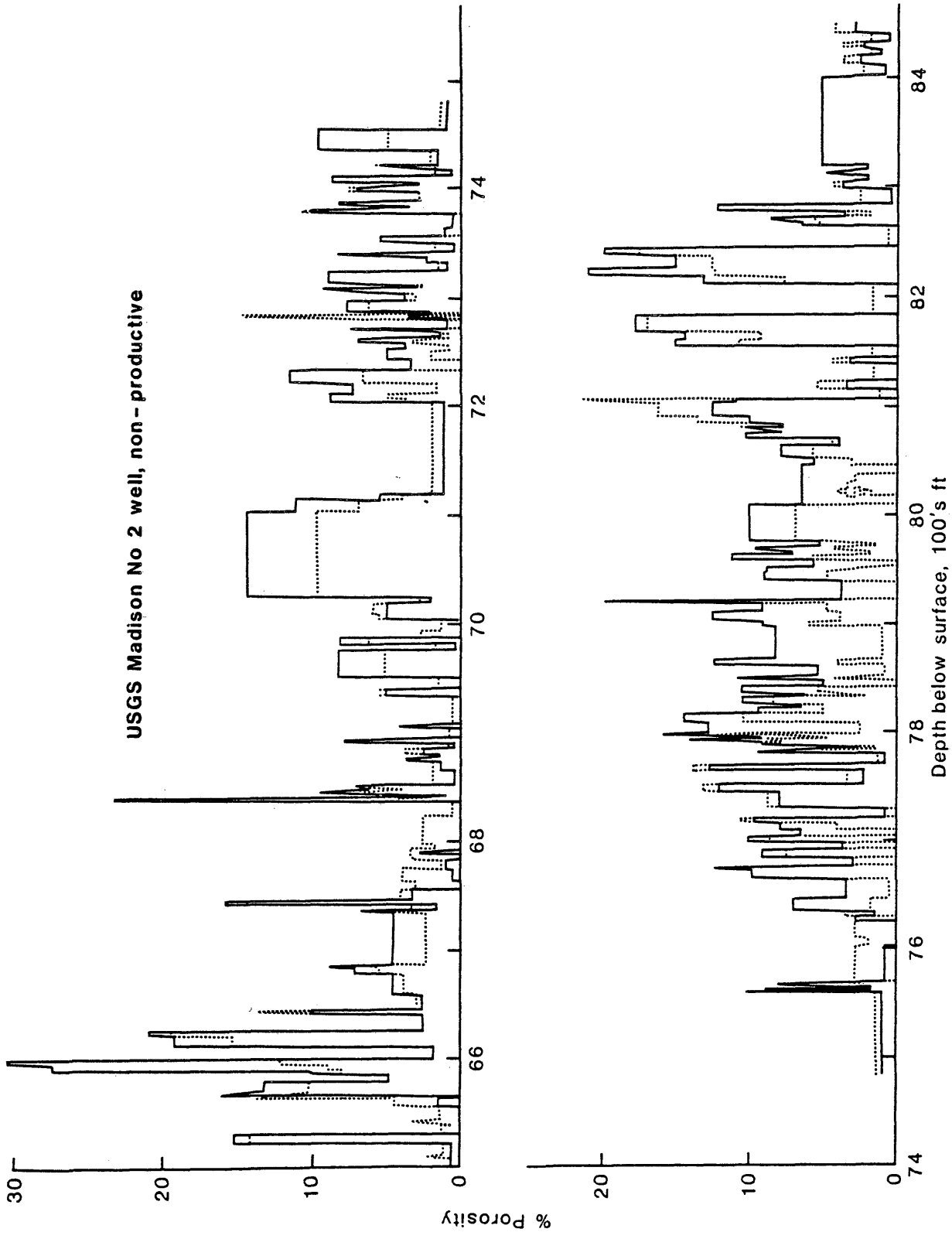

Figure 8. Porosity versus depth from the non-productive USGS Madison No. 2 well, using two blocked porosity curves to locate zones of secondary porosity. The solid curve is the neutron porosity log, and the dashed curve is porosity computed from the sonic travel time curve using limestone as the rock matrix.

Well Log Crossplots

The three porosity logs from the USGS Madison No. 1 and No. 2 wells were analyzed in crossplots to determine the lithologic trends in the Madison Formation and the Red River Formation. Crossplots were constructed of the density versus sonic travel time, neutron porosity versus sonic travel time, and neutron porosity versus density. Also, crossplots using combinations of the three porosity logs were constructed. Variables, called "M" and "N", are dependent on the three porosity logs, and produce a crossplot in which rock minerals are represented, in principle, by unique points on the crossplot regardless of their porosity. This graphical procedure allows quick identification of those zones in the Madison Formation and Red River Formation which may have aquifer characteristics (carbonate rock with high primary or secondary porosity), and those that are tight and non-productive.

The variable "M" is defined as

$$M = \frac{\Delta t_f - \Delta t}{\rho_b - \rho_f} \times .01$$

where Δt_f is the interval-transit-time of the fluid in the pores

Δt is the interval-transit-time from the

log data

ρ_f is the density of the fluid in the pores

ρ_b is the bulk density from the log data

The value "M", except for the scaling factor .01, is the slope of a line representing a particular mineral along its full range of porosity. Thus, in principle, the value "M" is dependent only on the fluid and matrix characteristics, and independent of porosity (Schlumberger, 1972). That is, if the porosity is written in terms of sonic travel time and density, then

$$\phi = \frac{\Delta t_f - \Delta t}{\Delta t_f - \Delta t_m} = \frac{\rho_b - \rho_f}{\rho_m - \rho_f}$$

so that

$$M = \frac{\Delta t_f - \Delta t}{\rho_b - \rho_f} = \frac{\Delta t_f - \Delta t_m}{\rho_m - \rho_f}$$

= constant, regardless of porosity

In a similar manner, N is defined as

$$N = \frac{(\phi_N)_f - \phi_N}{\rho_b - \rho_f}$$

where $(\phi_N)_f$ is neutron porosity of the fluid

ϕ_N is the neutron porosity from the

log data and

ρ_b and ρ_f are defined in the expression for M

The parameter "N" is the slope of a line representing a particular mineral along its full range of porosity on a crossplot of neutron porosity versus density. As in the case for the parameter "M", "N" is dependent only on the fluid and matrix characteristics of the rock. The values of "M" and "N" will be accurate only if the porosity is linear between the matrix point and fluid point.

The other types of crossplots used to analyze the Madison and Red River Formations were the sonic travel time versus density, sonic travel time versus neutron porosity, and neutron porosity versus density. These particular combinations of crossplots help to discriminate between different lithologies in the formations. Once a classification of rock types is accomplished, then it is a simple matter to compute acoustic impedance for the classes or rock types.

In addition to the log data described above, the gamma-ray log was checked for zones of shaliness to aid in the interpretation of the crossplots. Generally the values selected from the curves were clean, and quantitative corrections to the neutron, sonic, and density curves were not made. In zones where the caliper log indicated hole washout or damage, the corresponding values from the blocked

logs were simply not picked and used in the crossplots. Hole washout was not a significant problem through the Madison and Red River intervals.

Results of Crossplot Analysis

The family of crossplots were constructed on two primary zones of interest in the productive USGS Madison No. 1 well, and three zones from the non-productive USGS Madison No. 2 well. The two zones in the Madison No. 1 well were the Madison Formation, ranging in depth from 2,600 to 3,050 feet, and the Red River Formation, from 3,050 to 3,471 feet. Because the Madison Formation is a thicker unit at the USGS Madison No. 2 well, this interval was divided into two sections. Division of the Madison interval was made at an upper interval of 6,505 to 7,634 feet, and a lower interval of 7,646 to 8,087 feet. The Red River interval in this well ranges from 8,100 to 8,563 feet below ground level.

The crossplots are shown in Figures 9 through 16 for the USGS Madison No. 1 well, and in Figures 17 through 28 for the USGS Madison No. 2 well. Pure lithology lines are drawn on each figure and indicate the response of the logs for distinct rock types with varying porosities. Rock types and matrix values used (all after Schlumberger, 1972) were dolomite, with matrix density = 2.87 gm/cm^3 and matrix

velocity = 20,900 ft/sec, limestone, with matrix density = 2.78 gm/cm^3 and matrix velocity = 19,000 ft/sec, and anhydrite, with matrix density = 2.92 gm/cm^3 and matrix velocity = 22,800 ft/sec. The log calibration for the neutron porosity was computed using a limestone matrix, and so the pure dolomite line on the crossplots involving neutron porosity are compensated.

Fluid parameters selected for the crossplots of "M" versus "N" were 189 microseconds/ft for the sonic travel time, 1.0 gm/cm^3 for the density, and 100 percent for the neutron porosity.

USGS MADISON NO. 1

PRODUCTIVE CASE

Madison Interval

The neutron porosity versus density crossplot for the Madison interval (Fig. 9) shows in general that the higher porosity values correspond to lower values of density, and higher values of sonic travel times (Fig. 10). This trend is confirmed by the cuttings and core samples taken from the well (Blankennagel and others, 1977). Therefore the product of velocity and density, or the acoustic impedance, should follow the same trend, and would therefore be an indicator for porosity variations on a seismic reflection profile.

The data points of the Madison Formation are scattered on the plots of neutron porosity versus density, and neutron porosity versus sonic travel time, Figures 9 and 10, indicating a mixture of rock types. However, the points concentrate around the generalized limestone line at low porosities, and migrate toward the generalized dolomite line as porosities become higher. This indicates that porosity develops up to 30 percent in the limestone - dolomite mixture, as shown in Figure 9, as the concentration of dolomite increases.

Porosity development in carbonate rocks can occur in several ways because carbonate rocks originate in a variety of facies types and are later complexly altered through diagenetic influences. Diagenetic alterations can enhance porosity or completely destroy it. The diagenetic effects on limestone changing to dolomite is to create a slightly more compact crystal lattice, and therefore yield some 12 to 13 percent intercrystalline or sucrosic porosity to the porosity that originally existed in the rock (Murran, 1960).

The sonic travel time versus density crossplot, Figure 11, is confusing as it shows most of the data points plotting along a trend above the pure limestone line. In fact, this is the region where a pure silica line would plot, although the cuttings and cores indicate that the silica material is not present (Ryder, per. comm., 1979). This is probably because the sonic measurement responds differently to porosity in voids that is homogeneously distributed throughout the matrix than it does to vulgular porosity and porosity in voids created through fracturing of the rock. Thus, the sonic travel time log (Δt) is not affected as much by a unit of vuggy or fracture porosity, and the measurement is consequently smaller that the Δt would be in homogeneously distributred porosity. The result is that points on the sonic travel time versus density crossplot are shifted to the lower travel time values, and

this effect must be taken into account when attempting to determine lithology. However, the fairly linear trend of density with sonic travel time is easily recognized.

The density log and neutron log both respond to the total porosity of the formation. Thus the "M" and "N" crossplot would show these points plotting above the dolomite - limestone line since the value "N" is not affected by secondary porosity while the parameter "M" is affected, since it involves the sonic travel time data. The amount of increase in "M" is also dependent on the amount of primary porosity in the rock.

The "M" and "N" crossplot for the Madison interval (Fig. 12) agrees with the data from cuttings and cores (Blankennagel and others, 1977). The interval is composed primarily of a binary mixture of limestone and dolomite with good primary and secondary porosity development. Shale or anhydrite are not present in the interval.

Red River Interval

The Red River interval is dominated by a narrower range of rock mixtures as indicated by the density versus neutron porosity crossplot, Figure 13, the sonic travel time versus neutron crossplot, Figure 14, and the "M" versus "N" crossplot, Figure 15. The description of lithology from the

cuttings and cores (Blankennagel and others, 1977) shows this zone to be composed entirely of dolomite with fair to good fracture and vugular porosity. This zone also produced a very high water flow of about 700 gal/min during the testing of the well.

The sonic travel time versus neutron porosity crossplot, Figure 14, confirms the general rock type to be mainly dolomite, while the density versus neutron porosity crossplot, Figure 13, shows a relatively tight cluster of data points lying along a trend between the pure dolomite and limestone lines, indicating a mixture of carbonate rock types through the Red River Formation. The density versus sonic travel time crossplot, Figure 15, shows the same pattern as in the Madison interval for this well, in which points cluster along a trend to the left side of the plot due to the effects of secondary porosity on the interval transit time log. The "M" and "N" crossplot, Figure 16, shows a fairly tight cluster of points in the secondary porosity region of the plot.

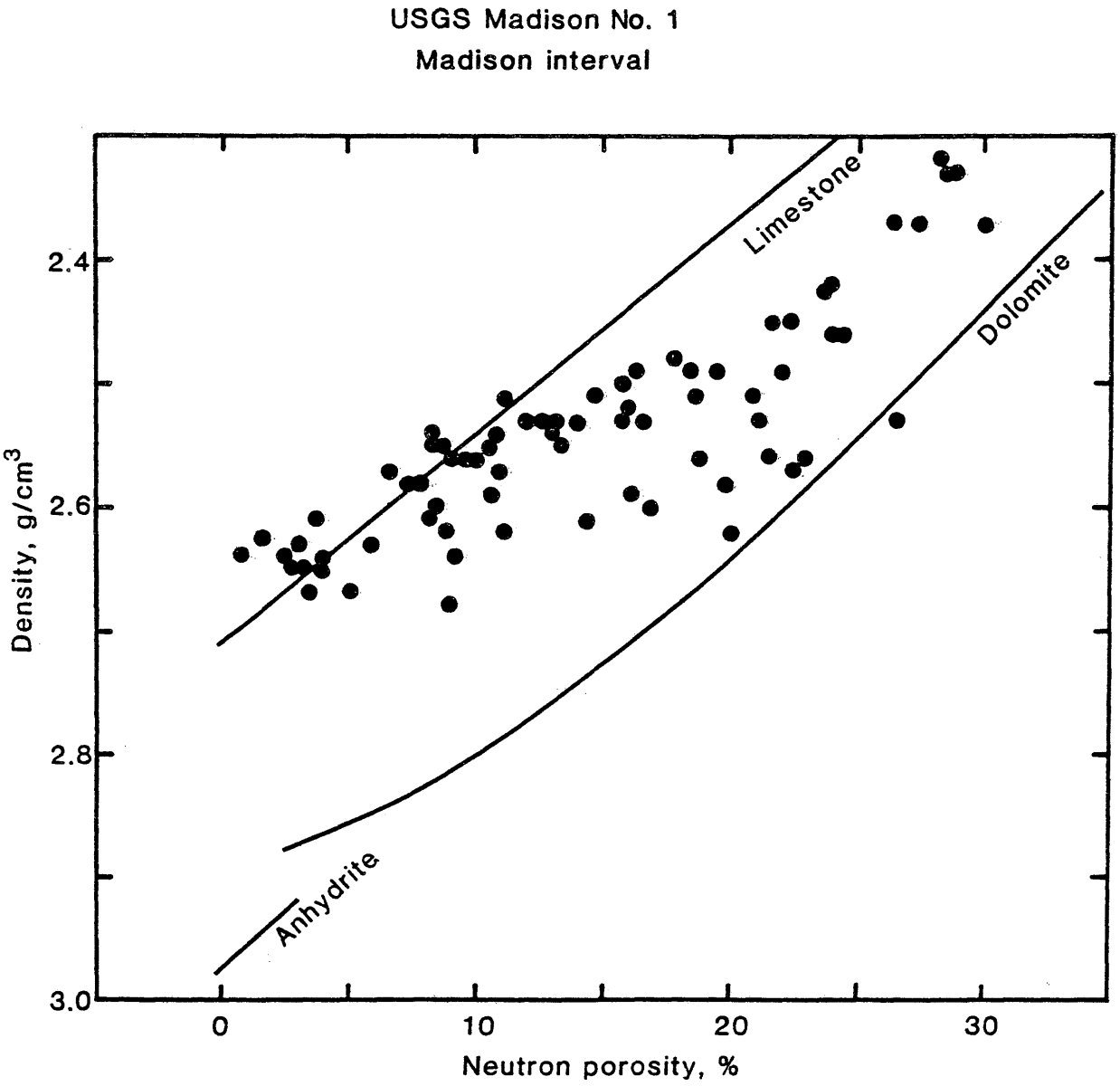

Figure 9. Relationship between density and porosity for the Madison Formation of the productive USGS Madison No. 1 well. The ideal response curves (solid lines) represent log values of distinct rock types for varying porosities (Schlumberger, 1979, p. 25).

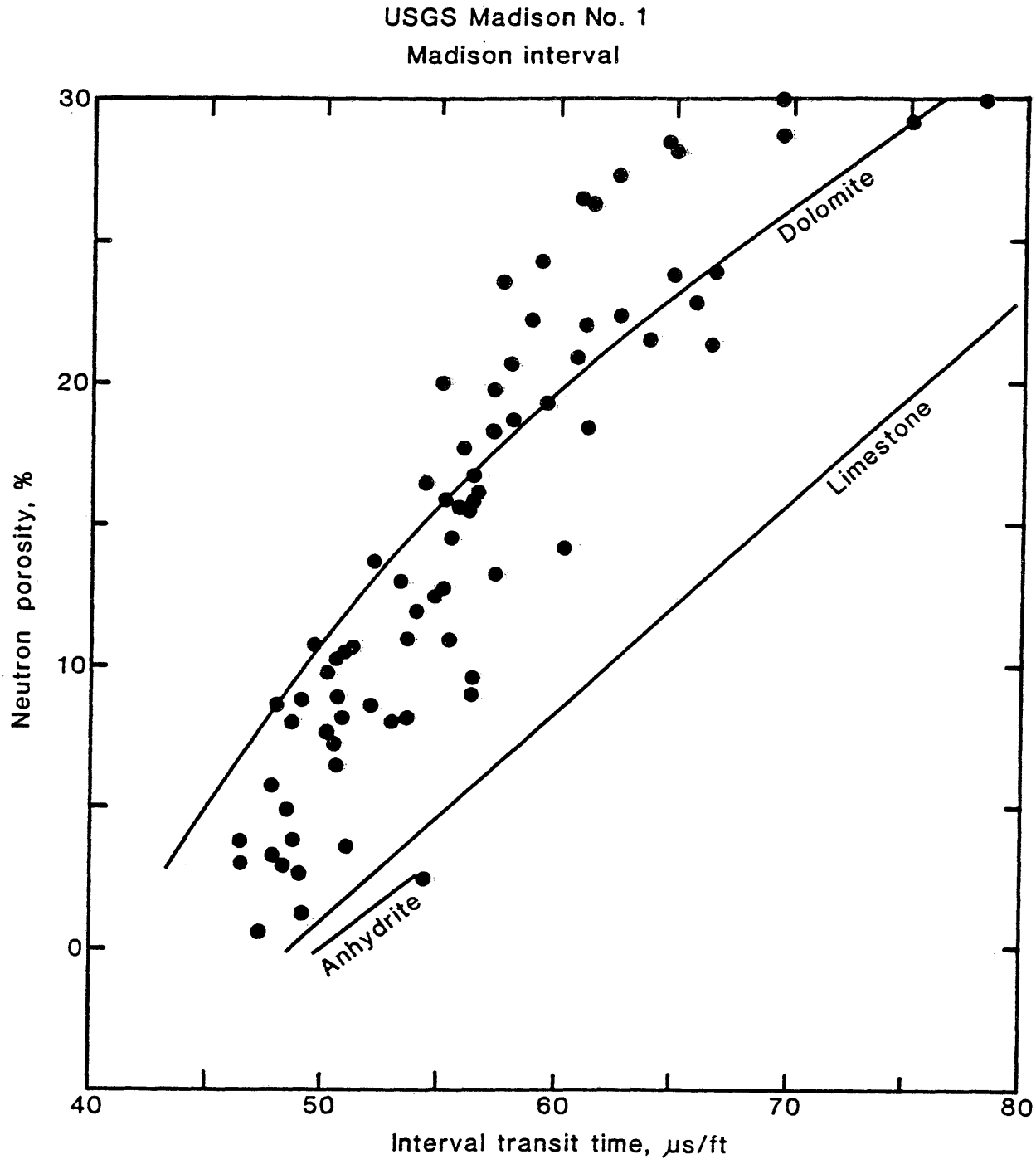

Figure 10. Relationship between porosity and interval travel time for the Madison Formation of the productive USGS Madison No. 1 well. The ideal response curves (solid lines) represent log values of distinct rock types for varying porosities (Schlumberger, 1979, p. 29).

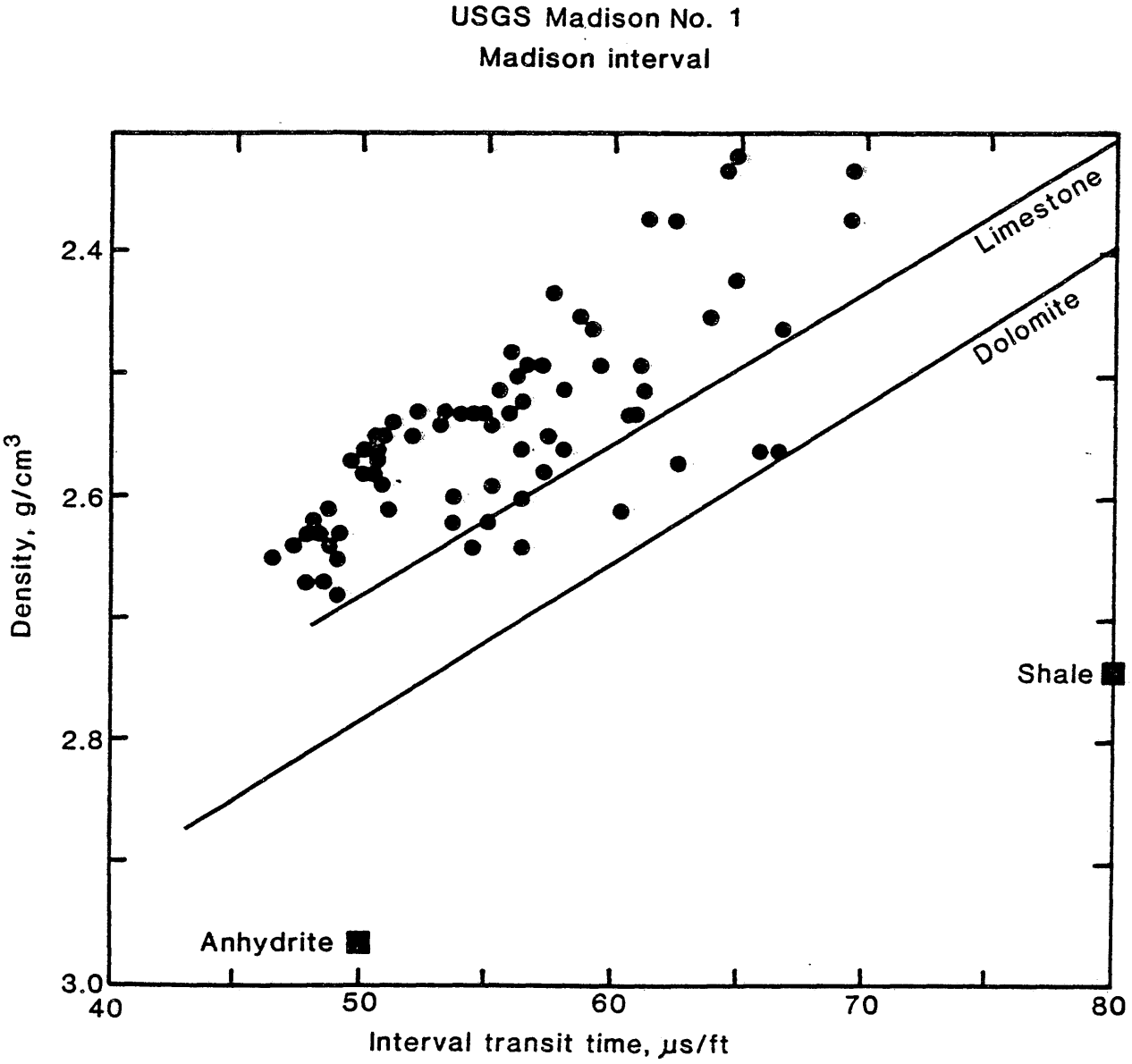

Figure 11. Relationship between density and interval transit time for the productive Madison interval of the USGS Madison No 1 well. The ideal response curves (solid lines) represent log values of distinct rock types for varying porosities (Schlumberger, 1979, p. 13).

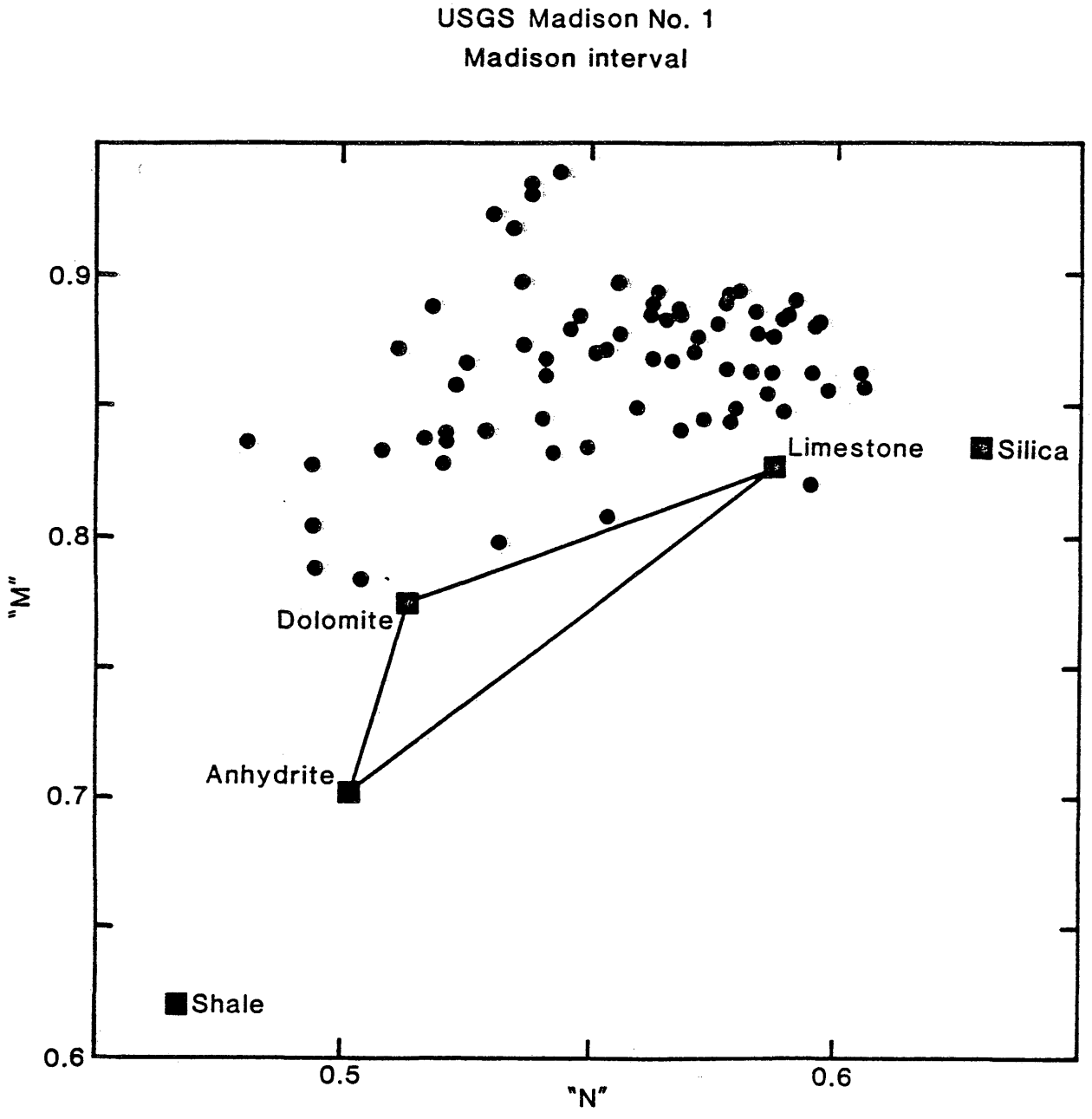

Figure 12. M versus N crossplot of the Madison interval from the productive USGS Madison No. 1 well. The variable "M" and "N" are defined in the text.

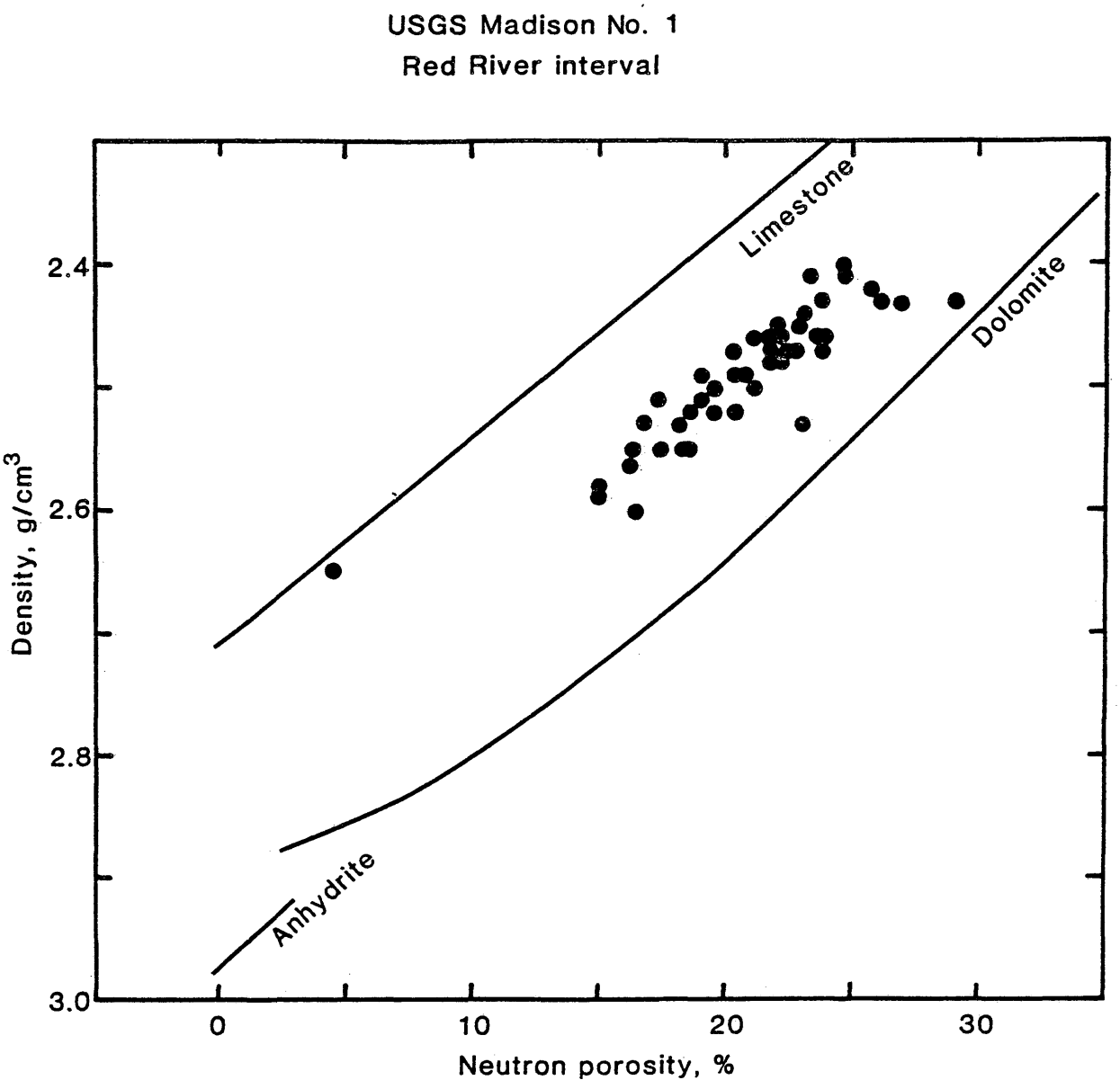

Figure 13. Relationship between density and porosity for the Red River Formation of the productive USGS Madison No. 1 well.

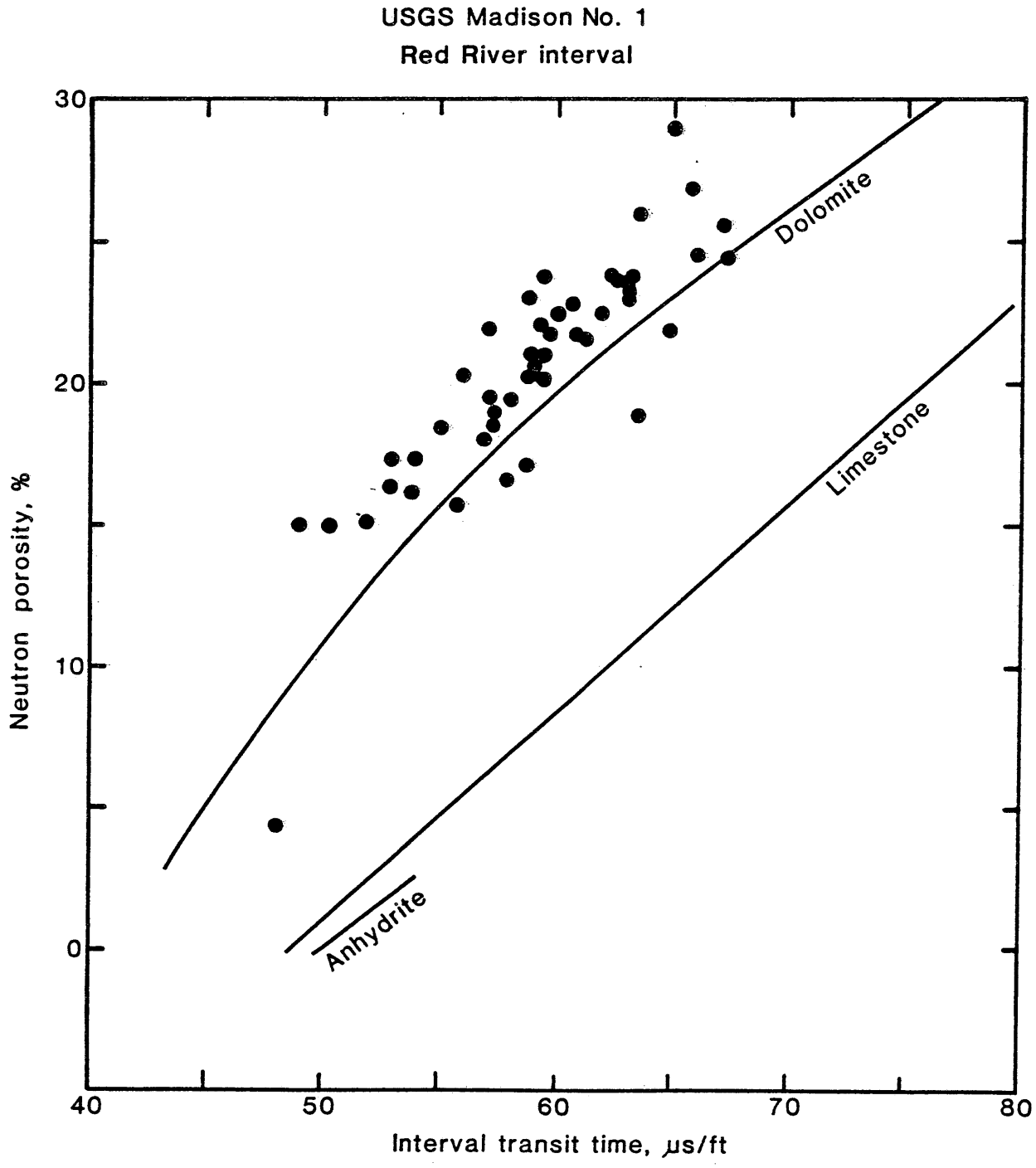

Figure 14. Relationship between porosity and interval transit time for the Red River Formation of the productive USGS Madison No. 1 well.

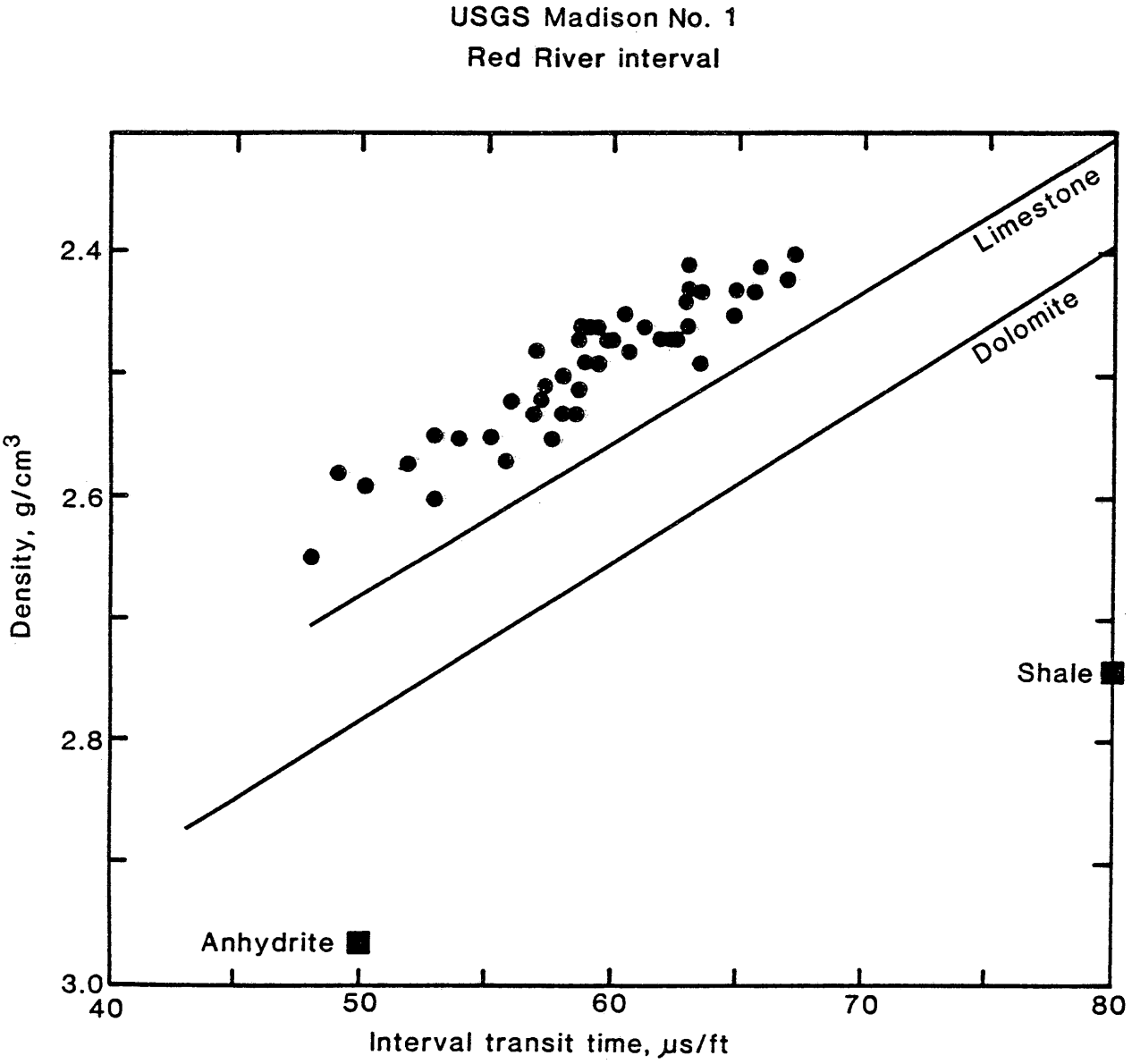

Figure 15. Relationship between density and interval transit time for the Red River Formation of the productive USGS Madison No. 1 well.

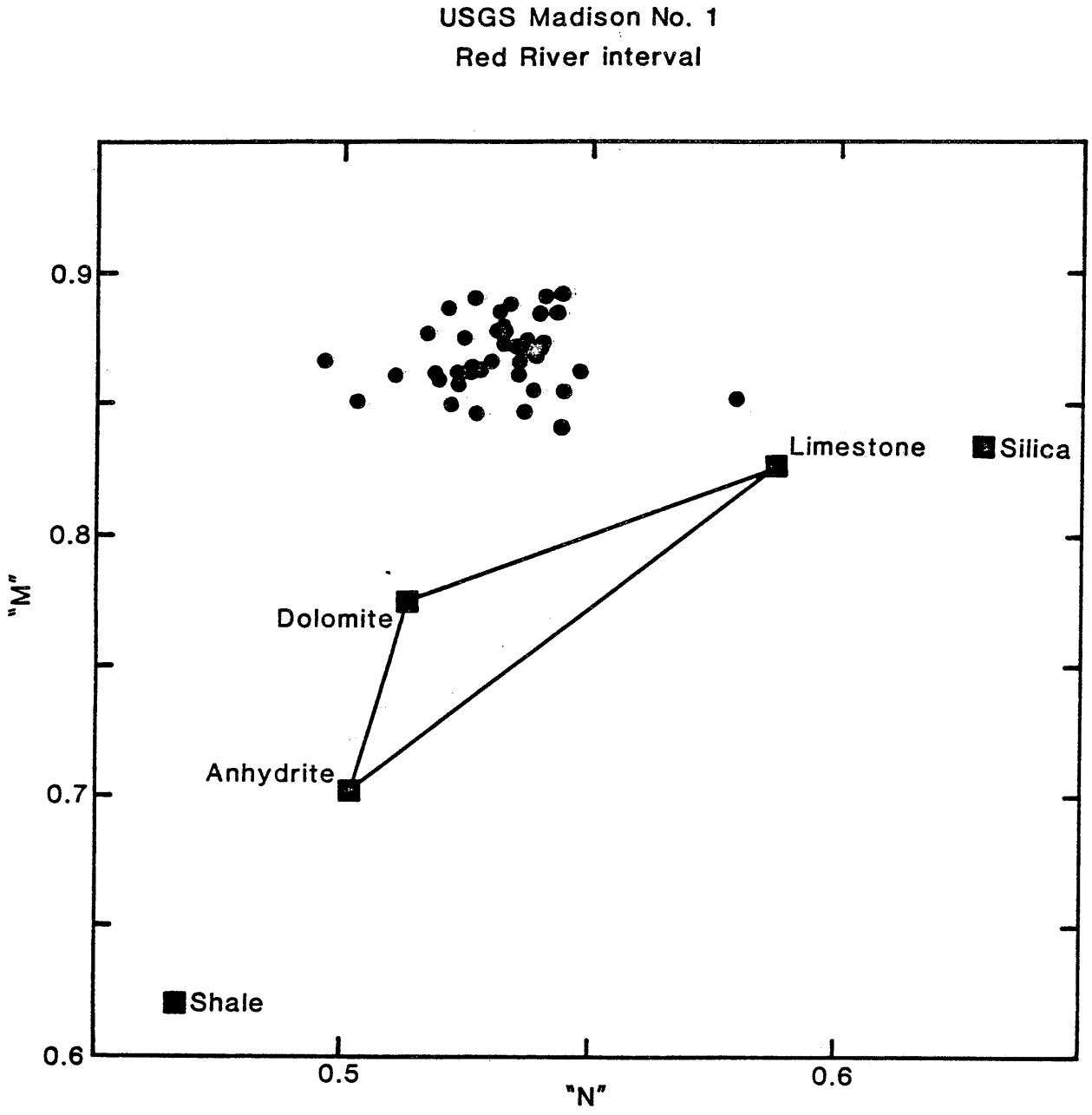

Figure 16. M versus N crossplot of the Red River interval from the productive USGS Madison No. 1 well.

USGS MADISON NO. 2 WELL

NON-PRODUCTIVE CASE

Madison Interval

The Madison Formation was divided into two sections because of the thickness of the unit at this well location. The break occurs at the approximate Mississippian - Devonian age boundary, in which the interval from 6,900 to 7,200 feet is called the upper Madison interval, and the interval from 7,200 to 7,400 feet is the lower Madison interval.

The crossplots of sonic travel time versus density, density versus neutron porosity, and sonic travel time versus neutron porosity (Figures 17, 18, and 19) all yield approximately the same interpretation of rock type and porosity distribution. This interval is composed primarily of a mixture of limestone and dolomite, with limestone being the dominant lithology. Some anhydrite is present in the interval, as indicated on all three crossplots by the points clustering around the pure anhydrite lithology line.

Most of the data points in the upper Madison interval cluster near the lower end of the porosity scale on the crossplots involving the neutron porosity log, Figures 18 and 19, indicating that the zone is tight. This observation was confirmed by the core samples recovered from the well.

According to Thayer (1981), the analysis of Madison cores showed that the limestone underwent early diagenetic cementation which filled interparticle pore spaces. As in the USGS Madison No. 1 well, the low porosity lithology is primarily limestone, and as the amount of dolomite increases, the average porosity increases.

A few points on the neutron porosity versus density, neutron porosity versus sonic travel time, and "M" versus "N" crossplots, fall in an area indicating gas effects. A small amount of gas was encountered in the well and detected by the gas chromatograph (Head, W.K., per. comm., 1978).

The velocities in the upper Madison interval do not have the linear relationship with porosity that was shown in the USGS Madison No. 1 case (see Figure 15), because of the apparent lack of porosity in the zone. As a result, the seismic reflection coefficient series would be expected to be more homogeneous, consisting of low values of reflection coefficients randomly distributed through the upper Madison interval. The only deviation from this distribution of reflection coefficients would come from the high density, high velocity anhydrite stringers. This interpretation is more closely evaluated over a range of seismic frequencies later in this thesis.

Crossplots of the lower Madison interval, Figures 21, 22, and 23, show fewer data points concentrating along the

limestone and anhydrite pure matrix lines, but generally the rocks still have low porosity values, much like that of the upper Madison interval. The slightly higher levels of dolomite in the lower Madison interval account for the higher average porosity values, ranging from 2 to 15 percent, but clustering around an average porosity of 15 percent, versus 4 to 5 percent for the upper Madison interval.

The "M" and "N" crossplot of the lower Madison interval (Fig. 24), also shows a majority of data values clustering between the pure dolomite point and pure limestone point, indicating a fairly even mixture of these two rock types. About a third of the data picked in this interval falls in the secondary porosity zone above the dolomite - limestone line, showing more of the porosity development in the lower part of the Madison Formation. The description of the cuttings from the well indicate that the zone contains a higher concentration of dolomite rock, some of it fractured with low to fair porosity development, and that the permeability is high enough to bleed water.

Red River Interval

Crossplots of the Red River interval in the USGS Madison No. 2 well, ranging from 8,100 to 8,560 feet below ground

surface, shows that there are rocks with low porosity clustering along the pure limestone line on the neutron porosity versus density crossplot (Fig. 25), and neutron porosity versus sonic travel time crossplot (Fig. 26). Data points that fall at the higher porosities are described as dolomite rocks in the well cutting descriptions, although on the crossplot most of the points fall between the pure limestone and pure dolomite lines.

The neutron porosity versus sonic travel time crossplot shows that the non-productive limestone rock has low interval transit time, or high velocity, and that as the porosity increases and the concentration of dolomite increases, the velocity decreases from 20,000 ft/sec to a range of 14,000 to 15,000 ft/sec, or a reduction of about 25 percent in velocity.

The neutron porosity versus density crossplot, Figure 25, shows the same relationship. The non-productive limestone rock clusters around 2.70 gm/cm^3, and decreases to 2.55 to 2.35 gm/cm^3 as the porosity and rock type change, representing a reduction in density of about 22 percent.

The "M" and "N" crossplot (Fig. 28) shows data points of this non-productive zone clustering around the limestone matrix point, and those points that plot at the higher porosity values are falling in the secondary porosity zone

above the limestone matrix - dolomite matrix line.

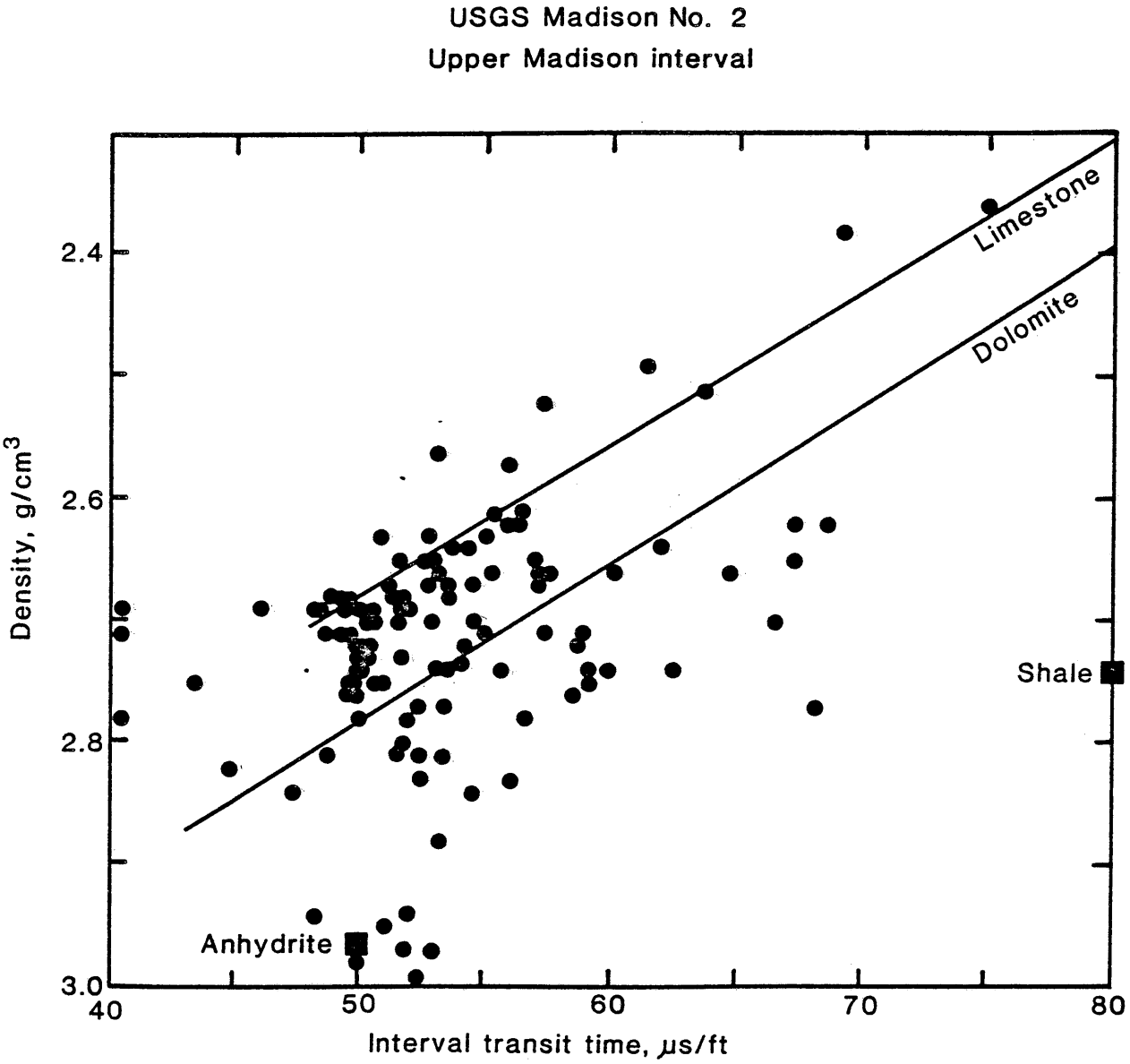

Figure 17. Relationship between density and interval transit time of the upper Madison interval from the non productive USGS Madison No. 2 well.

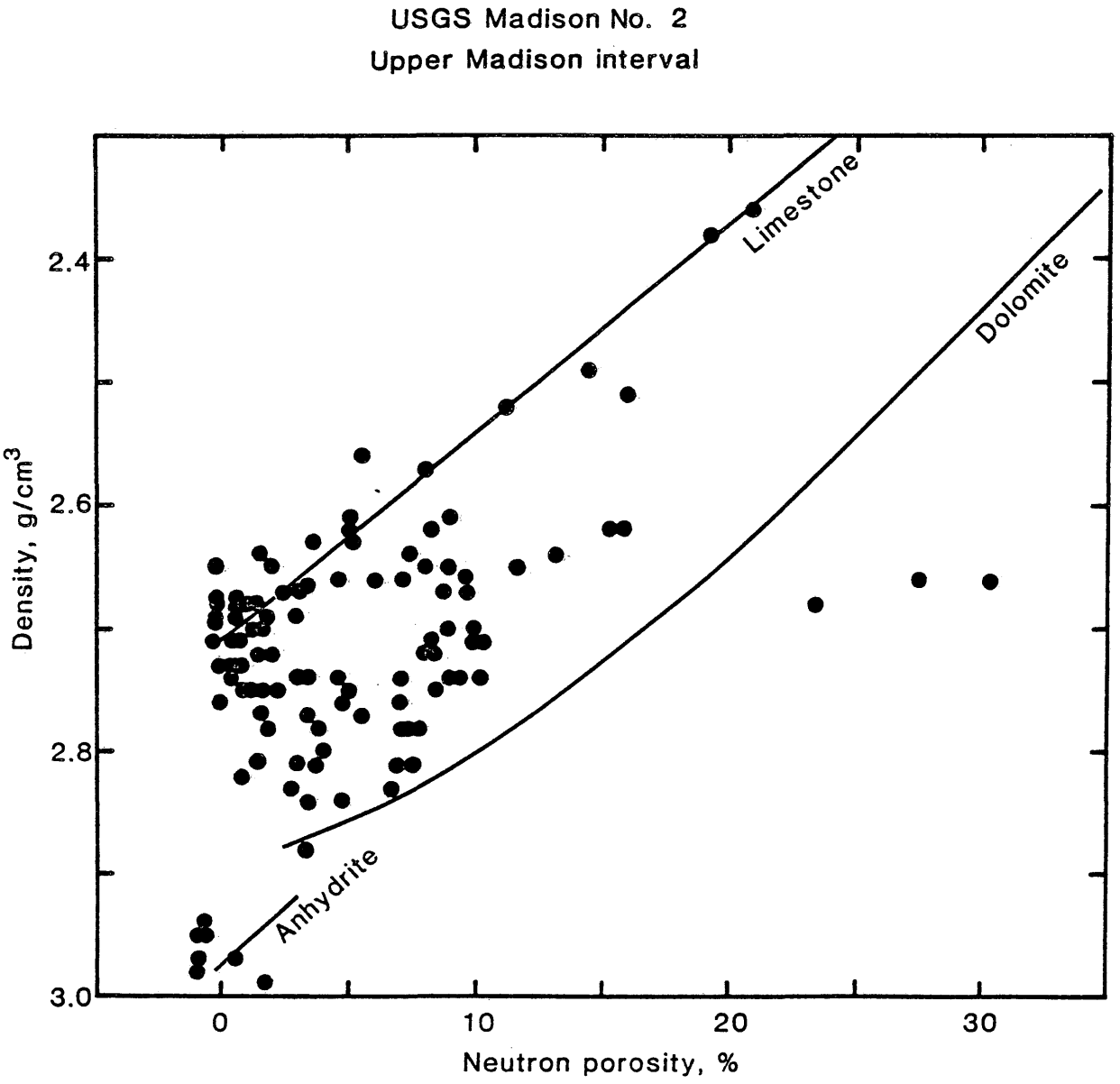

Figure 18. Relationship between density and neutron porosity of the upper Madison interval from the non productive USGS Madison No. 2 well.

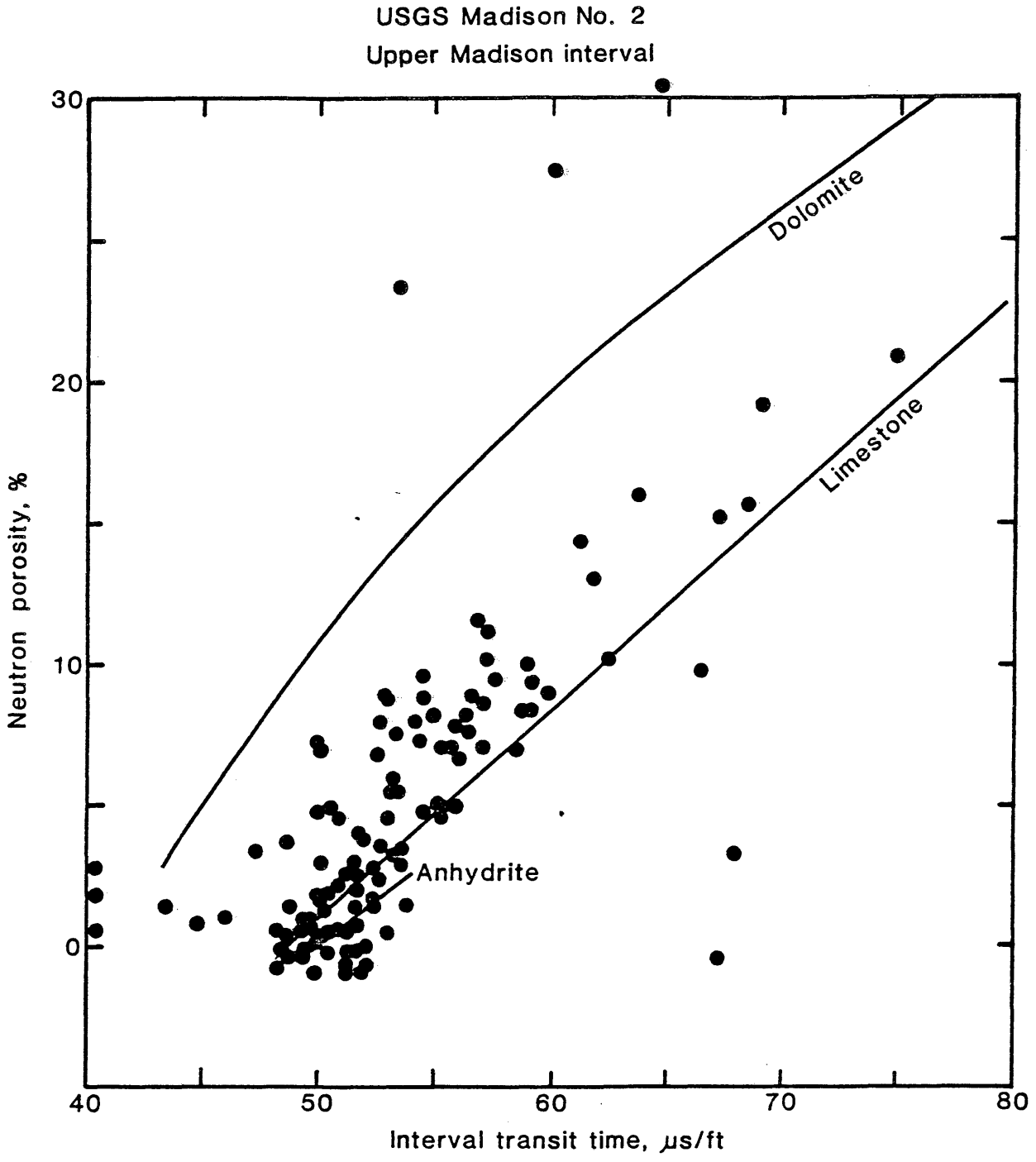

Figure 19. Relationship between porosity and interval transit time of the upper Madison Formation from the non productive USGS Madison No. 2 well.

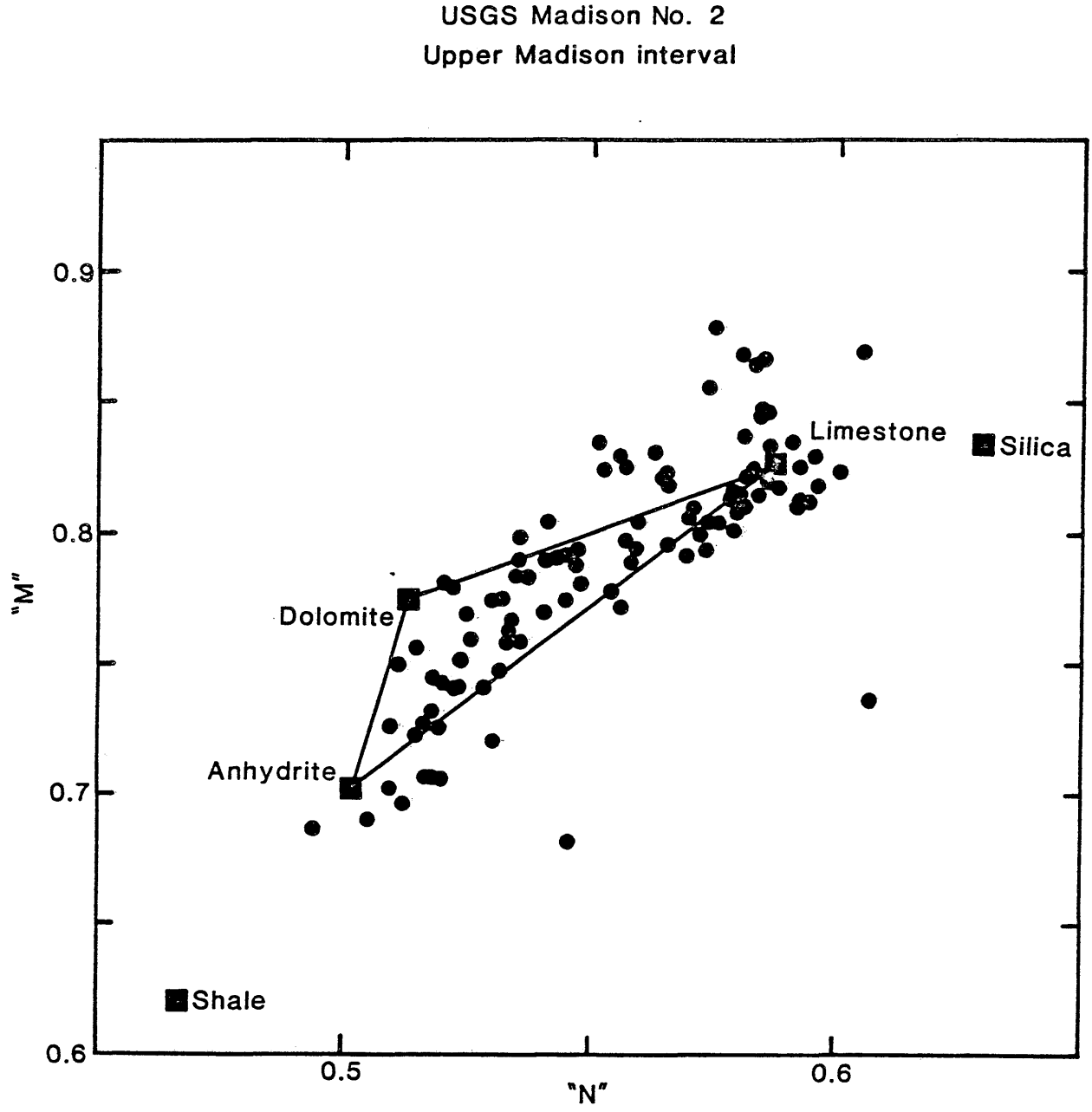

Figure 20. M and N crossplot of the upper Madison interval from the non-productive USGS Madison No. 2 well.

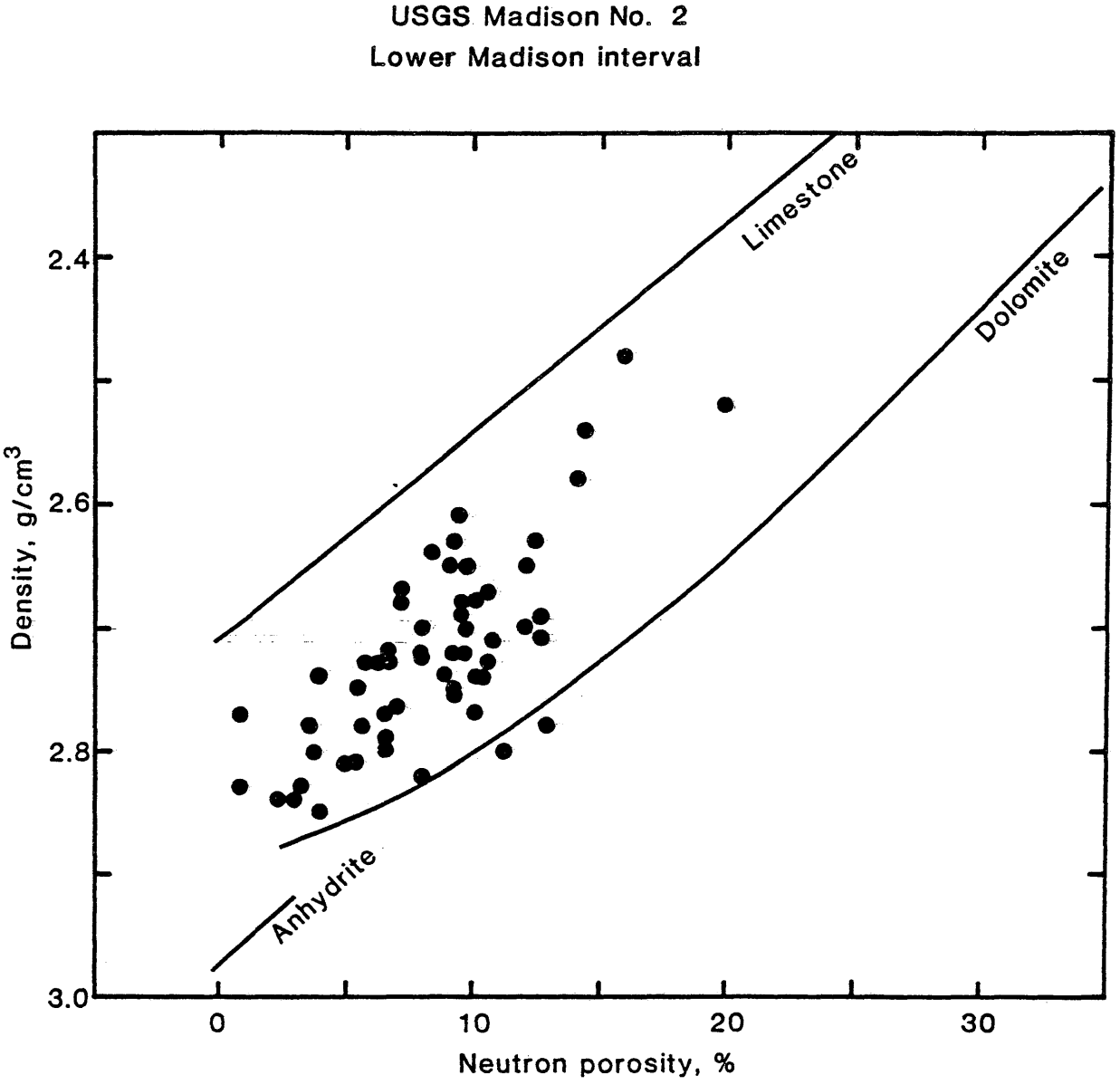

Figure 21. Relationship between density and neutron porosity of the lower Madison interval from the non productive USGS Madison No. 2 well.

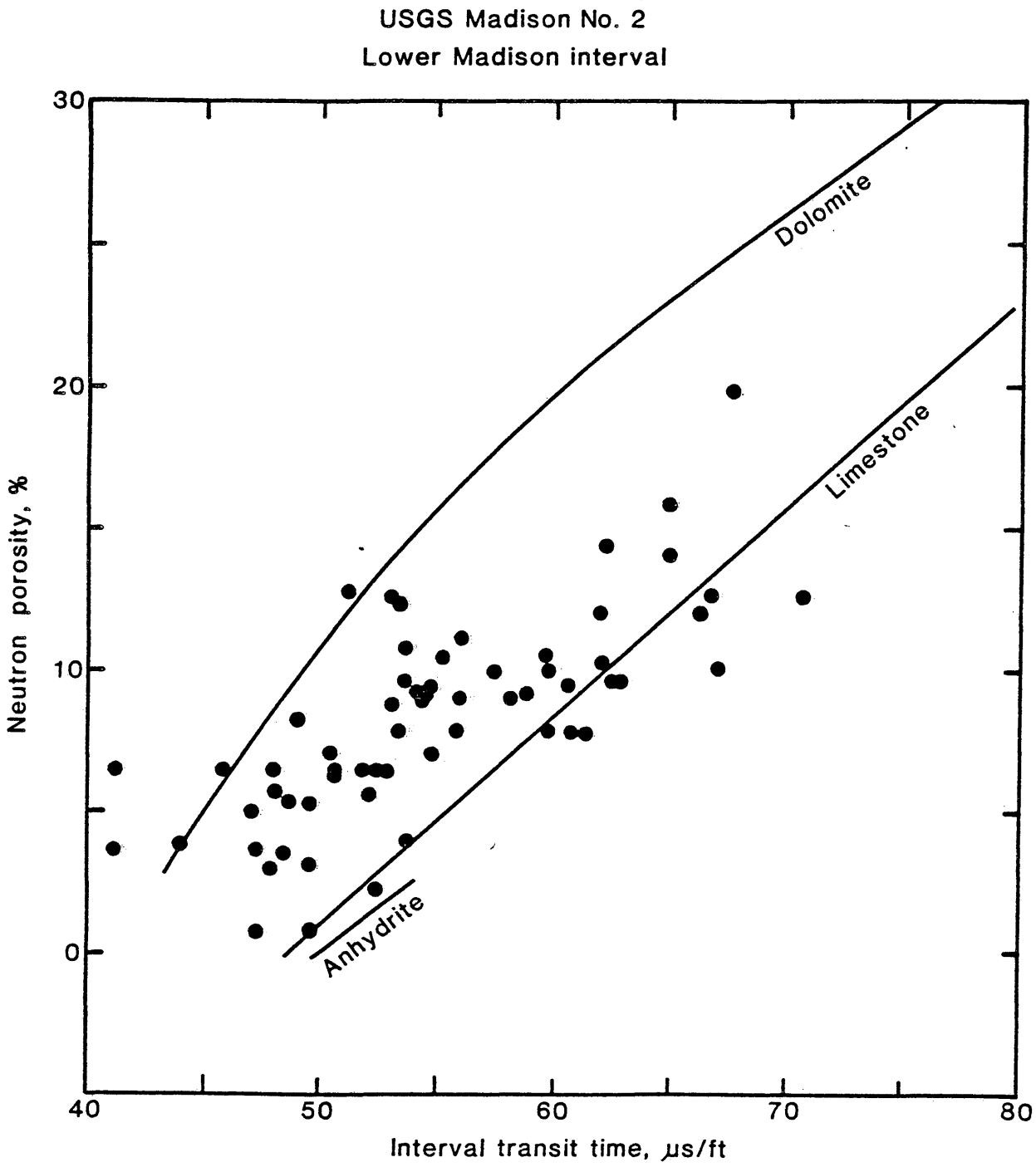

Figure 22. Relationship between porosity and interval transit time of the lower Madison Formation from the non productive USGS Madison No. 2 well.

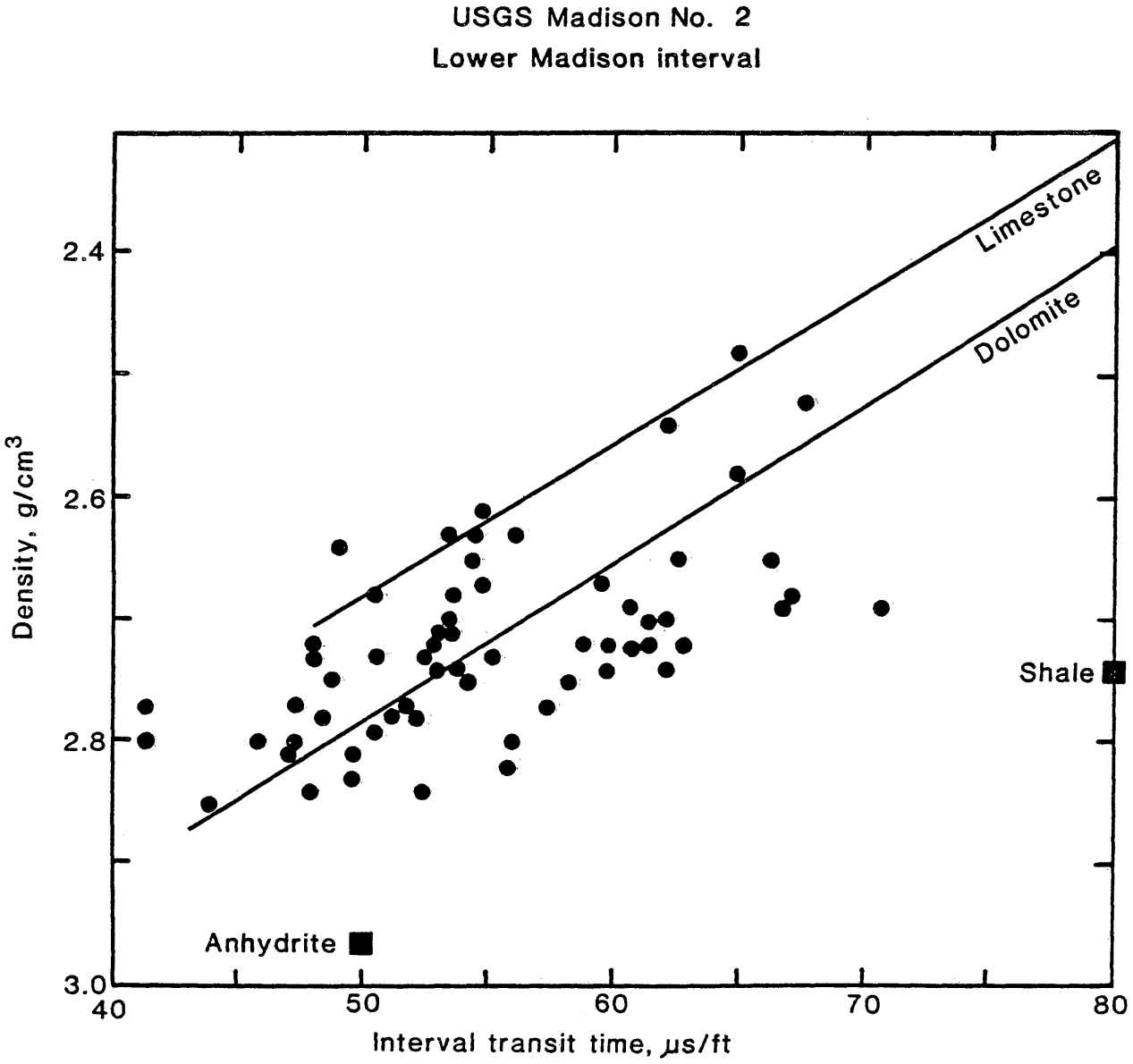

Figure 23. Relationship between density and interval transit time of the lower Madison interval from the non productive USGS Madison No. 2 well.

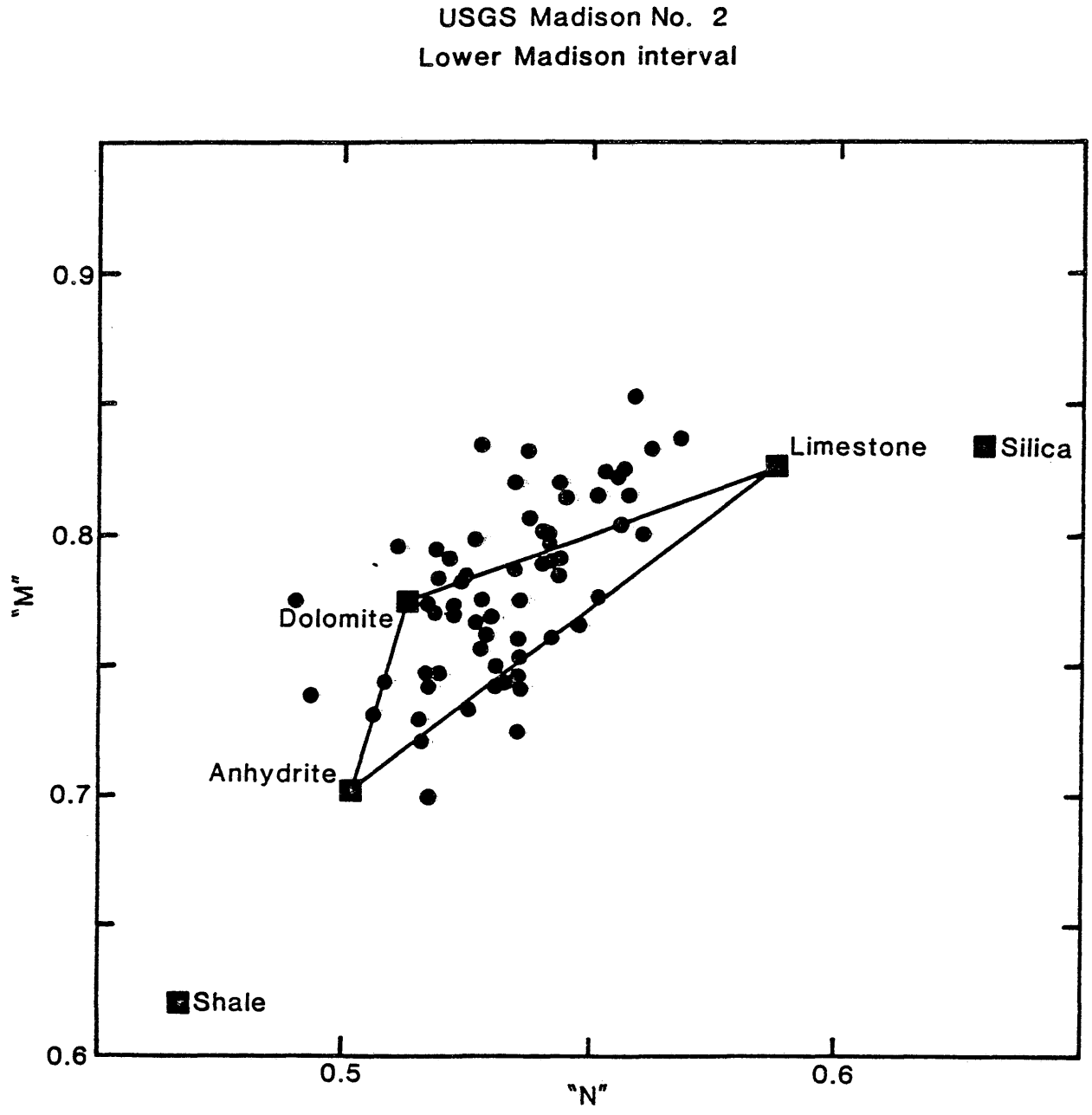

Figure 24. Relationship between M and N of the lower Madison interval from the non-productive USGS Madison No. 2 well.

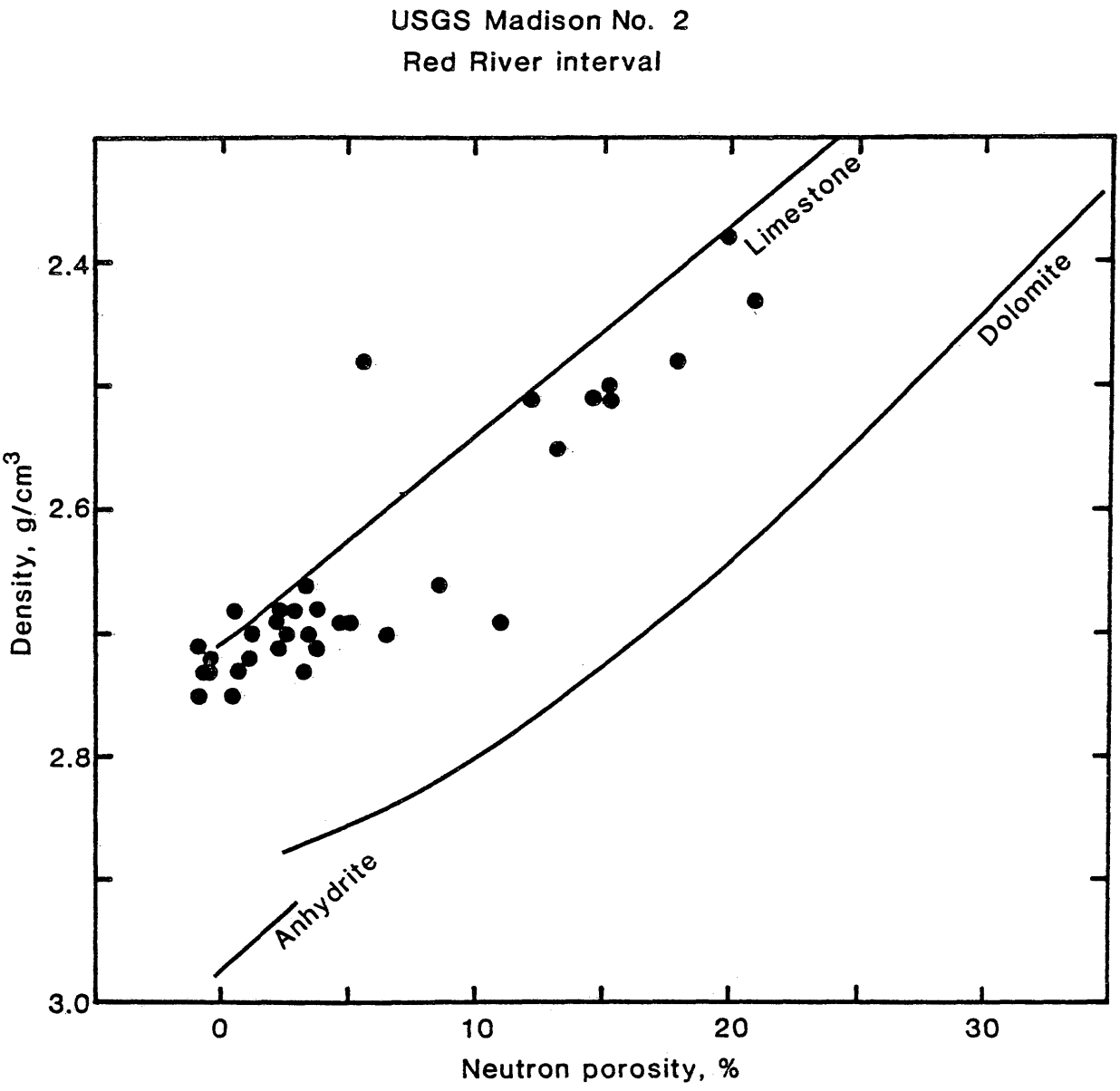

Figure 25. Relationship between density and neutron porosity of the Red River interval from the non-productive USGS Madison No. 2 well.

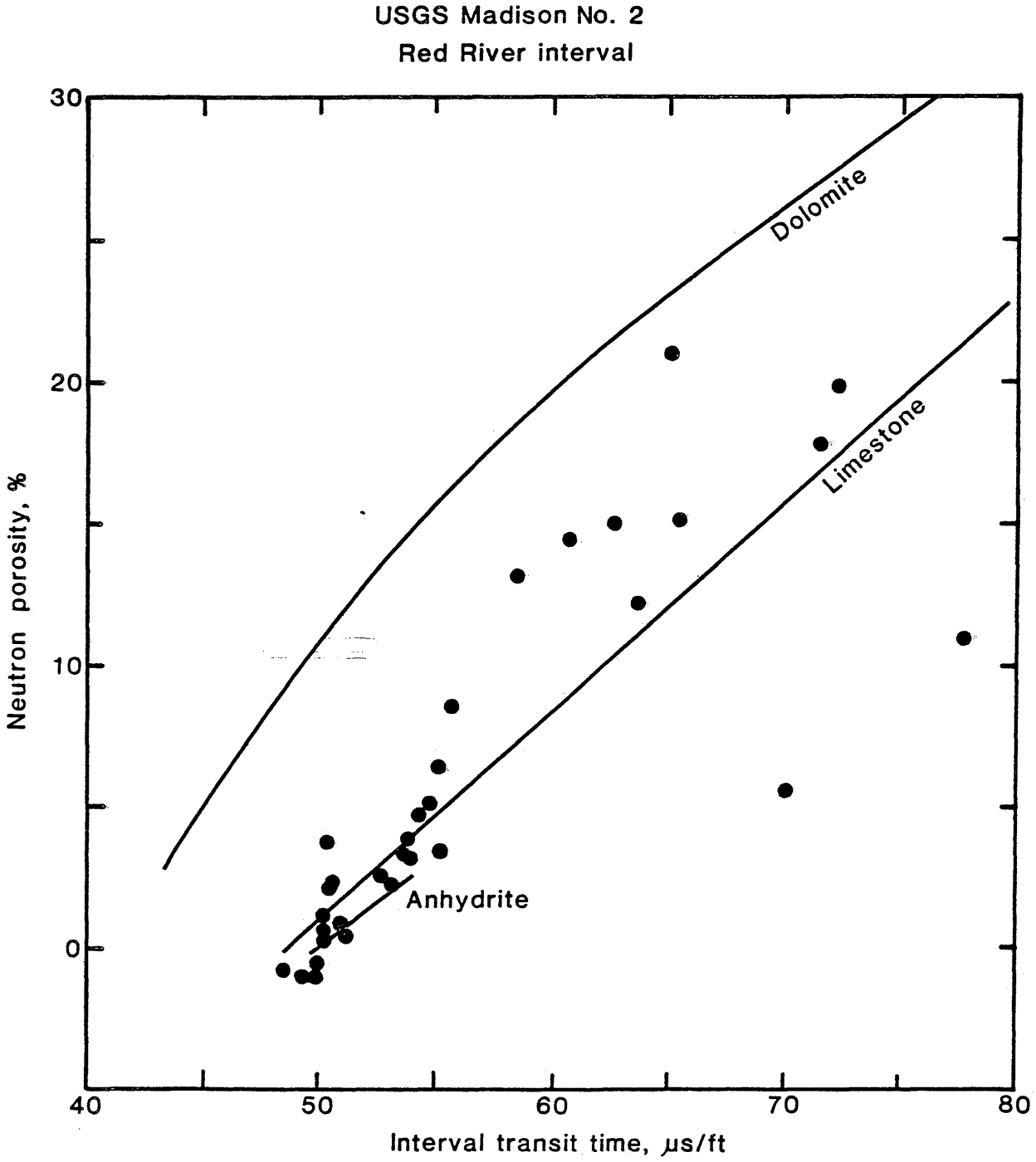

Figure 26. Relationship between neutron porosity and interval transit time of the Red River interval from the non productive USGS Madison No. 2 well.

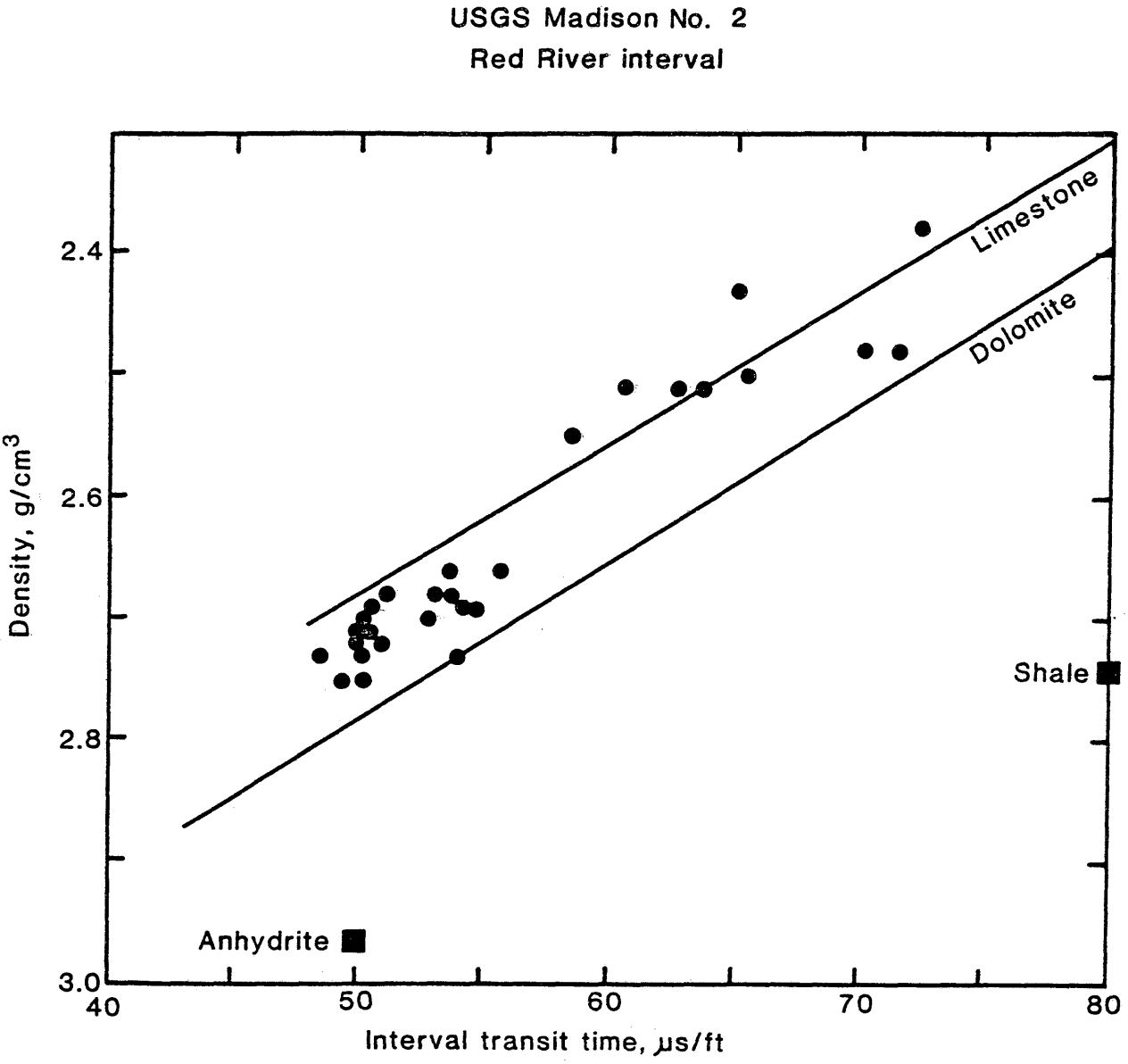

Figure 27. Relationship between density and interval transit time of the Red River interval from the non productive USGS Madison No. 2 well.

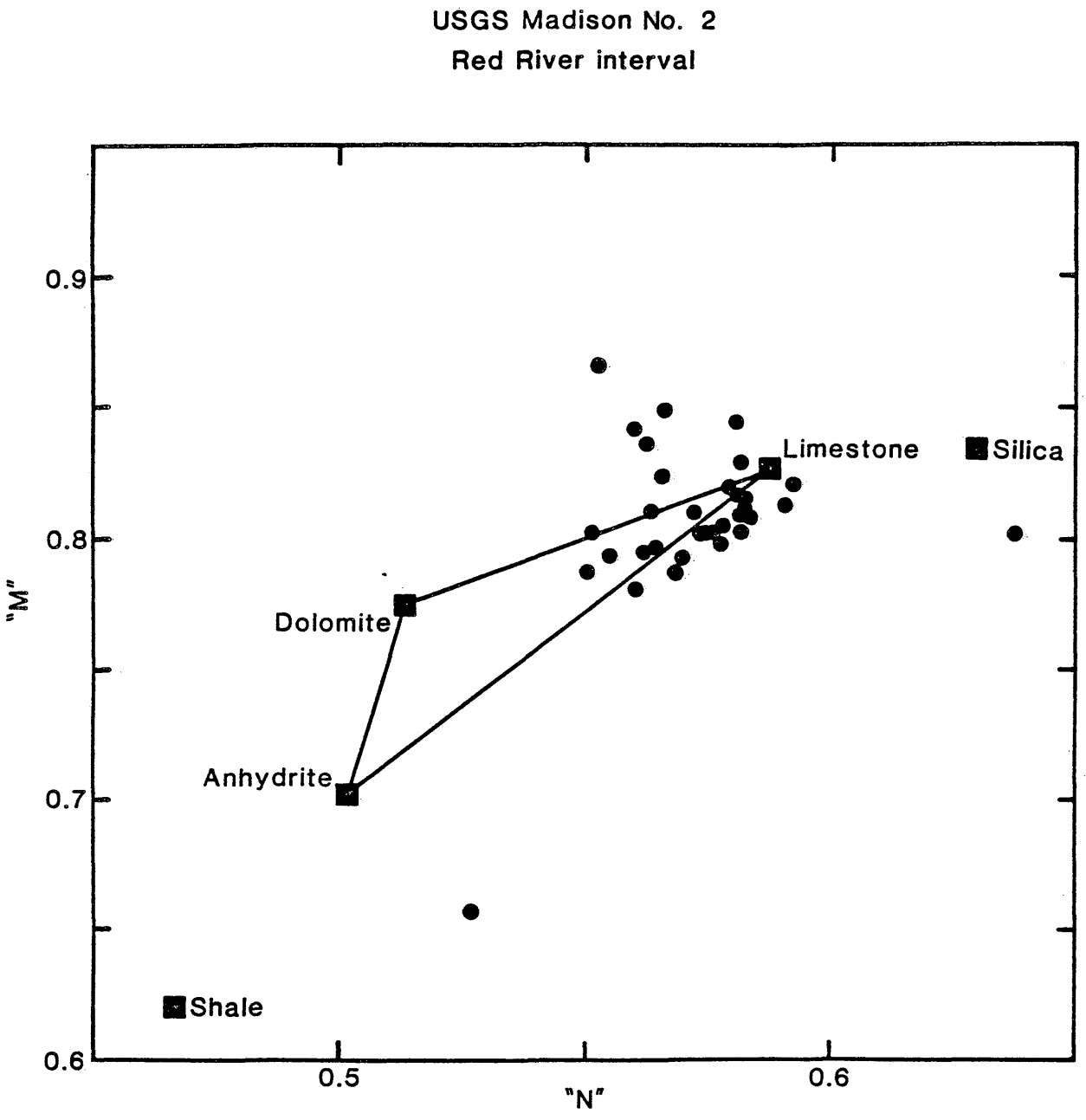

Figure 28. M and N crossplot of the Red River interval from the non-productive USGS Madison No. 2 well.

INTERPRETATION

General Trends

In the previous section, several crossplots were constructed using well log data from the water-producing USGS Madison No. 1 well, and the tight USGS Madison No. 2 well. The contrast of water production rates between the two wells is significant. Water flowed from the USGS Madison No. 1 well (from about 2,320 to 4,341 ft) at around 250 gal/min through a 2-inch valve, but if allowed to flow freely at the surface, it probably would have sustained a yield of 650 to 700 gal/min, which is considered to be a very good water well for the thickness of Madison and Red River rocks present (Blankennagel, and others, 1977). Water yield in the USGS Madison No. 2 well (about 50 gal/min under open-hole conditions), is considered to be poor, especially for the thickness of aquifer rocks present at this well location.

Because of the large contrast in water producing rates between the two wells, and the differences in porosity and permeability encountered, the rock types at these two locations probably are near the extreme geologic environments (tight, low porosity and permeabiity versus good porosity and permeability) of the Madison and Red River Formations. They should therefore provide information for determining an exploration criteria to detect high porosity

carbonate zones using seismic reflection techniques.

Figures 29 through 32 summarize the trends of porosity as a function of velocity and density that were evaluated on crossplots in the previous section on well log analysis. The plots summarize and contrast the distribution of the different rock types encountered in the two wells, and indicate where the seismic tool might have the best chance of discriminating between rock types. Figure 29 shows the distribution of sonic travel time with porosity for the Madison interval for both wells. Likewise, Figure 31 and 32 show the sonic travel time and density distribution respectively for the Red River interval in both wells.

Rocks in the lower part of the Madison Formation in the USGS Madison No. 2 well have nearly the same distribution of sonic travel time values as the Madison rocks in the USGS Madison No. 1 well. Consequently velocity information alone would not be a good exploration parameter to indicate porosity zones in the Madison carbonate facies. However, the density versus porosity plot (Fig. 30) shows the lower Madison rocks in the non-productive USGS Madison No. 2 well clustering at higher densities than rocks in the productive USGS Madison No. 1 well. Therefore the acoustic impedance contrast, which is the product of density and velocity, is slightly lower for porous rocks, and may be used as an indicator of porous carbonate rocks. In this case the

impedance is about 5 percent lower for porous Madison rocks than for tighter Madison rocks.

The Red River Formation distribution plots are generally similar for velocity and density, although the clusters are tighter, which suggests a more homogeneous rock matrix. As in the Madison interval, the densities of the rocks in the interval provide a distinction using acoustic impedance to be made between porous and tight facies of about 6 percent.

Based on these crossplots it would seem that there is some chance of discriminating high porosity, water-producing carbonate facies from tight, low porosity carbonate facies because the acoustic properties of these rock types are slightly different, due chiefly to rock densities. However, simply quantifying the lithologic properties of the beds in terms of acoustic impedance is just part of the exploration solution. What the crossplots do not show is the vertical distribution of the different rock types, and how this vertical arrangement of changing velocity and density zones controls the pattern of reflectivity spikes, which controls the amplitudes of the bandlimited seismic traces. The seismic response is sensitive to stratigraphic layering as well as acoustic impedance, and therefore the entire interval should be evaluated for its seismic patterns as well as specific bed boundaries.

Figures 33 and 34 show the vertical distribution of acoustic impedance as a function of depth for the two wells. Points are identified by their porosity ranges into three zones of 0 to 10 percent, 10 to 20 percent, and greater than 20 percent. The plots show that acoustic impedance is a good discriminator of porosity, and that the productive USGS Madison No. 1 well has more points falling at higher porosity values than the non-productive USGS Madison No. 2 well. Unfortunately the plots still do not relate to the shape of the seismic signal that will occur at seismic field frequencies.

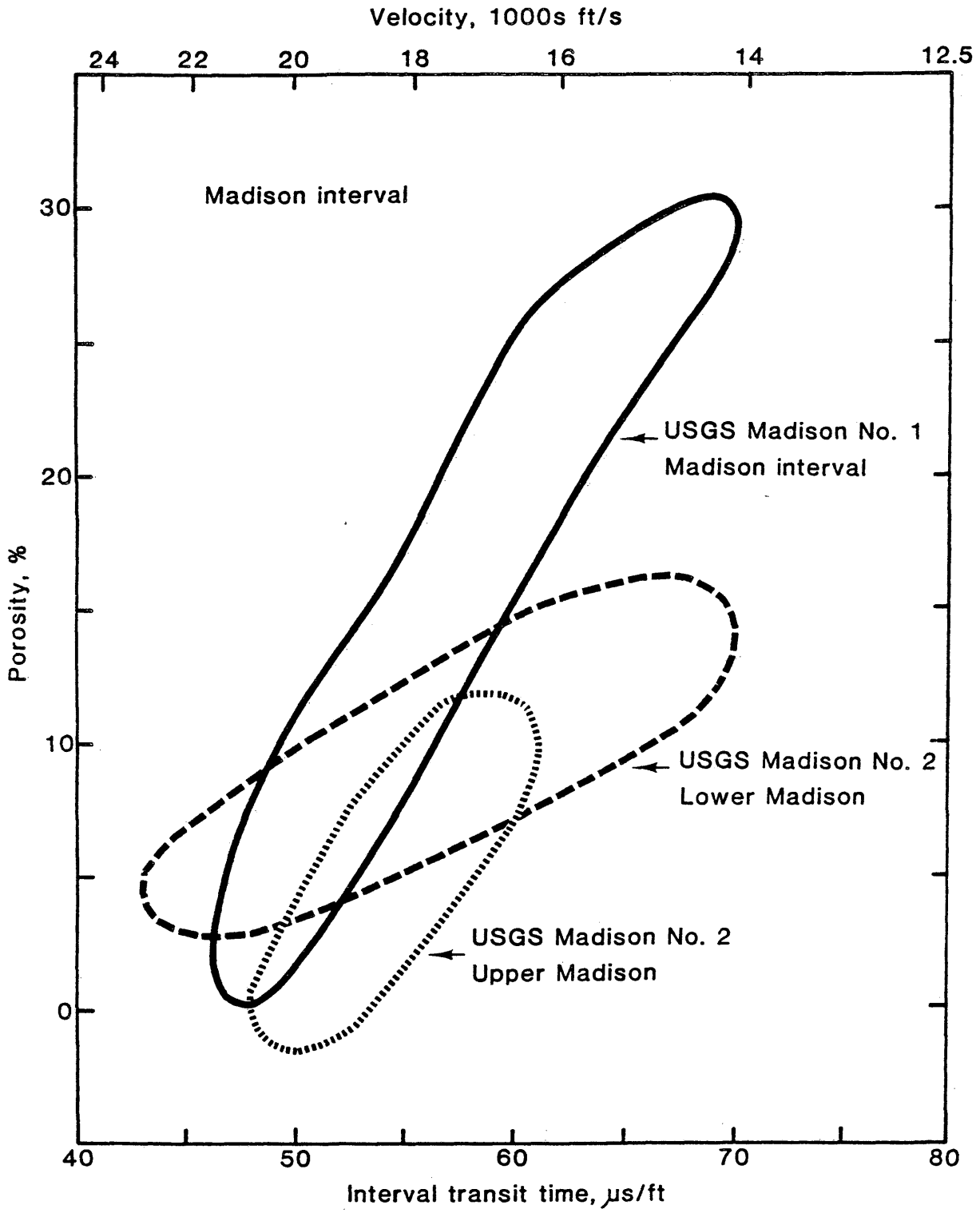

Figure 29. Crossplot of porosity and interval-transit-time values for the Madison interval showing the general outline of data clusters between the productive USGS Madison No. 1 well (solid lines), and the non-productive USGS Madison No. 2 well (dashed lines).

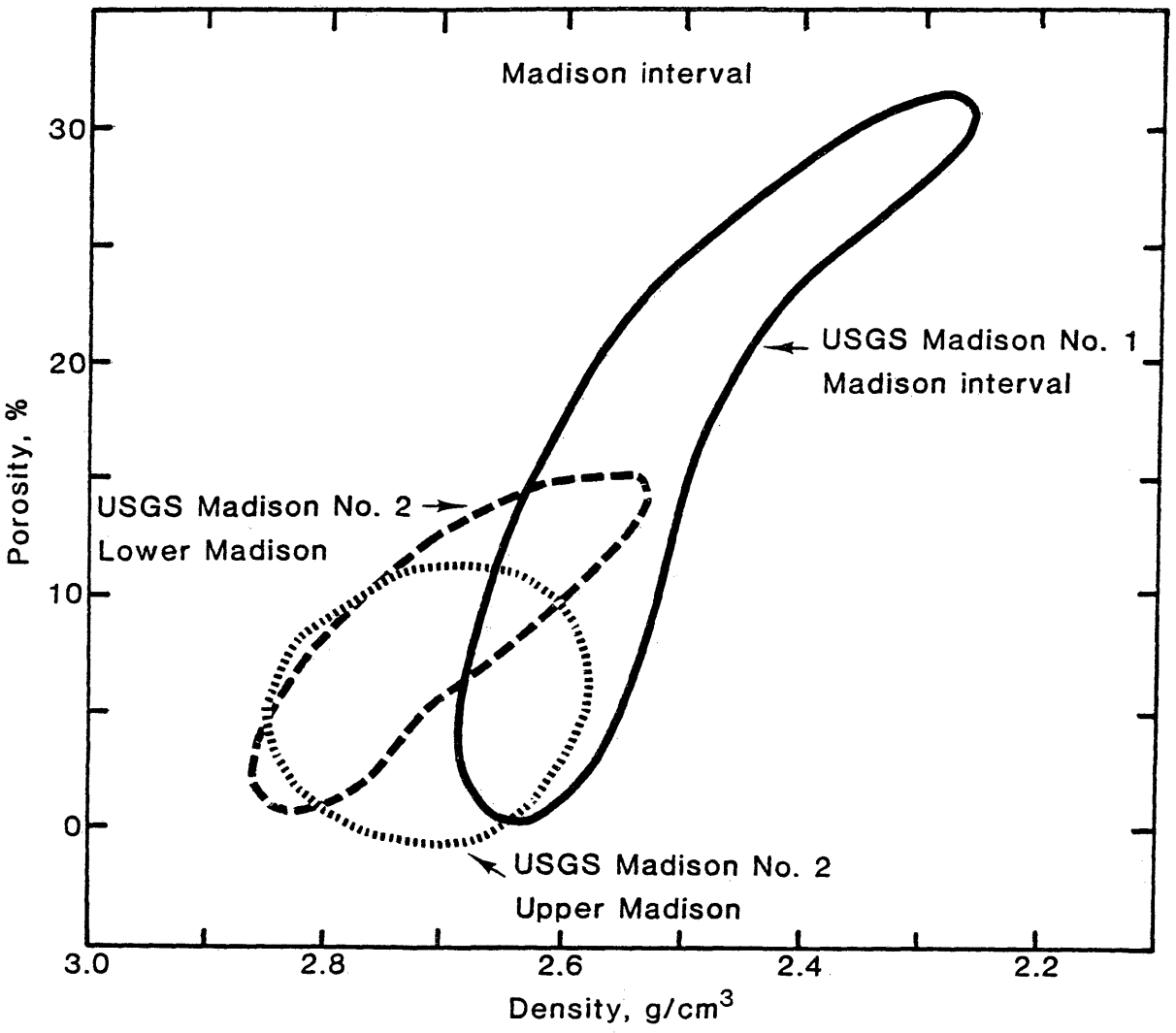

Figure 30. Crossplot of porosity and density values for the Madison interval showing the general outline of data clusters for the productive USGS Madison No. 1 well (solid line), and the non-productive USGS Madison No. 2 well (dashed lines).

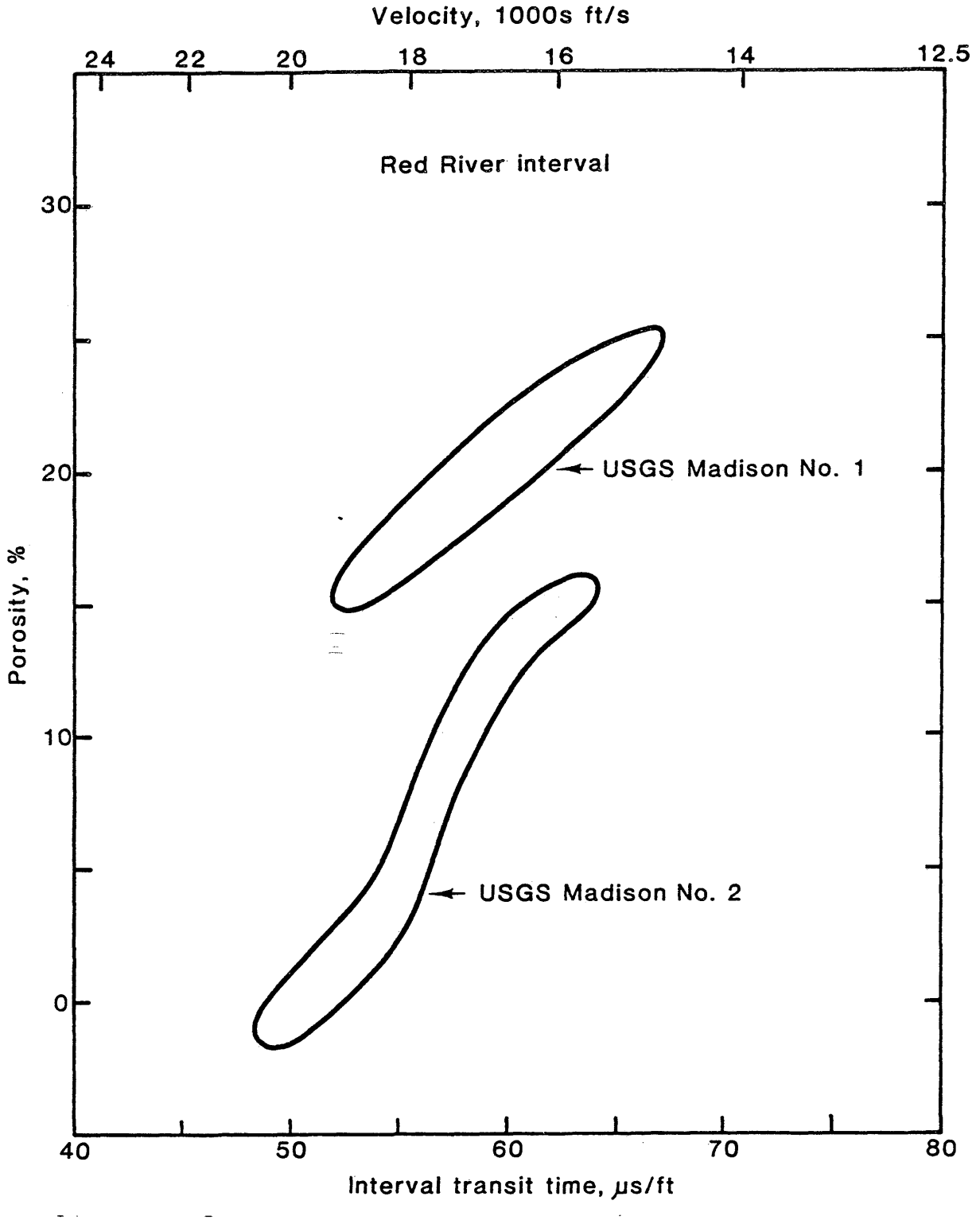

Figure 31. Crossplot of porosity and interval-transit-time values for the Red River interval showing the general outline of data clusters between the productive USGS Madison No. 1 well and the non-productive USGS Madison No. 2 well.

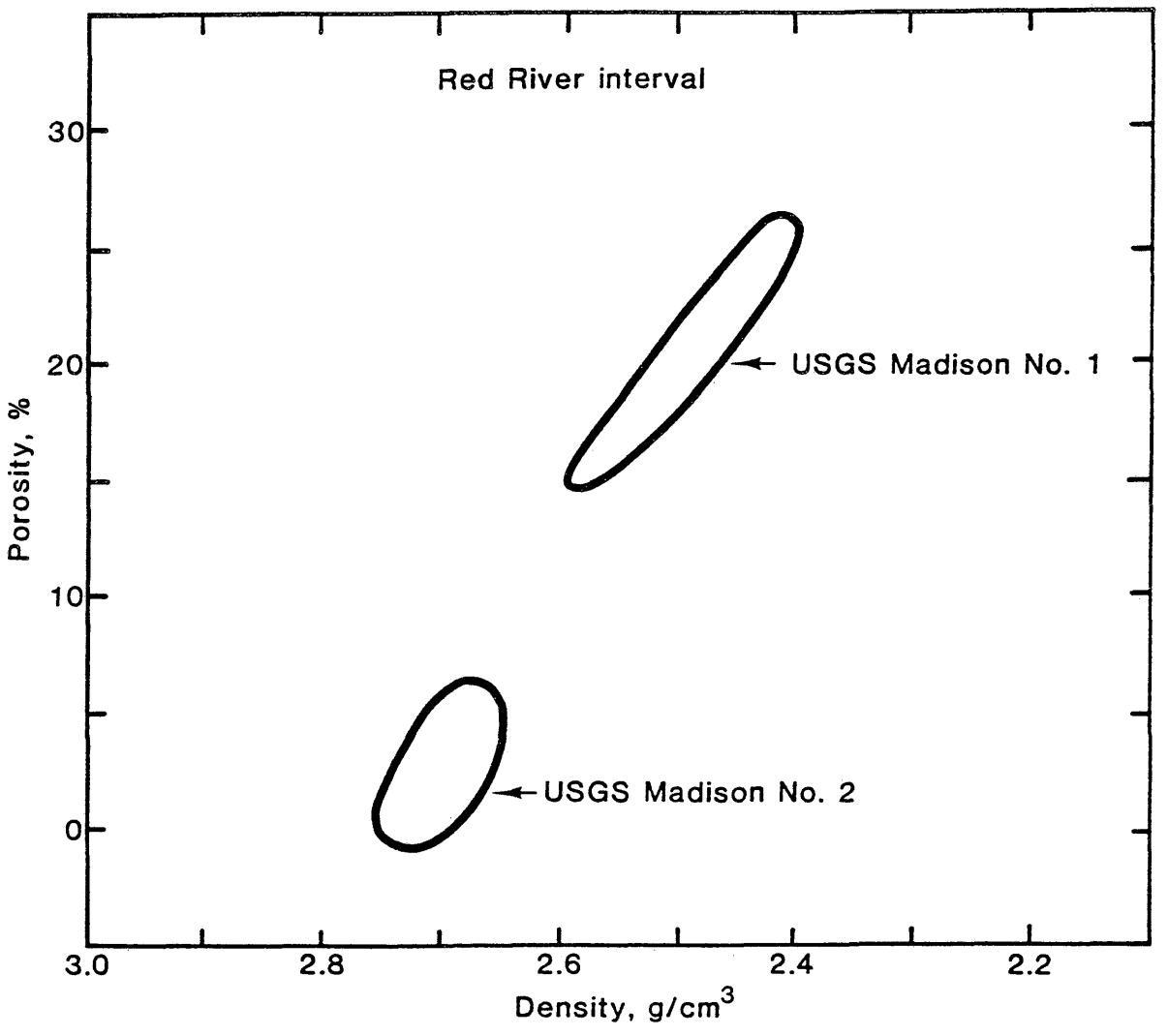

Figure 32. Crossplot of porosity and density values for the Red River interval showing the general outline of data clusters for the productive USGS Madison No. 1 well and the non-productive USGS Madison No. 2 well.

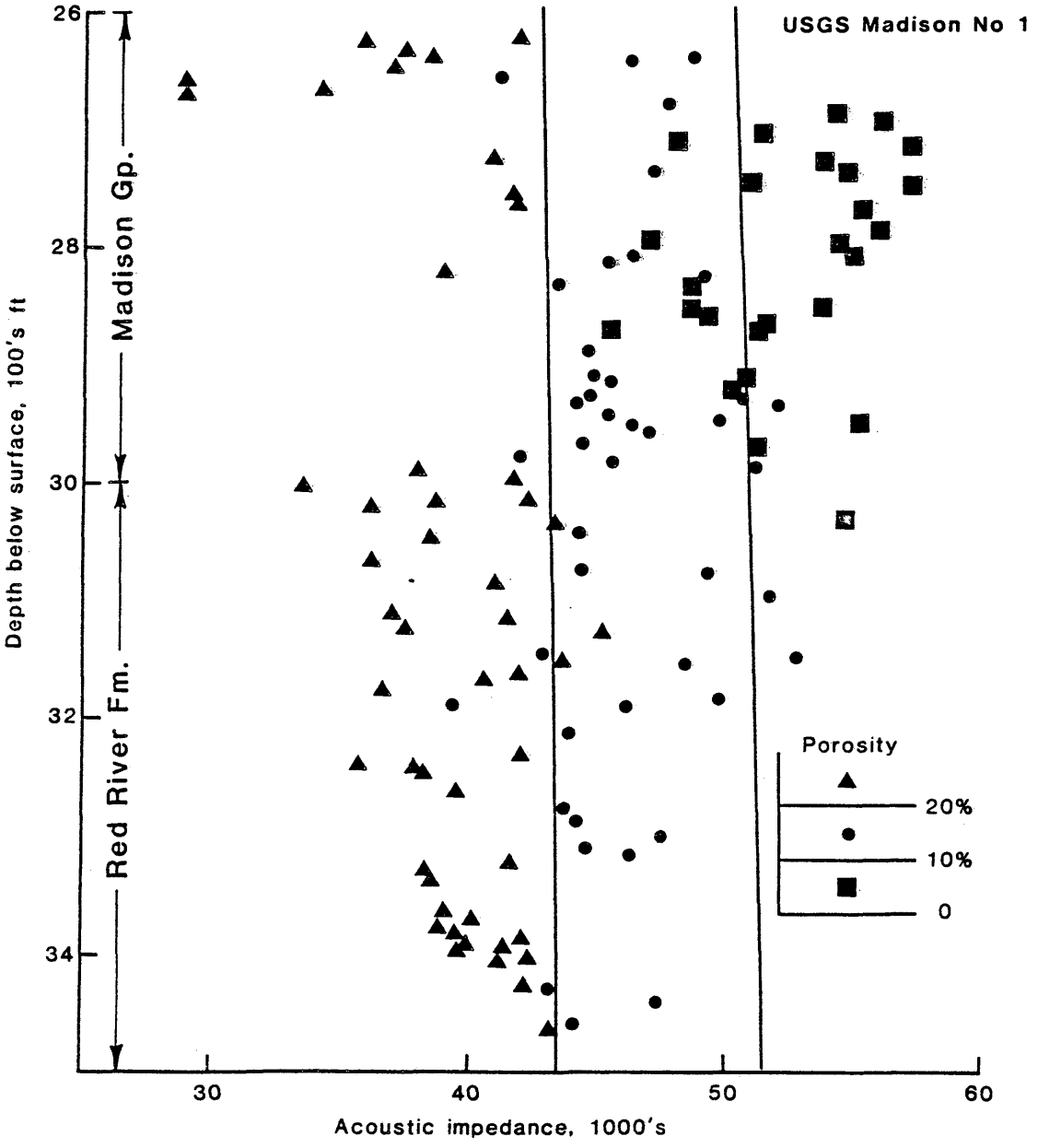

Figure 33. Acoustic impedance of rocks classified into three porosity ranges versus depth from the non-productive USGS Madison No. 1 well. The vertical line roughly divide the data points into two main classes of porosity.

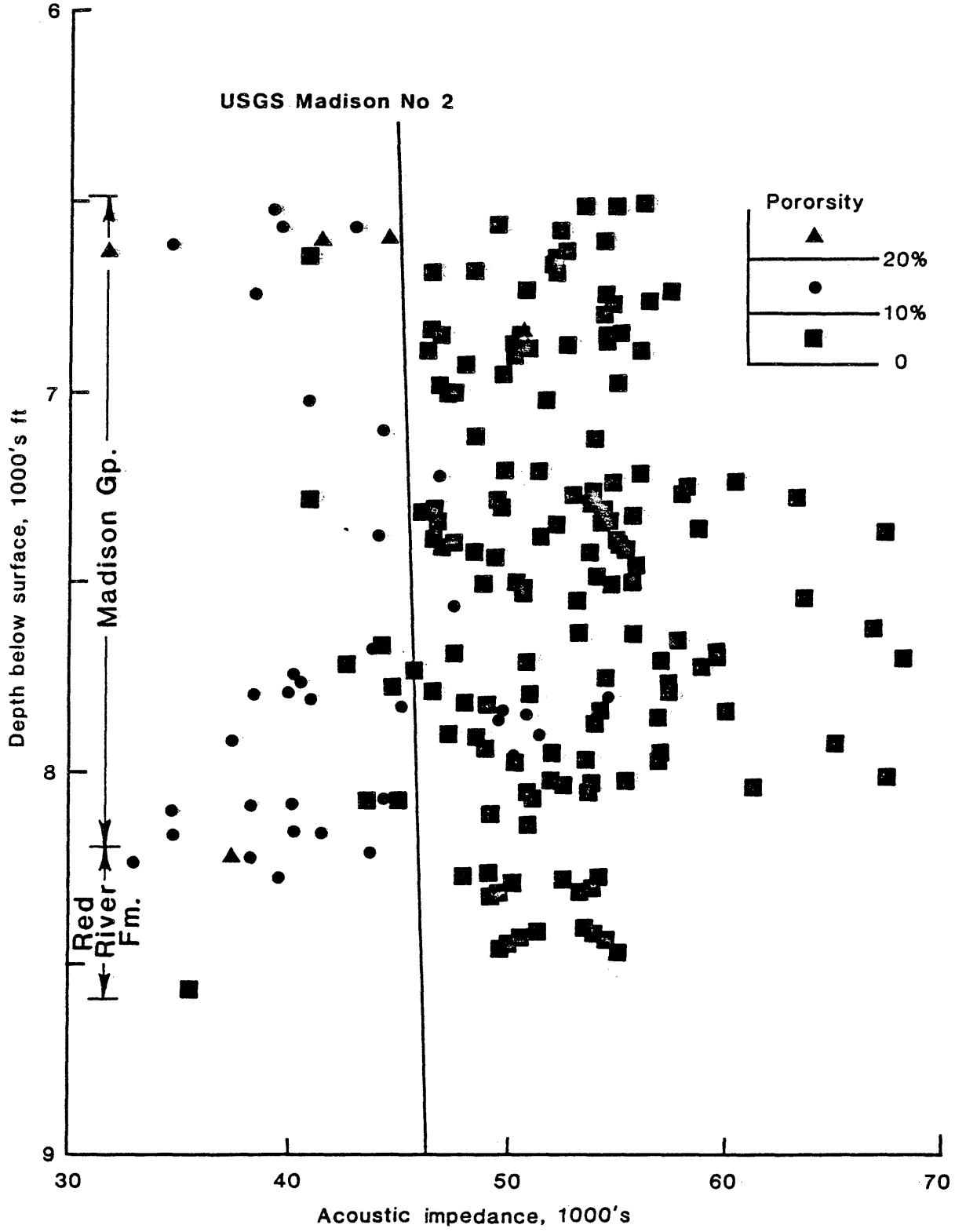

Figure 34. Acoustic impedance of rocks classified into three porosity ranges versus depth from the productive USGS Madison No. 2 well. The vertical lines roughly show the three porosity zones.

Relationship Between Porosity and Permeability

The previous sections have discussed the vertical distribution of porosity with the Madison and Red River Formations, and the relationship of porosity to velocity and density, which are the two main physical properties of a rock that directly affect the reflection characteristics of seismic reflection signals. While high porosity development is definitely an important characteristic for a reservoir rock to have, its identification alone will not guarantee that a rock will provie high water yields. Permeability of a carbonate rock plays an important role in the quality and productive capabilities of the reservoir.

Fortunately there were cores taken from the two test wells, with permeability and porosity measurements taken and reported in USGS Open File Reports 77-164 and 81-221. Figures 35 and 36 shows the crossplot of permeability with porosity for the different rock types identified within the Madison Formation. The mean porosity value for this data set is 8.4 percent, and the mean permeability is 15.8 md. The crossplot shows the large standard deviations for both porosity and permeability, which is common in most carbonate formations.

The limestones of the Madison have generally low values of porosity and permeability, which generally agreeing

with results of the crossplot analysis developed in the previous section of this thesis. According to Thayer (1981), the main reason for these low values of porosity and permeability in the Madison limestone is that early diagenetic cementation occured, and in most cases filled interparticle pore spaces.

Contrasted to the limestones are the dolomites, which have the higher porosities and permeabilities in the two wells. Although there is scatter in the crossplot, a rough positive correlation between porosity and permeability can be identified. According to the crossplot, the medium crystalline dolomites have the highest values of porosity and permeability, followed by finely crystalline dolomites. Dolomites have higher average porosities and permeabilities than limestones because of differences in crystal size, shape, and arrangment. Wardlow (1979) notes that at equivalent porosities, dolomites have higher average permeabilities than limestones.

One of the more interesting aspects of the crossplot is that there are a few data points with low porosity and moderately high permeability values. Analysis of the cores by the USGS (Thayer, 1981) shows these samples having fracture porosity. On the other hand, there are data samples with high porosity and low permeability values which have vuggy porosity with the pores not connected.

Because of these circumstances, the detection of porosity in the Madison with the seismic reflection tool would include the following limitations. If seismic data were to establish a zone of high porosity, it is possible that the permeability would be too low for adequate volumes of water to be produced. In the low porosity case, it is possible that there is sufficient permeability created through fracturing to provide adequate water flow rates. In either case the seismic data can only provide, at best, a partial interpretation of the water-producing qualities of an aquifer.

In some localities of the study area, tectonic fracturing of the Madison and Red River rocks has undoubtely enhanced their water productivity. However the degree to which fracturing contributes to production is extremenly difficult to document. An adquate interpretation of fracture controlled porosity and permeability requires complex well testing, coring, and pump tests (Blankennagel and others, 1977). Because the data shows a general positive correlation between porosity and permeability for the Madison Formation, the detection of porosity through the use of seismic methods can be an effective exploration tool.

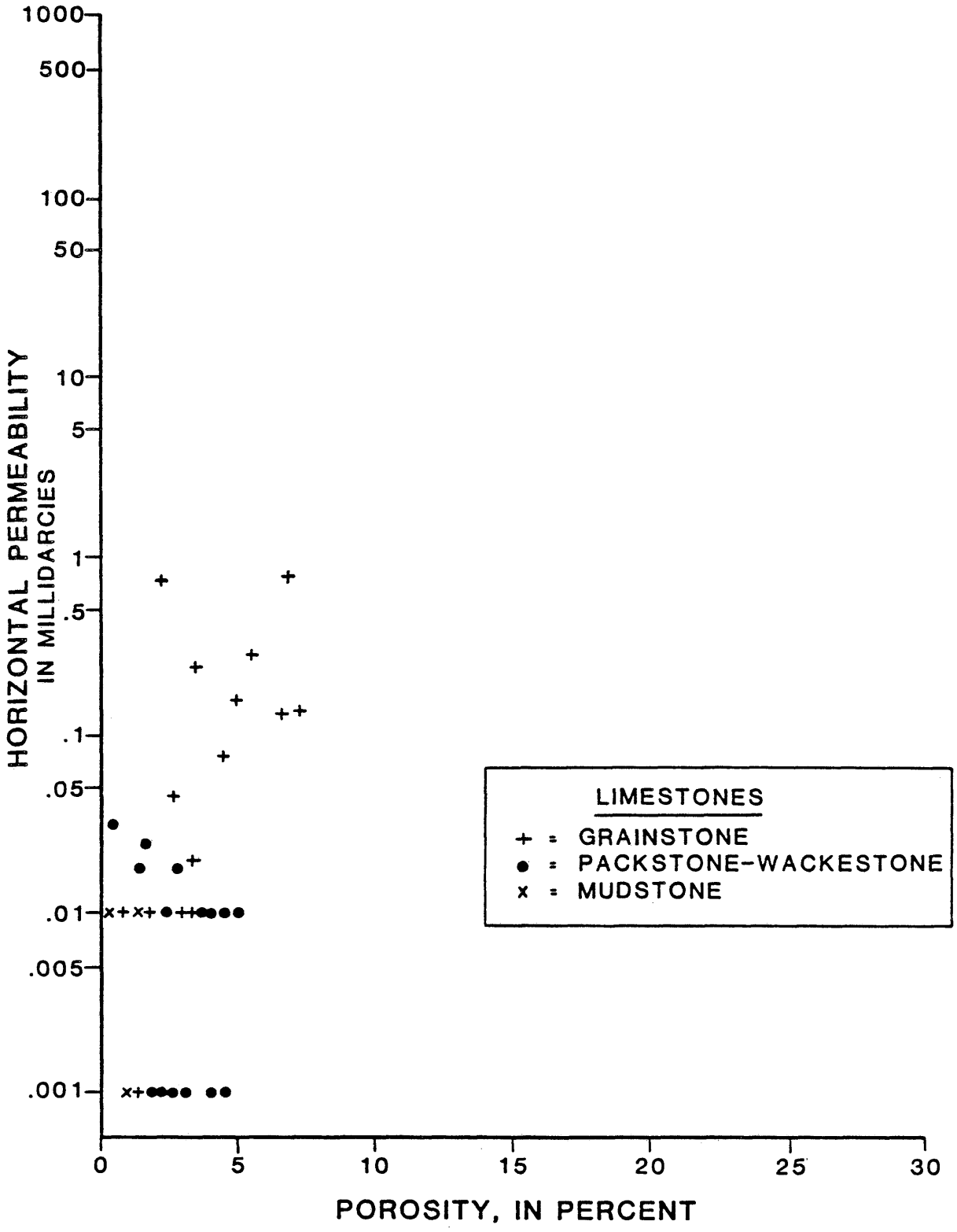

Figure 35. Porosity-permeability characteristics of Madison Formation limestones (after Thayer, 1981).

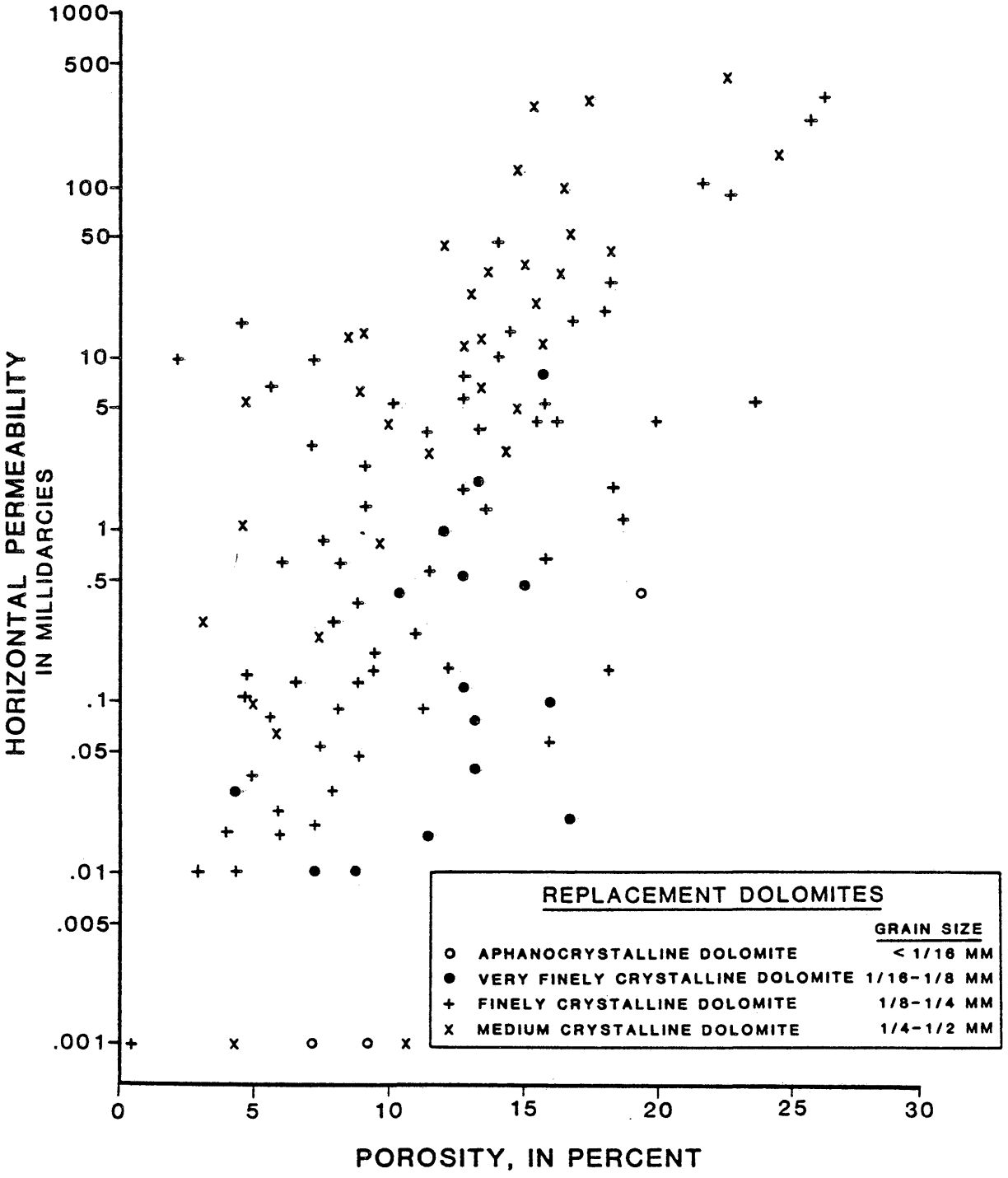

Figure 36. Porosity-permeability characteristics of Madison Formation replacement dolomites (after Thayer, 1981).

SYNTHETIC SEISMOGRAMS

The utility of synthetic seismograms as an exploration aid is well known. One-dimensional synthetic seismic traces were used in this study to demonstrate the detectability of high-water producing zones within the Madison and Red River Formations. The synthetic seismograms were computed for both the USGS Madison No. 1 and No. 2 wells using the sonic travel time log and density log. A minor amount of smoothing was applied to the acoustic logs of each well to reduce the large excursions due to noise and cycle skipping.

The computation of a reflection coefficient for each rock layer interface yields a reflection coefficient trace, consisting of a time series of spikes. This method for generating synthetic seismograms ignores transmission losses, absorption, the effects of multiples and noise. Further, the seismic response of a reflecting horizon on field data will usually differ from the response modeled by a synthetic seismogram derived from log data because the logs measure rock properties only a few inches from the borehole. A seismic wave will illuminate a stratigraphic horizon, and the resultant reflected wave is an average of reflections occuring from a circle that is several hundred feet in diameter, depending on depth and source frequency.

To compute the final version of the synthetic seismogram, a wave pulse, or wavelet, is convolved with the reflection coefficient series. The spectral characteristics of the wavelet are generally chosen to match the spectral characteristics of the surface seismic data, although this is never achieved perfectly. The resulting synthetic seismic trace can then be used to correlate geologic formations to their corresponding expression on seismic field data.

In this study, a set of synthetic seismograms were generated using symmetric bandpass wavelets with different lower and upper frequency limits. This approach demonstrates which seismic frequencies are necessary in the field data to allow detection of a particular geologic formation.

A set of synthetic seismograms generated using the product of velocity and density (acoustic impedance), and with varying bandpass filters applied, is shown in Figure 37 for the USGS Madison No. 1 well, and in Figure 38 for the USGS Madison No. 2 well. Bandpass filter cutoffs are listed below each seismogram group. Polarity of these seismograms is conventional, that is, a positive reflection amplitude represents a transition of lower to higher acoustic impedance between layers. Noise or multiple reflections were not added to these seismograms.

The first problem that is apparent on the two figures is that the Madison to Red River interval is thick for the non-productive No. 2 well, and thin for the productive No. 1 well. This will cause some correlation problems between synthetic seismograms of the two wells. Also, for the frequency range chosen, there is no outstanding characteristics or patterns between the two wells that would allow immediate discrimination of water producing zones from non-producing zones. The detection must manifest itself in a more subtle manner, which is discussed in the following sections.

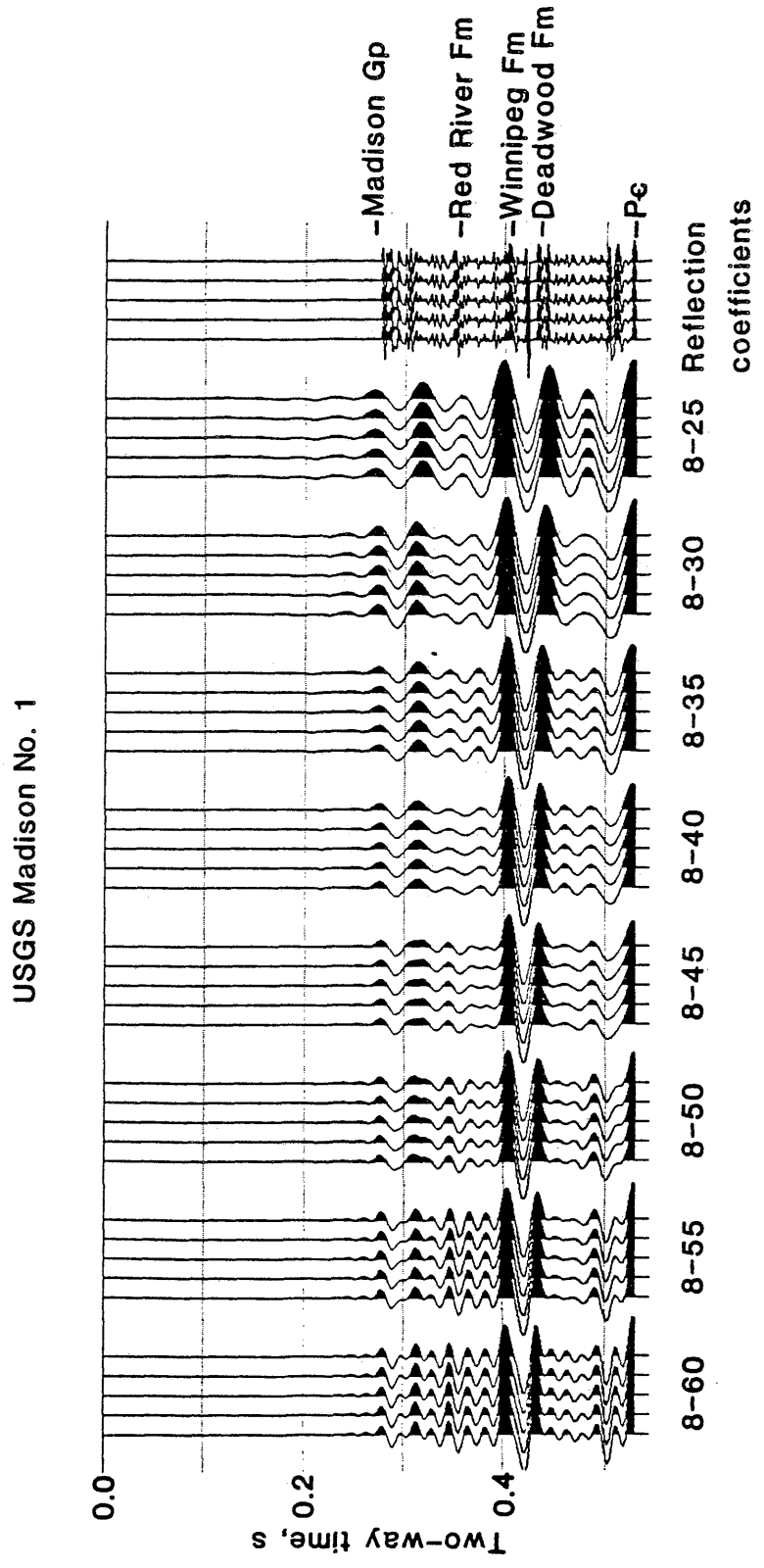

Figure 37. Synthetic seismograms derived from the interval-transit time and density log data of the USGS Madison No. 1 well filtered with seven different frequency ranges, which are listed below each group of traces. The unfiltered reflection coefficients are plotted as the last group of traces.

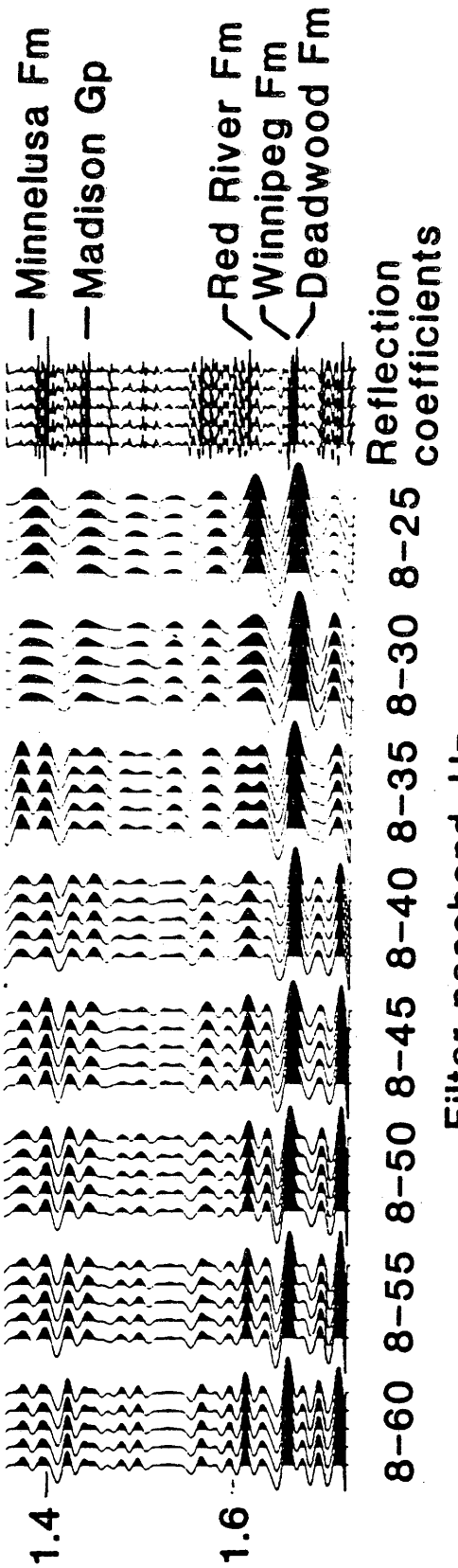

Figure 38. Synthetic seismograms derived from the interval transit time and density log data of the USGS Madison No. 2 well filtered with seven different frequency ranges, which are listed below each group of traces. The unfiltered reflection coefficients are plotted as the last group of traces.

RESOLUTION VERSUS DETECTABILITY

Usual methods of depicting the seismic response of a geological zone of interest involves creating a synthetic seismogram, which is a time series of filtered reflection coefficients derived from edited sonic travel time and density data. Correlation and identification of reflections on the synthetic seismogram with the seismic data is then made, and by using wavelet processing techniques, the data is converted to be broadband, and, in most cases, zero phase. Conversely, if the shape of the propagating wavelet is known, a synthetic seismogram can be constructed by filtering the reflection coefficients with the known wavelet, and correlating directly to the seismic data. In either situation, the goal is an attempt to match reflections occuring on seismic data with corresponding reflections on the synthetic seismogram. Once this is accomplished, a calibration of the synthetic and seismic data can be performed by determining characteristics of reflection waveform shapes which relate to information about lithology. For example, the amplitude of the reflection pulse may yield information about thickness of beds, porosity, or fluid content of a reservoir, and knowledge of this at the well can then be applied to seismic data traces away from the well.

A further refinement of the calibration method is the conversion of the seismic trace into relative acoustic impedance logs (Lindsey, 1977). The estimated acoustic impedance log derived from seismic data contains no additional information than the usual display of the wavelet processed seismic data; it is just another way of displaying the same information for information for interpretation. Interpretability is improved because acoustic impedance measures properties of the geologic interval, rather than properties of the bed interface. That is, acoustic impedance logs are interpreted as if they were well logs. Relationships that a geologist is familiar with on logs, such as bed thickness and relative values of velocity and density are available to him on an acoustic impedance trace, although the trace is bandlimited by the filtering action on seismic data by the earth.

Ideally the acoustic impedance log estimated from seismic data is an optimum method for interpreting stratigraphic changes of the subsurface, as it directly corresponds to the interpretation technique that a geologist uses when constructing geologic cross-sections from well log data. This technique is suggested in this report as a viable technique for studying Madison and Red River porosity changes from seismic data.

Analysis of the well log crossplots shows that there is

a definite relationship, roughly linear, between porosity and density, and between porosity and sonic travel time. Reflection strength is a function of acoustic impedance contrast between two dissimilar layers. Since acoustic impedance is the product of density and velocity (reciprocal of interval travel time measured from the sonic log), then the porosity should have a trend with acoustic impedance.

The relationship between porosity and acoustic impedance for the two wells is shown in Figure 39. A linear relationship of porosity with acoustic impedance can be identified for each of the wells, and is shown on the crossplot for each well. The main difference in the trend between the two data sets is that the trend line of the non-productive well has a smaller slope than the productive well. Therefore at any given value of acoustic impedance, the porosity will be lower in the non-productive case relative to the productive case.

This would seem to pose an obvious limitation in using seismic data to define zones of high porosity which would have a high probability of being good water-producing aquifers. That is, a given value of acoustic impedance can be associated with two porosity interpretations (with corresponding different rates of water production), and the utility of using seismic data to differentiate zones of high porosity from low porosity is somewhat restricted. The best

use of seismic data then would be to differentiate zones of high porosity from zones of low porosity.

A subtle aspect of the crossplot, however, is that more of the data samples of the non-productive data set tend to concentrate near the low-porosity region of the graph. This suggests that the probability of encountering higher porosity zones of a low water-yield carbonate reservoir using acoustic impedance will be low. The distribution of data samples for the high water-yield rock appears to be more uniform. Of course, several more wells would have to be analyzied before the distribution of porosity can be accurately characterized.

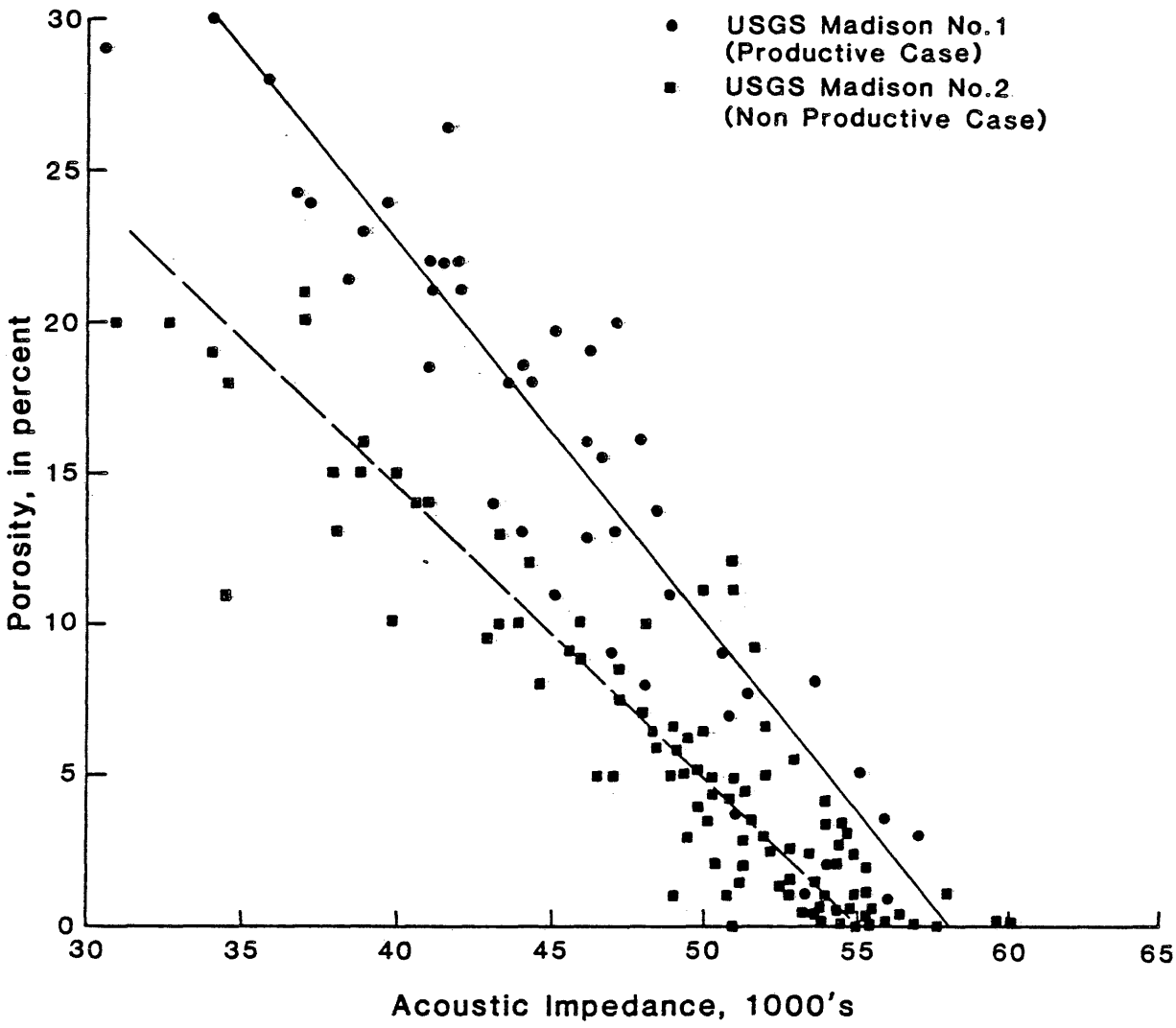

Figure 39. Porosity values measured from cores versus acoustic impedance for the USGS Madison No. 1 and USGS Madison No. 2 wells.

Resolution of Porosity Zones

Zones with porosity higher than ten percent are generally thin, and seismically have a two-way time thickness of about one to two milliseconds. The ability to detect a target bed and measure its relative acoustic impedance properties is not only a function of bed thickness and depth, but of the seismic signal's bandwidth, wavelet shape, and signal to noise ratio. Therefore the ability to detect thin Madison or Red River beds with seismic data, and map their acoustic impedance properties, would be a difficult task.

However, an earlier report by Farr (1976), showed that one-twelfh wavelength to be the practical lower limit to seismic resolution under typical field environments. For example, a ten foot bed with good porosity in either the Madison or Red River Formation would have a velocity of around 15,000 ft/sec, or one-way time thickness of 0.67 milliseconds. Using the one-twelfh criteria, a seismic signal would require an upper frequency of approximately 124 hz in order to resolve the bed discreetly.

However, there is further help in using seismic data, and that is when a bed becomes thin enough and disappears below the seismic's resolution limit, the thickness of the bed is encoded into the amplitude of the reflection pulse.

Recent work has been performed in quantifying the resolution of thin beds, based on amplitude changes, and an excellent example is given by Geoquest (1979). In this investigation, a simple model consisting of a thin bed encased in homogeneous materials is filtered with a normal incidence, zero-phase wavelet. By observing the composite waveform as a function of reservoir thickness, a relationship is derived to allow interpretation of very thin beds beyond the resolution limit, which is the point where the distinct and separate reflection peak from the top of the bed and from the bottom of the bed merge into a single reflection pulse. Interpretation is then based on the amplitude of the single reflection waveform. Lindsey (1975), Nath and Meckel (1976) have illustrated that below the tuning thickness, the amplitude of the event can still provide information concerning the true thickness of the bed, and provide calibration charts in their report based on bed thickness and seismic amplitude for a given passband of a wavelet.

While it is possible, then, to explore for Madison reservoirs using seismic data, it probably will be difficult in areas where the Madison and Red River Formations are deeper, and higher frequencies are not recoverable. Without the higher frequencies for resolution, the inversion of seismic traces to acoustic impedance traces will not yield the desired interpretation aid that is commonly obtained

with the thicker reservoirs. Therefore the next step was to search for other measurement techniques of seismic waveforms that would allow an interpreter to separate a porous, water-productive carbonate zone from a non-productive, tight zone.

Detectability of Target Zones

Because the zones with higher porosity in the USGS Madison No. 1 well are thin, the direct detection of each zone with seismic reflection data will be difficult within the resolution limitations of field data, particularly where target beds are deeper. However the detection of high porosity zones may be obtained by analyzing the composite of all reflections emanating from the interval. Since there are two wells in the study area that encountered different water producing environments, a comparison of the composite waveforms at different seismic frequencies can be made and evaluated. Widess (1958, 1973) noted that while a thin bed may not be discreetly resolved, it may be detectable in an indirect manner. Thin beds that have a time wavelength down to 1/40 of the dominant period of the seismic pulse can influence the overall composite response of a zone, and can be detected by careful analysis of the data. Applying this example to the Madison situation, then a bed as thin as .0005 seconds corresponds to a bed thickness of about eight feet. This thickness is about the lower range of bed thickness values for the highest porosity beds in the USGS Madison No. 1 well.

Based on the information already evaluated on the Madison and Red River Formations, an approach is suggested

to analyze the intervals and find methods for classifying the reflection spike series into two main classes, which are porous, water-producing lithology versus tight, non-water producing lithology. Two measurements of the reflectivity series were studied in an attempt to produce a reliable discrimination between the two classes, which individually may not be sufficient to discriminate between the classes. This method of classifying waveform patterns is essentially based on statistical decision theory.

Waveform analysis methods used in classifying speech segments involves measuring properties of short time-segments, and thereby build up a statistical distribution of the property being measured (Atal, 1976). Because of the small time distance involved in the Madison and Red River reflections, a reliable distribution function at seismic frequencies cannot be determined. Instead the approach used in this report will be to compute the features of the entire interval of interest for the two known classes of rock types over a range of realizable seismic frequencies, and look for those features and passband frequencies which best discriminate the two classes.

Waveform Measurements

The reflection coefficient series from the two classes of rock types were computed from the USGS Madison No. 1 well (productive class), and the USGS Madison No. 2 well (non-productive class). Reflection coefficients are derived by first performing a cumulative summation of the sonic travel time curve to yield a depth-time relationship of each well. Using the time-depth information, the sonic travel time data and density data can be converted to linear functions of time at evenly sampled intervals, which, in this case is one millisecond. Reflection coefficients are then computed according to the commonly used differencing equation

$$RC = \frac{\rho_{i+1} V_{i+1} - \rho_i V_i}{\rho_{i+1} V_{i+1} + \rho_i V_i}$$

where ρ_i = density of the i^{th} layer

V_i = velocity of the i^{th} layer

The reflectivity spike series was then bandpass filtered with a constant low cut of 5 hz, and varying upper frequency cutoffs, beginning at 20 hz and ending at 100 hz, in two hertz increments.

Two statistical measurements were made on each filtered block of data, and normalized by the length of the block

used. The waveform is represented by x(n), n=1.2....N. The following measurements were then computed for each block.

1) Energy of the interval, defined by

$$e = 10 \log (\epsilon + \frac{1}{N}\sum x^2(n))$$

where the small positive constant ϵ was added to prevent computing the logarithm of zero.

The energy measurement "e" is a function of the time and amplitude distribution of reflection spikes and the frequencies at which they are filtered. The distribution of reflection spikes will produce a complex combination of constructive and destructive interferences, or tuning, at the different frequency passbands.

2) Zero crossing rate, Nz, is the number of zero crossings in the interval normalized by the length of the interval. The zero-crossing measurement indicates the range of frequencies at which energy is concentrated. Obviously the zero-crossing count will increase for both classes as a function of the upper cutoff frequency.

Figure 40 shows the normalized log energy for the filtered reflectivity spikes from the Madison and Red River intervals as a function of the upper frequency cutoff for the filter. Seismic energy of the tight formation is greater than that of the porous formations at low frequencies (20 to 70 hz), and at higher frequencies the

porous zone and tight zone have about the same energy level.

The relatively flat curve for energy of the non-productive well is probably due to the nearly homogeneous distribution of velocities and densities throughout the interval. On the other hand, the mixture of thin beds of porous and tight carbonate zones in the water-productive case provides a low energy level at low frequencies, because of the averaging from the wavelet, and increases as a function of the wavelet's resolving power. Work performed by Lee (per. comm., 1979) using vertical seismic profiling methods showed that interbed multiple reflections in the porous wells produced a higher return of energy than did the tighter wells. Therefore, Figure 40 is probably only accurate at the lower frequency range (below 50 hz) since it was constructed assuming primary reflections only.

Figure 41 shows the number of zero crossings within the interval as a function of upper frequency cutoff. In general, the number of zero crossings for the porous case is higher than the zero crossings rate for the tight, non-productive case at the same frequency, although not by a significant amount. The figure shows that the alternating sequence of porous and non-porous thin beds in the productive case creates a pattern of low acoustic impedance next to high acoustic impedance, causing an oscillatory

pattern of reflections to develop at all frequencies. In the tight carbonate rock case, the oscillatory pattern is not as prevalent. Based on the analysis of these two wells, though, zero-crossing measurements would probably not be a useful discrimination tool. As in the energy level measurement, the effects of internal multiple reflections are not computed, but would probably cause the zero-crossing count to be higher for the porous case.

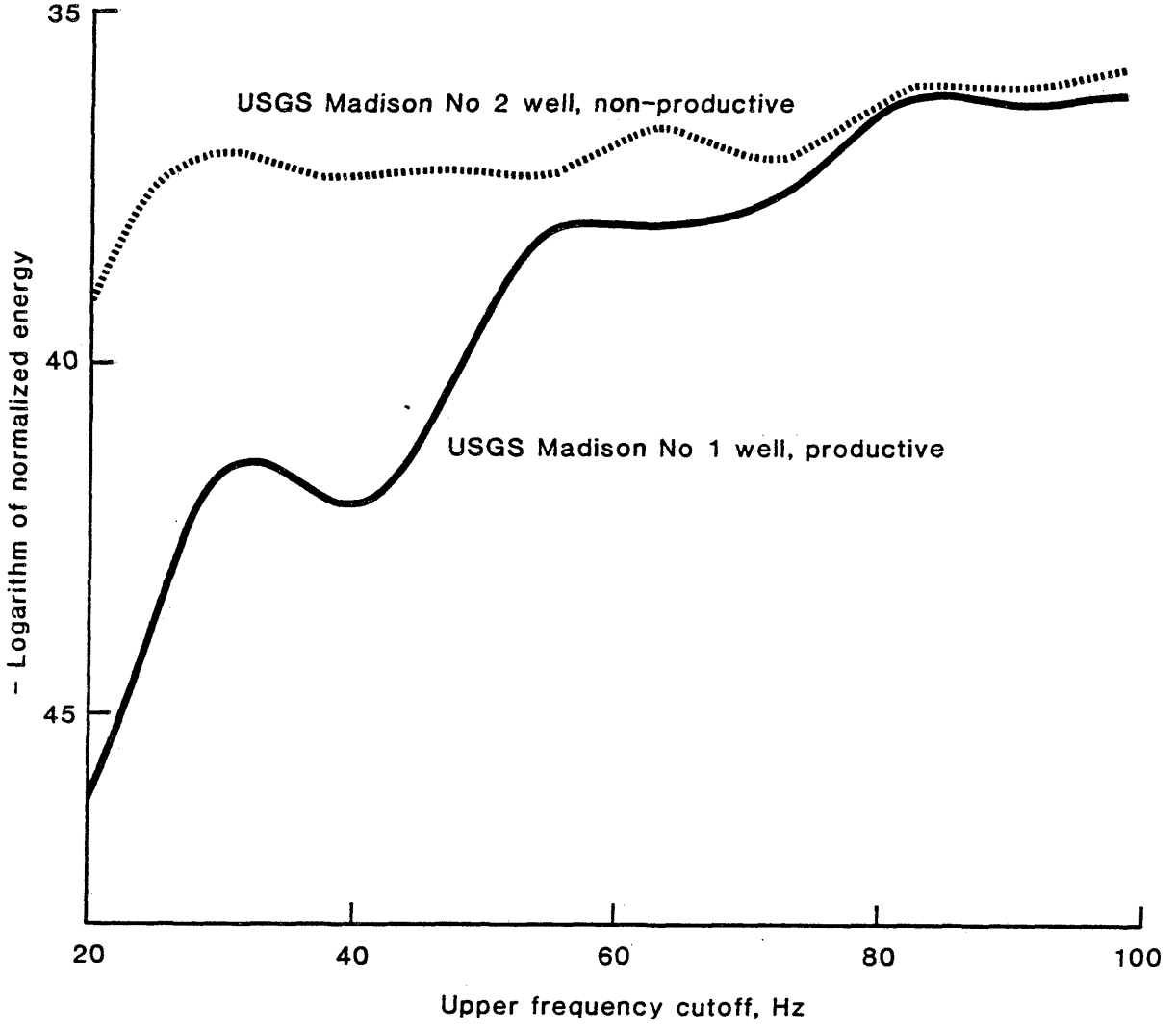

Figure 40. Normalized log energy of the Madison and Red River intervals for different passbands. The lower cut of the passband was 5 hz in each case, and the upper cut is plotted along the abscissa.

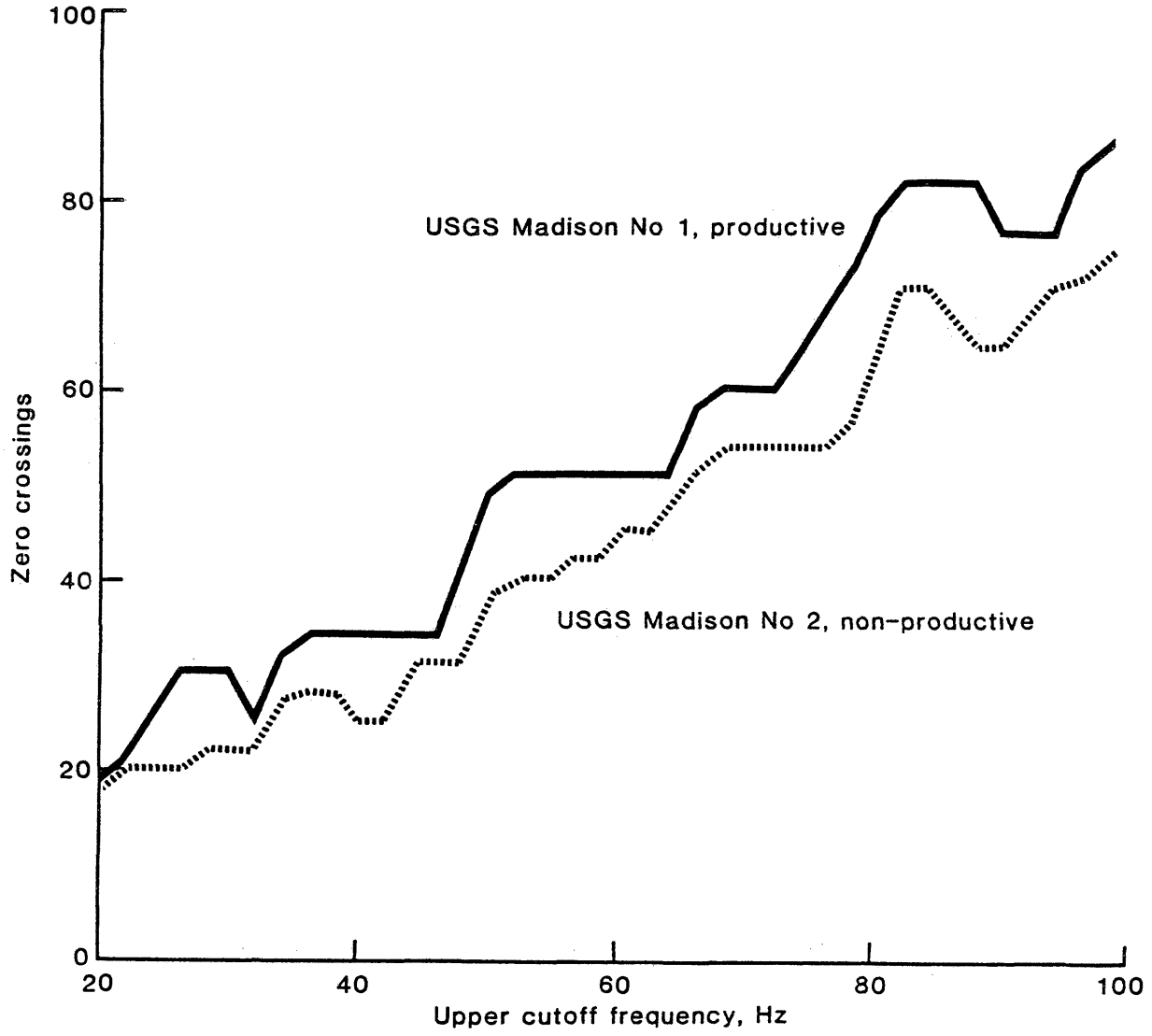

Figure 41. Number of zero crossings of the reflectivity series filtered at different passbands for the productive well (USGS Madison No. 1) and the non-productive well (USGS Madison No. 2).

RECOMMENDATIONS

The analysis of well log data from two wells representing contrasting reservoir environments demonstrated that trends of low acoustic impedance are associated with high porosity, and indicate that discrimination of water producing and non water producing zones using seismic data is possible. Although the individual high porosity zones are thin, and their spatial distribution is not well known, the composite response of an interval is suggestive of reservoir quality, and successful interpretations may be possible by classifying the response of the entire formation, rather than attempting to identify productive zones. Synthetic seismograms that are generated from the well logs using conventional plane-wave normal-incidence simulation methods have been done and shown to be useful in identifying major reflection boundaries, but may not provide the complete response that a seismic wave field might see.

In light of the studies made in this thesis, the following recommendations are made:

1. Further well log evaluations should be performed using available log data penetrating the Madison and Red River intervals in the study area. The analysis should follow the procedures described in this thesis, in order to determine the trends of porosity as a function of velocity,

density, and depth. This work will further substantiate the interpretability of porosity zones within the Madison and Red River Formations.

2. Develop synthetic seismograms from wells having velocity and density data to determine the reflectivity patterns of porous carbonate facies versus tight carbonate facies. Wells that do not have density information should be modeled, but with the understanding that density is an important parameter for detecting porosity from acoustic impedance measurements. The work done using vertical seismic profiling data (Lee, per. comm., 1980) shows that internal multiple reflections may be an indicator of porosity, and therefore the synthetic seismograms should include all orders of interbed multiple reflections.

3. Investigate the advantages of using vertical seismic profiles in place of the synthetic seismograms to understand the reflectivity pattern of carbonate facies. Because the VSP is a measurement of a seismic pulse in-situ at seismic field frequencies, with the effects of interbed multiples, absorption, scattering, and Fresnel zone averaging included, a more accurate determination of reflectivity patterns can be made.

4. The surface seismic data should be reasonable broadband to maximize the detectability of porous zones. Typically a range of 6 to 80 hz is now possible on land

acquisition, but will most likely require an explosive source. Trace spacing should be relatively close, on the order of 100 to 200 feet depending on the depth of the target, so that lateral variations of carbonate porosities can be tracked. Consider using an "experimental" field crew who have experience in obtaining high-quality seismic data initially, so that the best field parameters can be obtained.

5. Integrate the synthetic seismograms from well log data, and the VSP data, into the synthetic seismogram at the same effective bandwidth of that used in processing the seismic data. Also any phase spectrum differences between the synthetic seismogram and seismic data should be eliminated. Determine the reflectivity patterns associated with high porosity carbonate versus tighter carbonates, and compare with results presented in this work. Once a technique has been established for recognizing which group of waveforms indicates porosity development, the method can be applied directly to seismic field data. The method used will most likely be applied using computer methods, because the patterns on conventional seismic displays may be too subtle to be detected by visual inspection.

CONCLUSIONS

1. The best water-bearing aquifers in the Madison and Red River Formations occur where the carbonate rocks are predominantly coarsely-grained dolomite, and therefore have better porosity development. Zones of fracturing and secondary porosity are also good prospects. Locating fracture zones through analysis of the structural history and present day structural setting is feasible, but locating zones of high dolomite content by geologic subsurface and trend analysis is difficult due to the lack of subsurface information on Madison and Red River rocks in this area. Exploration for high-yield aquifers by random drilling may become prohibitively costly.

2. The best water-bearing zones have high porosity and permeability, but are generally thin units, usually ranging from two to ten feet. These zones are interbedded with tight, and generally thicker, dolomite and limestone units. There is no structural expression associated with porosity development in either the Madison or Red River interval.

3. Porosity in the Madison and Red River Formations is characterized by lower velocity and density, and therefore, by local acoustic impedance lows, relative to surrounding tight carbonate rocks with higher impedance. Because the high porosity zones are thin, direct detection using modern

seismic data is not likely to succeed because of the seismic's limited resolving capabilities.

4. High-porosity zones are thin, low acoustic impedance layers interbedded with generally thicker, tight carbonate layers of higher acoustic impedance. The high-porosity zones are not directly identifiable on noise-free synthetic seismograms at typical seismic frequencies. The usefulness of acoustic impedance logs to detect porosity zones in Madison and Red River rocks, based on the study of two wells, is marginal at best.

5. Limestones of the Madison have generally low values of permeability and porosity, while dolomites have higher porosities and permeabilities. A rough linear correlation exists between porosity and permeability, and therefore seismic detection of porosity will generally insure that the rock is premeable also. However, there are rock types with high porosity but low permeability, which would limit water production. On the other side of this, permeability in low porosity rocks is enhanced through tectonic fracturing, and aquifers in these rocks can produce adequate water productivity rates. Thus, porosity detection by itself is not sufficient to classify all of the carbonate aquifers that might exist in the Madison and Red River intervals.

6. In the case of thin beds, the seismic response is generally sensitive to stratigraphic layering as well as

changes in acoustic impedance. The thin, high-porosity zones produce an "influence" on the seismic waveform, and can be identified through special analysis of the seismic waveform.

7. The application of other detection schemes to identify the subtle "influence" effects included the measurement of the total RMS energy of the Madison and Red River intervals, and the number of zero crossings as a function of frequency bandwidth. These methods produced the following results:

(a) The seismic energy of tight formations is greater than that of the porous formations at low frequency (below 50 hz), but at higher frequencies the porous zone produced more energy. Work done by Lee (per comm., 1979) using vertical seismic profiling data showed that internal multiple reflections in the porous wells produced an even higher energy return than did the tighter wells. This is probably due to the porous carbonate rock having a heterogeneous mixture of velocities and densities associated with the porous carbonate, while the tight carbonate is more evenly distributed with constant velocities and densities.

(b) The number of zero crossings over the interval is roughly measuring frequency content. In the porous rock case, the number of zero-crossings is slightly

higher than for the tight rock case at similar frequencies, although the difference is small, and probably would not be a useful tool that can readily be applied to seismic field data.

REFERENCES

Andrichik, J.M., 1955, Mississippian Madison Group stratigraphic and sedimentation in Wyoming and southern Montana: Am. Assoc. Petro. Geol. Bull., v. 39, no. 11, p. 2170-2210.

Atal, B.S., and Rabiner, L.R., 1976, A pattern recognition approach to voiced-unvoiced-silence classifications with applications to speech recognition: IEEE Trans. on Acoustics, Speech, and Signal Processing, v. ASSP-24, no. 3, p. 201-212.

Asquith, G.B., 1979, Subsurface carbonate depositional models: A concise review: Okla., Petroleum Pub. Co., 116 p.

Blankennagel, R.K., Miller, W.R., Brown, D.L., and Cushing, E.M., 1977, Report on preliminary data for Madison Limestone Test Well No.1: U.S. Geol. Survey Open File Report 77-164.

Gray, A.H., and Marke, J.D., 1974, A spectral flatness measure for studying the autocorrelation method of linear prediction of speech analysis: IEEE Trans. on Acoustics, Speech, and Signal Processing, v. ASSP-22, no. 2, p. 207-217.

Head, W.J., and Merkel, R.H., 1977, Hydrologic characteristics of the Madison Limestone, the Minnelusa Formation, and equivalent rocks as determined by well-logging formation evaluation, Wyoming, Montana, South Dakota, and North Dakota in Jour. Res. U.S. Geol. Survey, v. 5, no. 4, p. 473-485.

Hilchie, D.W., 1977, Applied Open Hole Log Interpretation: Douglas W. Hilchie Inc., Golden Colorado.

Kerns, J.R., and Hegna, E.T., 1977, Geological report on the U.S. Geological Survey Madison Limestone Test No. 2:

Geological report prepared by Hegna, Kerns, and Traut, Casper, Wyoming.

Lageson, D.R., 1977, Depositional environments and diagenesis of the Madison Limestone, northern Medicine Bow Mountains, Wyoming: The Wyoming Geol. Assoc. Earth Sci. Bull., v. 10, no. 1, p. 3-12.

Lindseth, R.O., 1979, Synthetic sonic logs - a process for stratigraphic interpretation: Geophysics, v.44, no. 1, p. 3-12.

Lindsey, J.P., and Dedman, E.V., 1977, Seismic calibration techniques for exploration and exploitation: GeoQuest International, Inc., Houston, Texas, 33 p.

MacCary, L.M., Cushing, E.M., Brown, D.L., 1981, Potentially favorable areas for large-yield wells in the Red River Formation and Madison Limestone in parts of Montana, North Dakota, South Dakota, and Wyoming: U.S. Geol Survey Open File Report 81-220, 29 p.

Murray, R.C., 1960, Origin of porosity in carbonate rocks: Jour. Sedimentary Petrology, v.30, no. 1, p. 59-84.

Peterson, J.A., 1978, Subsurface geology and porosity distribution, Madison Limestone and underlying formations, Powder River Basin, northeastern Wyoming and southeastern Montana, and adjacent areas: U.S. Geol. Survey Open File Report 78-783, 9 p.

Rose, P.R., 1976, Mississippian carbonate shelf margins, western U.S: U.S. Geol. Survey Jour. Res., v. 4, no. 4, p. 449-466.

Sando, W.J., 1967, Madison Limestone (Mississippian), Wind River, Washakie, and Owl Creek Mountains, Wyoming: Am. Assoc. Petr. Geol. Bull., v. 51, no.4, p. 529-557.

_____, 1974, Ancient solution phenomena in the Madison Limestone (Mississippian) of north-central Wyoming: U.S. Geol. Survey Jour. Res., v. 2, no. 2, p. 133-141.

_____, 1976, Mississippian history of the northern Rocky Mountain region: U.S. Geol. Survey Jour. Res., v. 4, no. 3, p. 317-3338.

Schlumberger, 1972, Log Interpretation Manual, vol. I, Principles, 113 p.

Schlumberger, 1974, Log Interpretation Manual, vol. II, Applications, 116 p.

Schramm, Jr, M.W., Dedman, E.V., and Lindsey, J.P., 1977, Practical stratigraphic modeling and interpretation, in Am. Assoc. Petr. Geol. Mem. 26, p. 477-502.

Society of Petroleum Engineers, 1971, Well Logging, SPE Series No. 1.

Technica Resource Development Ltd, 1977, Seislogs: Houston, Texas, Technica Inc.

Thayer, P.A., 1981, Petrology and petrography for U.S. Geological Survey test wells 1, 2, and 3 in the Madison Limestone in Montana and Wyoming: U.S. Geol. Survey Open File Report 81-221.

U.S.G.S., 1975, Plan of study of the hydrology of the Madison Limestone and associated rocks in parts of Montana, Nebraska, North Dakota, South Dakota, and Wyoming: U.S. Geol. Survey Open File Report 75-631.

Wilson, J.L., 1975, Carbonate facies in geologic history: Springer-Verlag, New York, 471 p.

APPENDIX A

Tables of well log values used in all crossplot analysis.

Description of Variable Names Used for Column Headings

The depth value, Z is the depth to the top of each layer. All of the log measurements corresponds to the layer, or interval, between the depth at which the value appears, to the depth on the line immediately below.

Z	Depth below ground surface, in feet.
ITT	Interval transit time from the sonic log, in microseconds/ft
DEN	Density from the density log, in gm/cm^3
Ø	Porosity from the compensated neutron log, measured in limestone porosity percent
GR	Gamma-ray values from the gamma-ray log, in API units
V	Velocity, in feet per second, derived from the reciprocal of interval transit time
RHO-V	Acoustic impedance, derived by multiplying velocity by the density, in units of feet-gram/sec-cm^3
T	Two-way travel time from the surface to the top of the interval, in milliseconds
RC	Reflection coefficient at the interface between the layer at which the RC is listed, and the layer on the following line

U.S.G.S. Madison No. 1

Z	ITT	DEN	Ø	GR	V	RHO-V	T	RC
2604.	54.4	2.53	16.5	23.	18382.	46506.	271.08	-0.0330
2613.	57.2	2.49	18.4	25.	17483.	43533.	271.88	-0.0210
2620.	58.7	2.45	22.3	23.	17036.	41738.	272.23	-0.0773
2623.	64.9	2.32	28.3	20.	15408.	35747.	273.27	0.0211
2631.	64.9	2.42	23.9	22.	15408.	37287.	273.66	0.1304
2634.	52.2	2.53	13.8	24.	19157.	48467.	273.97	-0.1167
2637.	63.9	2.45	21.6	24.	15649.	38340.	274.48	0.0910
2641.	55.2	2.54	12.8	30.	18116.	46015.	275.04	-0.1102
2646.	66.7	2.46	24.0	34.	14993.	36883.	275.97	0.0522
2653.	61.3	2.51	18.5	20.	16313.	40946.	276.46	-0.1732
2657.	75.2	2.17	29.3	26.	13298.	28857.	277.66	0.0833
2665.	69.5	2.37	30.0	24.	14388.	34100.	278.22	-0.0832
2669.	78.3	2.26	30.0	26.	12771.	28862.	279.32	0.2437
2676.	53.3	2.53	13.0	22.	18762.	47468.	280.28	0.0651
2685.	49.0	2.65	2.8	20.	20408.	54081.	280.86	0.0158
2691.	47.3	2.64	0.7	21.	21142.	55815.	281.81	-0.0433
2701.	51.0	2.61	3.7	21.	19608.	51177.	282.52	-0.0338
2708.	53.1	2.54	8.2	22.	18832.	47833.	283.05	0.0873
2713.	46.5	2.65	3.1	25.	21505.	56988.	283.89	-0.1661
2722.	61.1	2.49	22.1	23.	16367.	40754.	284.26	0.1361
2725.	48.7	2.61	8.1	23.	20534.	53594.	285.04	-0.0664
2733.	55.2	2.59	16.0	26.	18116.	46920.	285.26	0.0743
2735.	48.3	2.63	3.0	42.	20704.	54452.	286.03	-0.0348
2743.	50.6	2.57	6.5	33.	19763.	50791.	286.33	0.0575
2746.	46.5	2.65	3.9	26.	21505.	56988.	287.08	-0.1568
2754.	60.9	2.53	26.5	26.	16420.	41543.	287.57	0.0683
2758.	55.0	2.62	20.0	33.	18182.	47637.	288.01	-0.0667
2762.	60.7	2.53	21.0	31.	16474.	41679.	288.61	0.1383
2767.	48.5	2.67	5.0	33.	20619.	55053.	289.49	-0.1457
2776.	62.6	2.57	22.4	37.	15974.	41053.	290.61	0.1517
2785.	47.9	2.67	3.4	21.	20877.	55742.	291.28	-0.0871
2792.	56.4	2.64	9.1	29.	17730.	46807.	291.62	0.0733
2795.	48.7	2.64	3.9	24.	20534.	54210.	292.50	-0.0809
2804.	56.4	2.60	16.8	27.	17730.	46098.	292.72	0.0853
2806.	49.0	2.68	8.9	30.	20408.	54693.	293.12	-0.0961
2810.	57.2	2.58	19.8	32.	17483.	45106.	294.03	-0.0745
2818.	65.9	2.56	22.9	29.	15175.	38848.	294.56	0.1144
2822.	53.6	2.62	11.0	40.	18657.	48881.	295.20	-0.0607
2828.	60.3	2.61	14.3	34.	16584.	43284.	295.44	0.0571
2830.	54.4	2.64	2.5	24.	18382.	48528.	297.62	0.0493
2850.	49.1	2.63	1.3	24.	20367.	53565.	297.91	-0.0495
2853.	53.6	2.60	8.3	28.	18657.	48508.	298.45	0.0054
2858.	52.0	2.55	8.7	24.	19231.	49039.	298.97	0.0244
2863.	50.1	2.58	7.7	25.	19960.	51497.	299.47	-0.0630
2868.	56.4	2.56	9.6	26.	17730.	45389.	299.70	0.0601
2870.	50.4	2.58	7.3	24.	19841.	51190.	301.41	-0.0707

Z	ITT	DEN	Ø	GR	V	RHO-V	T	RC
2925.	56.2	2.50	15.7	24.	17794.	44485.	305.85	0.0623
2927.	50.6	2.55	10.4	24.	19763.	50396.	306.05	-0.0678
2929.	56.6	2.49	16.2	24.	17668.	43993.	306.28	0.0816
2931.	49.6	2.57	10.8	25.	20161.	51814.	307.17	-0.0679
2940.	55.5	2.51	14.6	25.	18018.	45225.	307.73	0.0462
2945.	51.2	2.54	10.7	22.	19531.	49609.	308.04	-0.0359
2948.	54.8	2.53	12.5	20.	18248.	46167.	308.25	0.0865
2950.	47.9	2.63	5.9	21.	20877.	54907.	308.73	-0.0791
2955.	54.0	2.53	12.0	25.	18519.	46853.	309.81	-0.0282
2965.	56.0	2.48	17.8	23.	17857.	44285.	310.15	0.0704
2968.	50.2	2.56	9.9	21.	19920.	50995.	310.95	-0.0985
2976.	59.5	2.49	19.4	26.	16807.	41849.	311.43	0.0400
2980.	55.8	2.53	15.7	29.	17921.	45340.	311.76	0.0586
2983.	50.8	2.59	10.5	23.	19685.	50984.	312.27	-0.1469
2988.	62.5	2.37	27.4	23.	16000.	37920.	313.15	0.0457
2995.	59.2	2.46	24.4	23.	16892.	41554.	313.86	-0.1076
3001.	69.6	2.33	28.8	23.	14368.	33477.	315.25	0.1151
3011.	57.6	2.43	23.6	21.	17361.	42187.	315.59	-0.0444
3014.	61.4	2.37	26.4	27.	16287.	38600.	316.09	-0.0339
3018.	64.6	2.33	28.5	25.	15480.	36068.	317.38	0.2032
3028.	48.1	2.62	8.8	27.	20790.	54470.	317.76	-0.1145
3032.	58.0	2.51	20.8	32.	17241.	43275.	318.81	0.0099
3041.	58.0	2.56	18.8	50.	17241.	44137.	319.27	-0.0690
3045.	66.6	2.56	21.4	53.	15015.	38438.	321.80	-0.0311
3064.	67.0	2.42	25.7	48.	14925.	36119.	322.87	0.1014
3072.	57.6	2.55	18.3	24.	17361.	44271.	323.10	0.0532
3074.	52.8	2.60	16.5	24.	18939.	49241.	323.95	-0.0931
3082.	60.7	2.48	21.8	23.	16474.	40856.	325.41	0.1161
3094.	50.2	2.59	15.0	26.	19920.	51593.	326.81	-0.1649
3108.	65.7	2.43	27.0	19.	15221.	36987.	327.47	0.0565
3113.	59.4	2.46	23.9	19.	16835.	41414.	328.54	-0.0504
3122.	64.9	2.43	29.1	22.	15408.	37441.	328.93	0.0926
3125.	55.9	2.52	20.3	22.	17889.	45080.	330.94	-0.0264
3143.	58.7	2.51	17.3	19.	17036.	42760.	331.41	0.1037
3147.	49.0	2.58	15.0	24.	20408.	52653.	331.70	-0.0951
3150.	57.0	2.48	22.1	20.	17544.	43509.	332.04	0.0521
3153.	52.8	2.55	17.4	20.	18939.	48294.	332.78	-0.0716
3160.	58.8	2.46	21.1	21.	17007.	41837.	333.37	-0.0163
3165.	60.5	2.45	22.9	23.	16529.	40496.	334.46	-0.0509
3174.	65.9	2.41	24.7	25.	15175.	36572.	335.52	0.1513
3182.	51.8	2.57	15.2	24.	19305.	49614.	335.93	-0.1171
3186.	63.5	2.49	19.0	26.	15748.	39213.	336.31	0.0803
3189.	55.8	2.57	15.8	26.	17921.	46057.	338.77	-0.0251
3211.	57.3	2.51	19.0	25.	17452.	43805.	340.83	-0.0212
3229.	59.3	2.49	20.3	23.	16863.	41989.	341.90	-0.0815
3238.	67.3	2.40	24.6	27.	14859.	35662.	342.17	0.0292
3240.	64.8	2.45	22.0	24.	15432.	37808.	342.68	0.0059
3244.	63.0	2.41	23.3	21.	15873.	38254.	344.70	0.0163
3260.	62.5	2.47	22.7	23.	16000.	39520.	346.57	0.0493

Z	ITT	DEN	Ø	GR	V	RHO-V	T	RC
3298.	53.8	2.55	16.3	23.	18587.	47397.	350.40	-0.0319
3309.	56.9	2.53	18.1	23.	17575.	44465.	351.20	0.0200
3316.	55.1	2.55	18.5	27.	18149.	46280.	351.75	-0.0538
3321.	59.2	2.46	22.1	27.	16892.	41554.	352.58	-0.0412
3328.	63.5	2.43	26.1	26.	15748.	38268.	353.60	0.0032
3336.	63.1	2.43	23.8	26.	15848.	38511.	356.88	0.0069
3362.	63.0	2.46	23.6	26.	15873.	39048.	357.63	0.0137
3368.	61.3	2.46	21.6	19.	16313.	40130.	358.61	-0.0170
3376.	62.9	2.44	23.1	35.	15898.	38791.	359.37	0.0093
3382.	62.5	2.47	23.7	24.	16000.	39520.	359.74	0.0314
3385.	58.7	2.47	20.3	26.	17036.	42079.	360.21	-0.0265
3389.	61.9	2.47	22.5	26.	16155.	39903.	360.58	0.0181
3392.	59.7	2.47	21.8	26.	16750.	41373.	360.94	-0.0213
3395.	62.3	2.47	23.8	26.	16051.	39646.	361.57	0.0321
3400.	58.9	2.49	20.7	20.	16978.	42275.	362.15	-0.0133
3405.	60.0	2.47	22.5	27.	16667.	41167.	364.67	0.0119
3426.	59.3	2.50	21.1	24.	16863.	42158.	364.91	0.0111
3428.	58.0	2.50	19.5	28.	17241.	43103.	366.07	0.0465
3438.	53.9	2.55	17.4	25.	18553.	47310.	368.12	-0.0356
3457.	57.2	2.52	18.6	27.	17483.	44057.	368.69	-0.0101

U.S.G.S. MADISON NO. 2

Z	ITT	DEN	Ø	GR	V	RHO-V	T	RC
6505.	48.2	2.69	0.6	30.	20747.	55809.	1430.29	-0.0233
6508.	50.5	2.69	0.6	21.	19802.	53267.	1430.49	0.0120
6510.	49.3	2.69	0.6	21.	20284.	54564.	1431.67	-0.1672
6522.	67.3	2.62	15.2	63.	14859.	38931.	1432.75	0.1644
6530.	49.4	2.68	-0.1	37.	20243.	54251.	1433.44	0.0121
6537.	48.4	2.69	-0.1	22.	20661.	55578.	1433.73	-0.0349
6540.	51.9	2.69	-0.1	32.	19268.	51831.	1433.94	0.0218
6542.	49.5	2.68	-0.1	32.	20202.	54141.	1434.73	0.0147
6550.	49.5	2.76	-0.1	46.	20202.	55758.	1435.23	-0.0629
6555.	53.7	2.64	1.5	26.	18622.	49162.	1436.09	-0.1105
6563.	67.3	2.65	-0.3	59.	14859.	39376.	1436.36	0.0004
6565.	63.7	2.51	16.0	27.	15699.	39404.	1436.74	0.0395
6568.	61.9	2.64	13.1	31.	16155.	42649.	1437.98	0.0999
6578.	54.5	2.84	4.8	18.	18349.	52111.	1438.85	-0.0622
6586.	58.9	2.71	10.0	25.	16978.	46010.	1439.20	-0.0194
6589.	60.1	2.66	27.5	25.	16639.	44260.	1439.80	-0.0369
6594.	64.7	2.66	30.4	25.	15456.	41113.	1440.45	0.1362
6599.	50.3	2.72	1.9	20.	19881.	54076.	1441.66	-0.2225
6611.	69.2	2.38	19.2	35.	14451.	34393.	1443.04	-0.0445
6621.	75.0	2.36	20.9	33.	13333.	31466.	1443.64	0.2483
6625.	51.1	2.67	2.6	23.	19569.	52249.	1445.28	-0.1254
6641.	66.5	2.70	9.8	94.	15038.	40603.	1445.68	0.1215
6644.	51.7	2.68	2.6	26.	19342.	51837.	1447.12	-0.0013
6658.	53.0	2.74	4.6	27.	18868.	51698.	1449.14	-0.0360
6677.	55.3	2.66	7.1	21.	18083.	48101.	1449.80	-0.0202
6683.	56.5	2.61	8.9	21.	17699.	46194.	1450.03	0.0569
6685.	50.8	2.63	4.6	21.	19685.	51772.	1455.00	-0.0130
6734.	56.1	2.83	6.7	15.	17825.	50445.	1455.23	0.0625
6736.	52.3	2.99	1.6	15.	19120.	57169.	1455.75	-0.1990
6741.	68.6	2.62	15.7	37.	14577.	38192.	1456.30	0.1727
6745.	53.2	2.88	3.3	17.	18797.	54135.	1457.26	0.0287
6754.	51.8	2.97	-0.9	16.	19305.	57336.	1457.98	-0.0105
6761.	52.9	2.97	0.5	23.	18904.	56145.	1459.25	-0.0161
6773.	49.3	2.68	1.0	23.	20284.	54361.	1460.04	0.0206
6781.	51.9	2.94	-0.7	12.	19268.	56648.	1460.66	-0.0229
6787.	52.3	2.83	2.8	25.	19120.	54110.	1460.98	0.0493
6790.	49.9	2.98	-0.9	13.	20040.	59719.	1461.48	-0.0169
6795.	51.1	2.95	-0.9	13.	19569.	57729.	1461.99	0.0000
6800.	51.1	2.95	-0.7	0.	19569.	57729.	1464.03	0.0275
6820.	48.2	2.94	-0.7	0.	20747.	60996.	1465.58	-0.0981
6836.	53.5	2.68	23.4	0.	18692.	50095.	1465.90	0.0459
6839.	48.8	2.68	1.4	0.	20492.	54919.	1466.29	-0.0856
6843.	57.5	2.66	9.5	0.	17391.	46260.	1466.52	0.0398
6845.	53.1	2.66	6.0	0.	18832.	50093.	1466.84	-0.0363
6848.	57.1	2.66	7.1	0.	17513.	46585.	1467.18	0.0754
6851.	50.2	2.72	0.4	0.	19920.	54182.	1468.48	0.0000

Z	ITT	DEN	Ø	GR	V	RHO-V	T	RC
6890.	55.9	2.57	7.9	0.	17889.	45975.	1471.57	0.0962
6894.	48.6	2.71	-0.3	0.	20576.	55761.	1472.54	-0.0554
6904.	53.5	2.67	2.9	0.	18692.	49908.	1472.75	0.0585
6906.	48.3	2.71	-0.4	0.	20704.	56108.	1475.36	-0.0807
6933.	55.1	2.63	5.1	0.	18149.	47732.	1476.02	0.0674
6939.	49.6	2.71	0.0	0.	20161.	54636.	1477.11	-0.0507
6950.	54.9	2.71	8.2	0.	18215.	49363.	1479.86	0.0514
6975.	49.9	2.73	0.3	0.	20040.	54709.	1480.46	-0.0807
6981.	56.3	2.62	8.2	0.	17762.	46536.	1481.02	0.0578
6986.	51.3	2.68	-0.2	0.	19493.	52241.	1481.64	0.0217
6992.	49.3	2.69	-0.2	0.	20284.	54564.	1482.72	-0.0724
7003.	55.3	2.61	5.0	0.	18083.	47197.	1483.27	-0.0035
7008.	55.9	2.62	5.0	0.	17889.	46869.	1484.39	0.0466
7018.	51.5	2.65	2.0	0.	19417.	51455.	1485.01	-0.1177
7024.	61.3	2.49	14.4	0.	16313.	40619.	1494.57	0.0397
7102.	57.3	2.52	11.2	0.	17452.	43979.	1495.95	0.0459
7114.	53.1	2.56	5.5	0.	18832.	48210.	1496.37	0.0537
7118.	50.3	2.70	1.2	0.	19881.	53679.	1505.02	-0.0243
7204.	52.8	2.70	8.9	24.	18939.	51135.	1505.45	-0.0158
7208.	54.5	2.70	8.9	18.	18349.	49542.	1505.77	0.0586
7211.	49.9	2.78	7.3	21.	20040.	55711.	1506.77	-0.0893
7221.	56.9	2.65	11.6	25.	17575.	46574.	1508.02	0.1263
7232.	47.3	2.84	3.4	17.	21142.	60043.	1508.97	-0.0488
7242.	50.5	2.75	5.0	13.	19802.	54456.	1509.88	0.0300
7251.	48.6	2.81	3.8	15.	20576.	57819.	1510.56	-0.0376
7258.	52.4	2.81	6.9	20.	19084.	53626.	1510.98	0.0366
7262.	48.7	2.81	1.4	19.	20534.	57701.	1511.66	-0.0451
7269.	53.3	2.81	7.5	25.	18762.	52721.	1511.87	0.0884
7271.	44.8	2.82	0.9	23.	22321.	62945.	1512.68	-0.2149
7280.	68.1	2.77	3.4	23.	14684.	40675.	1512.95	0.2570
7282.	40.4	2.78	1.8	25.	24752.	68811.	1513.27	-0.1661
7286.	56.5	2.78	7.7	29.	17699.	49203.	1514.40	0.0424
7296.	51.9	2.78	3.8	25.	19268.	53565.	1515.13	-0.0416
7303.	55.6	2.74	7.1	26.	17986.	49282.	1515.46	-0.0305
7306.	59.1	2.74	9.4	31.	16920.	46361.	1515.82	0.0776
7309.	51.7	2.80	4.0	22.	19342.	54158.	1516.23	-0.0842
7313.	59.9	2.74	9.0	35.	16694.	45742.	1517.43	0.0949
7323.	49.7	2.75	0.9	17.	20121.	55333.	1518.33	-0.0119
7332.	50.9	2.75	2.2	20.	19646.	54027.	1518.83	-0.0746
7337.	59.1	2.75	8.4	31.	16920.	46530.	1519.19	0.0788
7340.	50.1	2.73	0.5	16.	19960.	54491.	1520.09	-0.0237
7349.	53.3	2.77	5.5	25.	18762.	51971.	1520.73	0.0589
7355.	46.0	2.69	1.1	23.	21739.	58478.	1521.37	0.0685
7362.	40.4	2.71	0.6	15.	24752.	67078.	1522.51	-0.2095
7376.	62.5	2.74	10.2	32.	16000.	43840.	1523.01	0.0776
7380.	53.5	2.74	3.5	25.	18692.	51216.	1523.33	-0.0500
7383.	58.7	2.72	8.4	35.	17036.	46338.	1523.80	0.0815
7387.	51.5	2.81	3.0	22.	19417.	54562.	1524.72	-0.0726
7396.	58.5	2.76	7.0	34.	17094.	47179.	1525.31	0.0737

Z	ITT	DEN	Ø	GR	V	RHO-V	T	RC
7410.	49.9	2.74	0.4	15.	20040.	54910.	1526.98	-0.0661
7417.	55.3	2.66	4.6	15.	18083.	48101.	1527.31	0.0528
7420.	50.5	2.70	1.6	14.	19802.	53465.	1528.72	-0.0437
7434.	54.5	2.67	9.6	20.	18349.	48992.	1530.69	0.0628
7452.	49.5	2.75	1.0	17.	20202.	55556.	1541.38	-0.0803
7560.	57.3	2.71	10.2	22.	17452.	47295.	1531.98	0.0643
7478.	50.0	2.69	1.7	16.	20000.	53800.	1533.78	-0.0357
7496.	52.9	2.65	8.8	19.	18904.	50096.	1533.99	0.0495
7498.	49.9	2.76	4.8	23.	20040.	55310.	1534.29	-0.0644
7501.	54.3	2.64	7.3	20.	18416.	48618.	1534.73	0.0571
7505.	49.9	2.72	1.8	16.	20040.	54509.	1535.43	-0.0394
7512.	52.6	2.65	8.0	18.	19011.	50379.	1537.00	-0.0010
7527.	54.1	2.72	8.0	20.	18484.	50276.	1537.98	0.1152
7536.	43.4	2.75	1.5	17.	23041.	63363.	1538.85	-0.0899
7546.	51.6	2.73	0.8	25.	19380.	52907.	1544.62	0.0128
7602.	50.3	2.73	-0.2	22.	19881.	54275.	1545.33	-0.0201
7609.	51.6	2.69	-0.2	22.	19380.	52132.	1546.98	0.1217
7625.	40.4	2.69	2.8	24.	24752.	66583.	1547.30	-0.1139
7629.	52.3	2.77	1.5	24.	19120.	52962.	1547.83	0.0233
7634.	50.1	2.78	7.1	28.	19960.	55489.	1549.03	0.0183
7646.	48.3	2.78	3.5	21.	20704.	57557.	1550.77	-0.1338
7664.	61.4	2.70	9.7	82.	16287.	43975.	1551.87	-0.0041
7673.	61.9	2.70	12.1	23.	16155.	43619.	1552.12	0.1533
7675.	47.8	2.84	3.0	19.	20921.	59416.	1552.88	-0.1132
7683.	58.1	2.75	9.1	42.	17212.	47333.	1553.81	0.1789
7691.	41.2	2.80	3.7	17.	24272.	67962.	1553.98	-0.0679
7693.	47.2	2.80	3.7	17.	21186.	59321.	1554.45	-0.1276
7698.	59.7	2.74	10.0	73.	16750.	45895.	1555.05	0.1061
7703.	47.9	2.72	6.5	17.	20877.	56785.	1555.62	-0.0570
7709.	53.3	2.70	7.9	30.	18762.	50657.	1556.37	-0.0887
7716.	62.5	2.65	9.6	81.	16000.	42400.	1556.87	0.1611
7720.	47.2	2.77	0.8	15.	21186.	58685.	1557.72	-0.1259
7729.	59.7	2.72	7.9	40.	16750.	45560.	1559.51	-0.0646
7744.	66.2	2.65	12.1	103.	15106.	40031.	1560.44	0.1513
7751.	52.3	2.84	2.3	25.	19120.	54301.	1561.80	-0.1476
7764.	66.7	2.69	12.7	81.	14993.	40331.	1562.46	0.1727
7769.	49.5	2.83	0.8	17.	20202.	57172.	1563.45	-0.1250
7779.	60.5	2.69	9.5	53.	16529.	44463.	1563.82	0.1250
7782.	49.5	2.83	3.2	25.	20202.	57172.	1564.21	-0.1047
7786.	58.7	2.72	9.2	25.	17036.	46338.	1564.80	-0.0765
7791.	64.9	2.58	14.1	52.	15408.	39753.	1565.06	0.1223
7793.	54.1	2.75	9.2	21.	18484.	50831.	1565.38	-0.1417
7796.	64.9	2.48	15.9	24.	15408.	38212.	1565.64	0.1748
7798.	51.1	2.78	12.8	18.	19569.	54402.	1566.67	-0.1424
7808.	62.2	2.54	14.4	28.	16077.	40836.	1567.66	0.0786
7816.	54.6	2.61	9.4	18.	18315.	47802.	1568.21	0.0105
7821.	54.7	2.67	7.1	24.	18282.	48813.	1568.64	-0.0420
7825.	59.5	2.67	10.5	36.	16807.	44875.	1569.36	0.0928
7831.	50.5	2.73	6.3	24.	19802.	54059.	1569.76	-0.0436

Z	ITT	DEN	Ø	GR	V	RHO-V	T	RC
7847.	53.5	2.71	10.8	18.	18692.	50655.	1571.18	0.0553
7849.	48.6	2.75	5.4	18.	20576.	56584.	1572.25	-0.0683
7860.	53.3	2.63	12.4	18.	18762.	49344.	1572.79	0.0439
7865.	49.0	2.64	8.3	21.	20408.	53877.	1575.83	-0.0677
7896.	55.9	2.63	9.1	14.	17889.	47048.	1576.27	0.0426
7900.	52.9	2.71	12.6	19.	18904.	51230.	1577.22	-0.0290
7909.	54.4	2.63	9.2	16.	18382.	48345.	1578.10	-0.1292
7917.	67.6	2.52	19.9	49.	14793.	37278.	1578.37	0.2705
7919.	43.9	2.85	3.9	11.	22779.	64920.	1579.95	-0.1417
7937.	54.3	2.65	9.0	13.	18416.	48802.	1580.92	0.0298
7946.	52.9	2.74	8.8	16.	18904.	51797.	1581.24	0.0467
7949.	48.0	2.73	5.7	16.	20833.	56874.	1581.91	-0.0634
7956.	55.9	2.80	11.2	36.	17889.	50089.	1582.47	0.0309
7961.	50.3	2.68	7.1	15.	19881.	53281.	1582.87	-0.0308
7965.	53.5	2.68	9.6	21.	18692.	50095.	1583.20	0.0624
7968.	49.5	2.81	5.3	21.	20202.	56768.	1583.69	-0.0802
7973.	57.3	2.77	10.0	46.	17452.	48342.	1587.47	0.1635
8006.	41.2	2.77	6.5	33.	24272.	67233.	1588.21	-0.1314
8015.	52.7	2.72	6.5	21.	18975.	51612.	1588.53	0.0340
8018.	50.5	2.79	6.5	21.	19802.	55248.	1588.73	-0.0284
8020.	52.3	2.73	6.5	25.	19120.	52198.	1589.36	0.0130
8026.	51.7	2.77	6.5	20.	19342.	53577.	1590.19	0.0659
8034.	45.8	2.80	6.5	16.	21834.	61135.	1591.01	-0.0670
8043.	52.0	2.78	5.6	28.	19231.	53462.	1591.74	-0.0272
8050.	55.7	2.82	7.9	35.	17953.	50627.	1592.85	0.0039
8060.	53.7	2.74	4.0	18.	18622.	51024.	1593.60	-0.0717
8067.	62.0	2.74	10.3	67.	16129.	44193.	1594.22	0.0069
8072.	60.7	2.72	7.9	57.	16474.	44809.	1594.59	-0.0162
8075.	62.7	2.72	9.6	72.	15949.	43381.	1594.84	0.0113
8077.	61.3	2.72	7.8	63.	16313.	44371.	1595.33	-0.0518
8081.	67.0	2.68	10.1	74.	14925.	39999.	1596.13	-0.0243
8087.	70.6	2.69	12.6	84.	14164.	38101.	1597.97	-0.0485
8100.	77.8	2.69	11.0	88.	12853.	34575.	1598.44	0.2347
8103.	49.3	2.75	-1.0	18.	20284.	55781.	1599.32	-0.0647
8112.	55.1	2.70	3.4	19.	18149.	49002.	1600.21	0.0514
8120.	49.9	2.71	-1.0	19.	20040.	54308.	1601.70	-0.0349
8135.	53.9	2.73	3.2	22.	18553.	50650.	1602.35	0.0375
8141.	50.0	2.73	-0.6	18.	20000.	54600.	1603.45	-0.1539
8152.	62.7	2.51	15.1	21.	15949.	40032.	1604.20	0.0162
8158.	60.7	2.51	14.5	19.	16474.	41350.	1605.05	-0.0884
8165.	71.6	2.48	17.9	19.	13966.	34636.	1607.20	0.2229
8180.	49.9	2.72	-0.5	18.	20040.	54509.	1610.09	-0.1113
8209.	58.5	2.55	13.2	42.	17094.	43590.	1610.91	-0.0774
8216.	65.1	2.43	21.0	27.	15361.	37327.	1611.82	0.0111
8223.	65.5	2.50	15.2	23.	15267.	38168.	1613.40	-0.0745
8235.	72.4	2.38	19.9	23.	13812.	32873.	1614.41	0.2626
8242.	48.5	2.73	-0.8	13.	20619.	56290.	1616.35	-0.0692
8262.	55.1	2.70	6.5	15.	18149.	49002.	1616.90	-0.0129
8267.	55.7	2.66	8.6	20.	17953.	47755.	1617.23	0.0602

Z	ITT	DEN	Ø	GR	V	RHO-V	T	RC
8282.	51.1	2.68	0.5	14.	19569.	52445.	1620.14	-0.0248
8297.	53.7	2.68	3.8	18.	18622.	49907.	1620.78	0.0363
8303.	50.5	2.71	2.2	17.	19802.	53663.	1621.39	-0.0400
8309.	54.3	2.69	4.7	15.	18416.	49539.	1621.82	0.0363
8313.	50.5	2.69	2.1	15.	19802.	53267.	1622.33	-0.0399
8318.	54.7	2.69	5.1	16.	18282.	49179.	1631.30	0.0415
8400.	50.9	2.72	0.9	20.	19646.	53437.	1632.42	-0.0211
8411.	52.7	2.70	2.5	21.	18975.	51233.	1633.36	0.0243
8420.	50.2	2.70	1.2	20.	19920.	53784.	1634.07	-0.0318
8427.	53.1	2.68	2.3	19.	18832.	50470.	1634.60	0.0373
8432.	50.2	2.73	0.6	18.	19920.	54382.	1635.40	-0.0429
8440.	53.7	2.68	2.9	15.	18622.	49907.	1636.80	-0.0037
8453.	53.7	2.66	3.3	20.	18622.	49535.	1638.09	0.0503
8465.	50.2	2.75	0.3	19.	19920.	54780.	1647.93	-0.2159

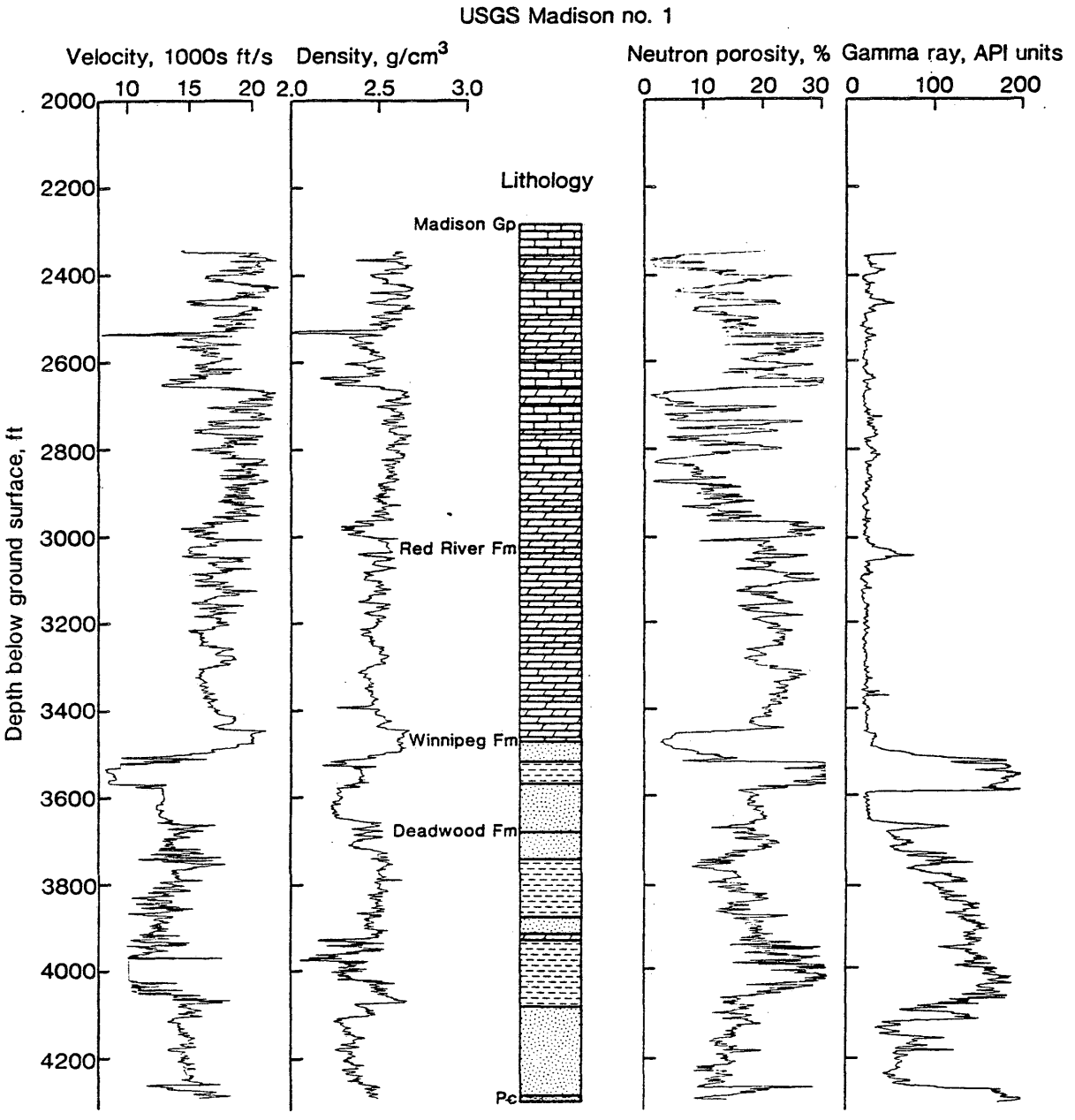

Curves used in the well log analysis from the USGS Madison No. 1 well plotted as a linear function of depth.

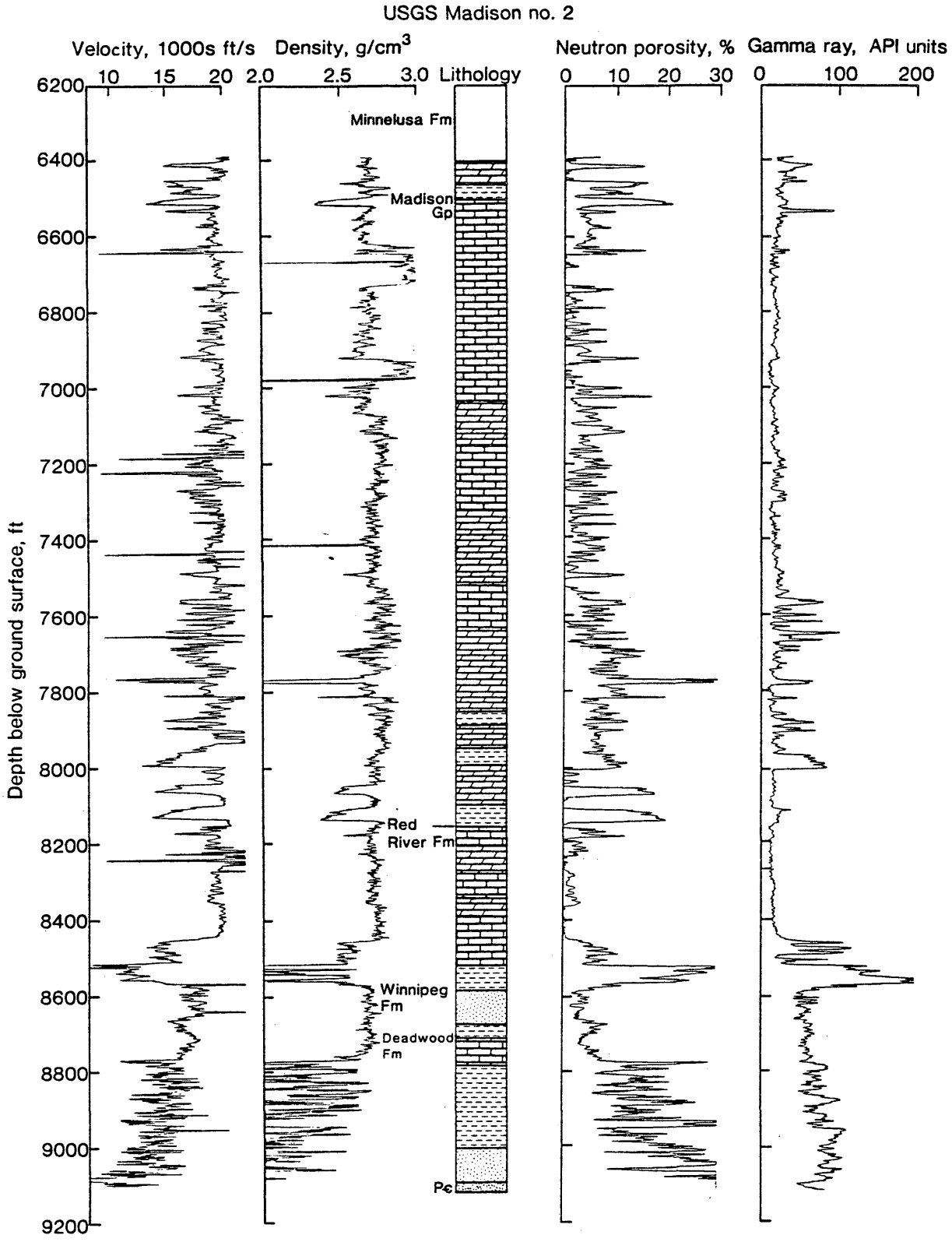

Curves used in the well log analysis from the USGS Madison No. 2 well plotted as a linear function of depth.